DEVELOPMENTS IN THE FIELD OF ENGINEERING 2024

Editor:

Assoc. Prof. Mehmet HASKUL

Assoc. Prof. Asaf Tolga ÜLGEN

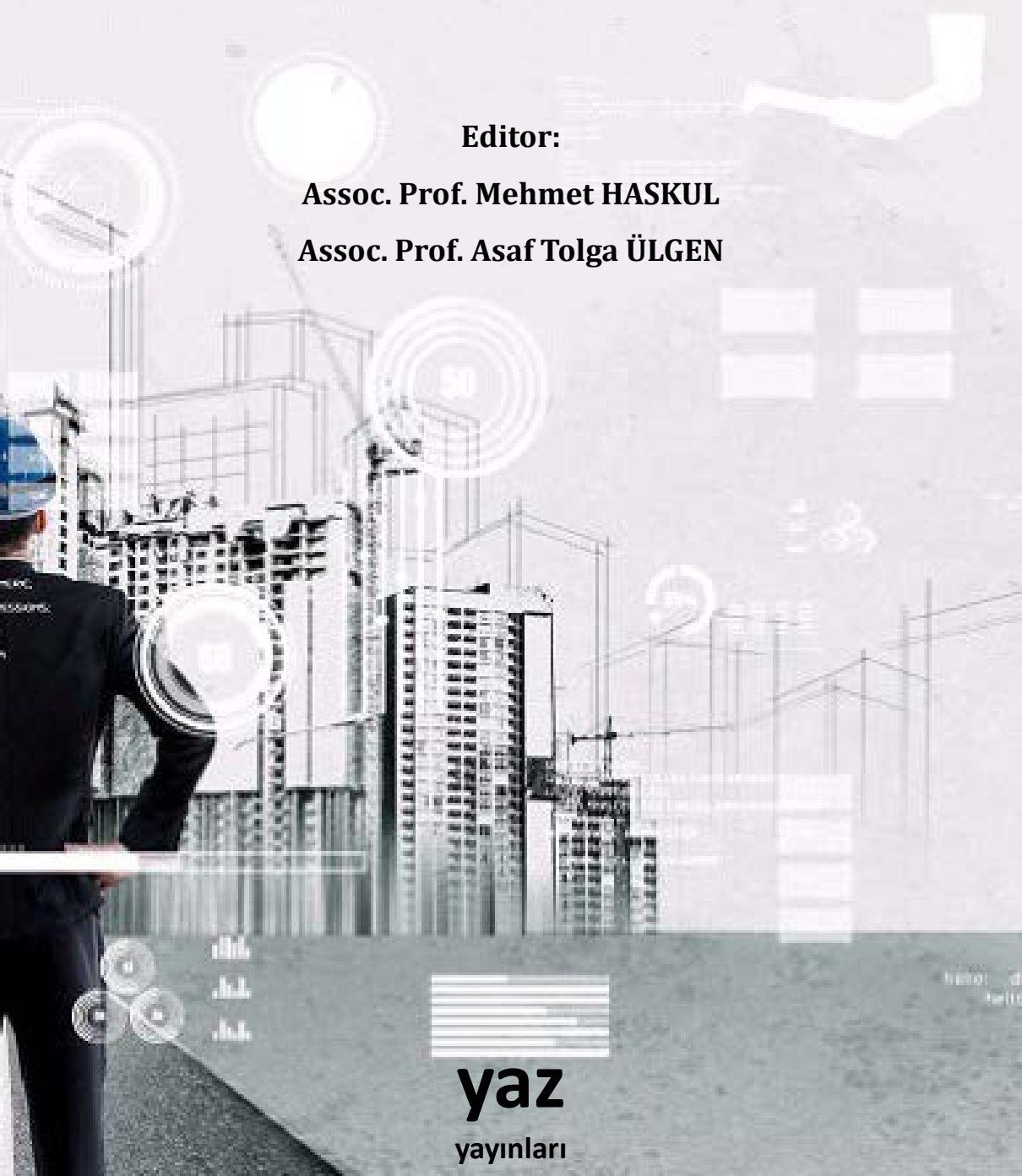

yaz

yayınları

DEVELOPMENTS IN THE FIELD OF ENGINEERING 2024

Editors

Assoc. Prof. Dr. Mehmet HASKUL

Assoc. Prof. Dr. Asaf Tolga ÜLGEN

yaz yayınları

2024

yaz yayınları

DEVELOPMENTS IN THE FIELD OF ENGINEERING 2024

Editor: Assoc. Prof. Dr. Mehmet HASKUL

ORCID NO: 0000-0001-8671-4597

Editor: Assoc. Prof. Dr. Asaf Tolga ÜLGEN

ORCID NO: 0000-0002-7112-5607

E_ISBN 978-625-6171-18-3

Aralık 2024 – Afyonkarahisar

Dizgi/Mizanpaj: YAZ Yayınları

Kapak Tasarım: YAZ Yayınları

YAZ Yayınları. Yayıncı Sertifika No: 73086

M.İhtisas OSB Mah. 4A Cad. No:3/3
İscehisar/AFYONKARAHİSAR

www.yazyayinlari.com

yazyayinlari@gmail.com

info@yazyayinlari.com

CONTENTS

INSPECTION OF SOME FUNDAMENTAL CHARACTERISTICS OF 2,4,6-TRIBROMOANILINE MOLECULE WITH MODERN COMPUTATIONAL CHEMISTRY MODELS

Muhammed ÖZ[1]

Ümit ERDEM[2]

Mustafa Burak TÜRKÖZ[3]

1. INTRODUCTION

Modeling experimental results for polymer-based compounds provides us with a preliminary indication of some of the problems that may be encountered. Besides, the model provides valuable information on how long the newly synthesized polymer materials can be used under what conditions and how long they can be used under operational stress or harsh environmental conditions, and at what points they may fail. On this basis, theoretical models play an important role in simplifying complex real-

1 Assoc. Prof. Dr. Bolu Abant İzzet Baysal University, Gerede Vocational School, Chemistry and Chemical Processing Technology, oz_m@ibu.edu.tr, ORCID: 0000-0003-0049-0161.

2 Assoc. Prof. Dr. Kırıkkale University, Kırıkkale Vocational School, Department of Electronıcs and Automation, erdem.umit@gmail.com, ORCID: 0000-0002-0480-8176.

3 Assoc. Prof. Dr. Karabuk University, Faculty of Engineering, Electric-Electronics Engineering, mbturkoz@karabuk.edu.tr, ORCID: 0000-0002-4127-7650.

world systems, breaking down complex processes, behaviors, and relationships into more manageable components. This simplification makes it easier to understand, analyze, and interpret the systems. Among different modeling techniques, modern computational chemistry models stand out for their ability to blend theoretical principles with empirical data, allowing for accurate and rapid predictions with reduced computational demands. This makes the models especially useful for handling complex systems and situations where data availability is limited. As well known, modern computational chemistry model approaches focus sensitively on critical interactions and deliberately omit unnecessary details to reveal patterns, trends, and potential outcomes that are of invaluable value in fields as diverse as science, engineering, and economics. Correspondingly, the quantum chemistry models enable researchers to test hypotheses, simulate various scenarios, and predict system behavior without the need for extensive real-world experimentation. This way, the high costs and risks associated with physical application conditions are avoided while early diagnosis of potential problems is possible. Furthermore, the chemistry modeling provides a rational basis for decision-making by exploring the potential consequences of various factors. The ability of quantum mechanical models to simulate the various conditions allows for better planning, design, and risk management, and improves decision-making, supporting problem solving and contributing to the development of innovative solutions. Despite the major advantages, there is a noteworthy gap in scientific investigations on the

specific application of modern computational chemistry models. More examination is required to recognize wholly the potential benefits and limitations pertaining to the modeling approaches in practical applications. Addressing the gap emphasized could lead to advances in modeling techniques and contribute to future innovations in various fields.

Modern computational chemistry relies on theoretical techniques such as ab initio Hartree-Fock (HF) and density functional theory (DFT), which have gained widespread popularity to study numerous important properties including physical, structural, and electronic of newly synthesized molecules. The quantum mechanical methods are particularly effective for investigating molecular geometries, thermodynamics, structural, vibrational frequencies, physical, mechanical, dipole moments, chemical shifts, charge transfer mechanisms, electrochemical, molecular electrostatic potential, spectroscopic, and optical properties. Similarly, the models are also effective in determining the lone pairs, electron engagements, conjugative effect as well as possible intra-molecular charge (ICT) transfer regions along the new synthesized organic molecules. All in all, modern computational chemistry models have widely been used for the characterization of organic molecules. In the literature, numerous studies have focused on 2,4,6-Tribromoaniline molecule, with a growing body of research dedicated to both theoretical and experimental analyses and its related organic derivatives. For example, 2,4,6-Tribromoaniline compound is used for the production of larger molecules such as brominated dioxins and

bromodioxin analogs (Brillas, Costa, & Pastor 1984; Alsabbagh, Gierthy, Narang, Aldous, & O'Keefe, 1988; Alsabbagh, Aldous, & Narang, 1992; Kulakov, et al., 2008). Hydrogen bonding and electrochemical oxidation behavior in different solvents have also been studied (Brillas, Costa, & Pastor, 1983; Pavlenko & Rubalio, 1985; Kádár, Nagy, Karancsi, & Farsang, 2001). Jaiswal et al investigated the intermolecular vibrational coupling characteristics along the crystalline 2,4,6-Tribromoaniline compound (Jaiswal, Katon, &Tripathi, 1983). The main reasons for our preference for the title compound are that 2,4,6-Tribromoaniline is a halogenated aromatic amine and can easily find key applications in various fields due to its chemical properties. The molecule has been used as a precursor or intermediate in pharmaceutical compound synthesis, agrochemicals, and azo dyes/pigments including pesticides, herbicides, and fungicides. Besides, due to its brominated structure, the material allows its use in the formulation of flame retardants used to reduce flammability in various materials such as plastics, textiles and electronics. The 2,4,6-Tribromoaniline is utilized as a reagent or a standard for bromination reactions and analytical testing. Similarly, it is possible to see the use of a marker or standard in the detection and quantification of halogenated organic compounds in environmental samples. Owing to the superior electronic properties, 2,4,6-tribromoaniline can be explored in the development of organic semiconductors or conducting polymers. Moreover, the material with remarkable characteristic features can be used in modifying polymers to improve thermal stability or flame resistance. Also, the scientific

studies based on potential uses of 2,4,6-tribromoaniline molecule in functionalizing nanomaterials for specialized applications are ongoing. It was also reported that studying the antibacterial properties of herbal and organic compounds is important for their use in more areas in the future (Ulgen, Yildirim, & Turker, 2023). Having deep knowledge about the reactions of these kinds of compounds under electric fields, electric currents and magnetic fields helps us analyze their areas of use more easily (Ulgen, & Turker, 2024; Vashisth, & Nagarajan, 2008). Here, theoretical modelling studies pave the way for such untouched fields. Moreover, theoretical investigations have become increasingly important for characterizing these molecules, providing insights into their structural, thermodynamic, electronic, optical, spectroscopic, and electrochemical properties, including aspects like charge distribution, dipole moments, and molecular charge transfer regions. Accurate theoretical results not only enhance our understanding of these molecular characteristics but also play a vital role in predicting and elucidating experimental findings in a cost-effective manner.

The successful correlation between theoretical and experimental findings highlights the value of modern calculation techniques such as HF and DFT in molecular characterization. These approaches provide a powerful tool for predicting compound properties and gaining deeper insights into experimental phenomena, facilitating advances in understanding the behavior of complex organic molecules. To illustrate, in the year of 2022, 2,4,6-tribromoaniline adsorption behavior onto the surface of

coronene types, fullerene or fullerene-like nano-cages has theoretically been serached based on the noteworthy variations in chemical descriptive and non-linear optics features using DFT computational study (Al-Otaibi, Mary, Mary, Kaya, & Serdaroglu, 2022). Similarly, Haruna et al. in 2016 investigated the conformation, structure natural bond orbital, surface morphology, frontier molecular orbitals, and vibrational spectra belonging to the tribromoaniline structure (Haruna, Saleh, Thagfi, & Al-Saadi, 2016). Besides, the authors have inspected the detection of 2,4,6-tribromoaniline prepared silver colloids as surface-enhanced Raman scattering active substrates. However, the atomic charge distributions-dipole moments, thermodynamic quantities, electronic properties, nuclear magnetic resonance chemical shifts, electronegativity, electrophilic index, softness, molecular charge transfer regions, chemical hardness, as well as simulations (molecular electrostatic potential (MEP), lowest unoccupied molecular orbital (LUMO), electrostatic potential (ESP), highest occupied molecular orbital (HOMO), nucleophilic and electrophilic reactive regions) have not been studied in detail. In the current work, it is aimed to theoretically fill these gaps as much as possible using both HF and DFT approaches. In particular, the calculations utilize the B3LYP functional, which integrates Becke's three-parameter hybrid exchange functional with the nonlocal correlation functional developed by Lee, Yang, and Parr. The 6-31G+(d,p) calculation level is employed in these computations. The results obtained from the quantum mechanical models are systematically compared with experimental data from the SDBS (10011) database

and the paper in Ref. (Haruna, Saleh, Thagfi, & Al-Saadi, 2016), revealing a strong correlation between theoretical predictions and experimental observations. This consistency demonstrates the reliability and accuracy of the applied computational methods in predicting molecular properties. Further, here a comprehensive analysis is performed on the UV-visible (UV–vis) spectra, numerous thermodynamic properties, and nuclear magnetic resonance chemical shifts of 2,4,6-tribromoaniline molecule. Additionally, atomic charge distributions are assessed to understand the dipole moments and ICT regions. The findings indicate that the compound exhibits the potential for metallic bonding and intermolecular interactions. At the same time, the investigation extends to the visualization of key electronic properties, including LUMO, ESP, HOMO, and MEP maps. The visualizations provide insights into transition states, electronegativity, energy band gaps, chemical hardness, molecular softness, and electrophilicity quantities. The calculated values for the transition states and energy band gaps offer a deeper understanding of the reactivity and stability of the studied molecule. To sum up, the primary goal of this research is not only to compare theoretical predictions with some experimental data for the first time but also to provide a detailed characterization of the molecular properties. Accordingly, the current study aims to pave a way for future examinations and practical applications of these molecules in areas, viz., physics, chemistry, biology, and industry, by offering a foundation for understanding their behavior and potential uses.

2. COMPUTATIONAL DETAILS

This study presents a comprehensive analysis of the 2,4,6-tribromoaniline molecule (presented in Fig. 1), covering various molecular and electronic properties for the first time using computational methods. The research was performed with a Gaussian 09 characterization package (Frisch, et al., 2009; Dennington, Keith, & Millam, 2009), employing HF and DFT with B3LYP/6-31+G(d,p) computational method (Swiderski, Kalinowska, Swislocka, Wojtulewski, & Lewandowski, 2013; Karabacak, Cinar, Kurt, Babu, & Sundaraganesan, 2013; Milanovic et al., 2021a; Milanovic et al., 2021b). Key aspects investigate include the dipole moments, atomic charge distributions, ICT areas, thermodynamic quantities at 300 K, functional group identifications, molecular charge transfer characteristics, UV-vis spectra, 13C-NMR, and 1H-NMR chemical shifts.

Additionally, electronic properties were examined, focusing on electrochemical behavior. This included simulating the MEP, LUMO, HOMO, and ESP pictures. Energy band gaps and transition state parameters are also analyzed to get further perceptions for the stability, reactivity, and potential applications of 2,4,6-tribromoaniline molecule. This research not only provides a detailed characterization of the structural and electronic features but also offers a valuable reference for future experimental and theoretical studies. Furthermore, theoretical nuclear magnetic resonance (NMR) calculations are carried out using B3LYP//6-31+G(d,p) calculations. Computations utilized from GIAO method, which is

widely recognized for providing accurate NMR shifts predictions. Moreover, the visible electronic absorption maxima are calculated in vacuum by CIS-B3LYP and HF/6-31+G(d,p) (Furche, & Ahlrichs, 2002) levels of theory.

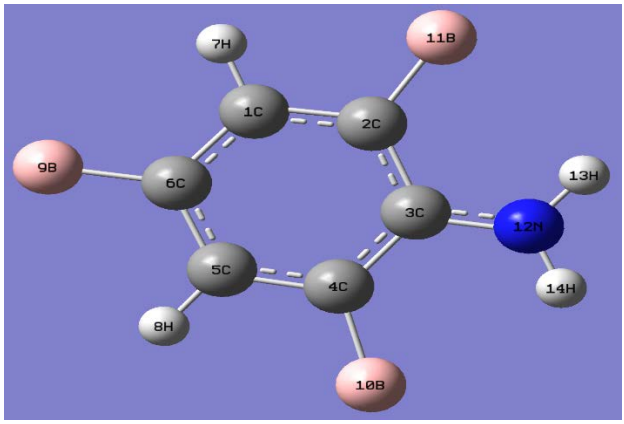

Fig. 1. Image of 2,4,6-Tribromoaniline molecule.

The electronic features are determined based on total energy calculations and principles from theorem associated with Koopmans. Ionization potential (IP) calculation is performed by using the energy variation between the radical cation, which results from the loss of an electron, and the energy of the neutral molecule. This difference indicates how readily a molecule can be ionized, offering insight into its electronic behavior. The formulas can be arranged as:

$$IP_{TE} = E_{cation} - E_n \quad (1)$$

$$IP_{KE} = - E_{HOMO} \quad (2)$$

Furthermore, the electron affinity (abbreviated as EA) is determined by energy differentiation stemmed from the anion and neutral compounds:

$$EA_{TE}=E_n - E_{anion} \quad (3)$$

$$EA_{KE}= - E_{LUMO} \quad (4)$$

At the same time, the IP and EA parameters enable us to define the crucial thermodynamics and physical features including electronegativity (χ), softness (ζ), electrophilicity index (ψ), and hardness (η) were inferred from the EA and IP parameters (Kohn, Becke, & Parr, 1996; Politzer & Awwad, 1998). Also, the chemical hardness and related electronegativity parameters are calculated from the following formulas.

$$\mu \approx - \chi = - (IP+EA)/2 \quad (5)$$

$$\eta \approx (IP-EA)/2 \quad (6)$$

Likewise, the parameters of softness and electrophilicity index are computed from the equations given below:

$$\zeta = 1/(2\eta) \quad (7)$$

$$\psi = (\mu 2/2\eta) \quad (8)$$

3. RESULTS AND DISCUSSION

ICT, atomic charge distributions-dipole moments, thermodynamic properties, electron donating groups, dipole moment, ζ, χ, ψ, η, 1H and 13C NMR results, electron engagement, visible absorption maxima, conjugation of π bonds, lone (non-bonding) pairs, energy band gap, HOMO, LUMO, MEP and ESP including 2D total

charge contours are inspected for 2,4,6-tribromoaniline molecule.

3.1.Atomic Charge Distributions

In this study, the atomic charge distributions for the 2,4,6-tribromoaniline molecule is analyzed using the Mulliken population computation method (Olsen & Jørgensen, 1985; Helgaker, Jensen, & Jørgensen, 1986; Foresman & Frisch, 1996; Buyukuslu, Akdogan,. Yildirim, & Parlak, 2010). Calculations are carried out at both DTF/B3LYP//6-31+G(d,p) and HF/B3LYP//6-31+G(d,p) quantum chemical methods, with the results for each atom presented in Table 1. The Mulliken charges for carbon atoms show a range of positive and negative values with charge magnitudes varying from -1.525129 to 1.259217 at the B3LYP/6-3+G(d,p) level, and from the value of -0.841879 to 0.478950 at the HF/6-31+G(d,p) basis set.

Table 1. Atomic charge distributions for optimized geometry of 2,4,6-tribromoaniline molecule

Label	DFT(B3LYP/6-31+(d,p))	HF (6-31+(d,p))
C1	-1.525069	-0.841877
C2	1.259217	0.478950
C3	-1.193455	-0.695404
C4	1.258953	0.478941
C5	-1.525129	-0.841879
C6	0.200264	-0.618757
H7	0.157296	0.192685
H8	0.157294	0.192685
Br9	0.339545	0.509914
Br10	0.346190	0.509231
Br11	0.346190	0.509231
N12	-0.463760	-0.556871
H13	0.321227	0.341576
H14	0.321238	0.341577

For nitrogen atom, the calculated charge is found to be about -0.463760 and -0.556871 in the DFT/B3LYP and HF/B3LYP basis sets, respectively. According to the atomic positions, spatial chemical environment, and strong existence of electron engagement, bromine atoms indicate positive charge values in the different calculation levels. The B3LYP/6-31+G(d,p) basis set yields charges intervals 0.339545 to 0.346190 while the HF/6-31+G(d,p) basis set shows a range from 0.509231 to 0.509914.

Hydrogen atomic charges (loss of electrons) are found to vary from 0.157294 to 0.321238 because of the existence of lone pairs on the hydrogens in the quantum chemistry models. In spite of differences between the HF and B3LYP molecular modeling results being attributed to some factors such as π-conjugation in carbon ring, non-bonding lone pairs, uneven charge distribution, and ICT, the agreement for the computations is satisfactory. All in all, the atomic charge distributions stem from the strong existence of electron engagement in bonds, electron donating groups, conjugation of π bonds, ICT regions, and lone pairs in the organic compound.

3.2.Uv–vis Spectra for 2,4,6-tribromoaniline Molecule

Electronic transitions in 2,4,6-tribromoaniline material can be classified based on the orbitals involved or specific regions along with the organic molecule. The two most common types of transitions are π → π* (donor to acceptor) and n → π*, where the π → π* transitions are generally stronger while the n → π* transitions are weaker. To define the electronic transitions in 2,4,6-tribromoaniline

molecule, theoretical calculations related to the electronic absorption spectra are performed using the TD-B3LYP/6-31+G(d,p) computation technique in vacuum conditions. The computation methods provide us the absorption maxima (λ), Cl-expansion coefficients, excitations, Singlet-A, oscillator strength (f), and translations. In the parameters, the value of λ parameter relates to electron availability, along with the Singlet A values are summarized in Table 2. The observed visible absorption peaks correspond to electronic transitions between frontier molecular orbitals such as transitions from the HOMO to LUMO or related other transitions. In this respect, for the excited state 1, transition occurs from HOMO-1 state to LUMO state and HOMO-1 state to LUMO+1 state. Similarly, the other transitions can be seen in Table 2 in detail.

Table 2. Theoretical electronic absorption spectra parameters

Cl-expansion coefficient					
Excitations	**Energy (eV)**	**Singlet-A**	**Wavelength (nm)**	**Oscillator strength (f)**	**Translations**
Excited State 1					
29→32		0.37367			LUMO-2→HOMO
29→33		-0.11294			LUMO-2→HOMO+1
29→46		-0.12091			LUMO-2→HOMO+14
30→32		0.38929			LUMO-1→HOMO
30→46	3.1789	-0.14509	390.02		LUMO-1→HOMO+14
31→32		-0.17917			LUMO→HOMO
31→33		-0.14223		0.0178	LUMO→HOMO+1
31→35		0.14119			LUMO→HOMO+3
31→46		0.14894			LUMO→HOMO+14
Excited State 2					
29→32		0.10163			LUMO-2→HOMO
29→33		0.12234			LUMO-2→HOMO+1
29→35		-0.13039			LUMO-2→HOMO+3
29→46		-0.13392	389.36		LUMO-2→HOMO+14
30→32	3.1843	0.13579		0.0820	LUMO-1→HOMO
31→32		-0.14634			LUMO→HOMO
31→33		0.48690			LUMO→HOMO+1

31→35		-0.25832			LUMO→HOMO+3
31→46		-0.19403			LUMO→HOMO+14
Excited State 3					
29→32		-0.13024			LUMO-2→HOMO
29→33		-0.19514			LUMO-2→HOMO+1
29→35		-0.18573			LUMO-2→HOMO+3
29→46		-0.10329			LUMO-2→HOMO+14
30→32		0.21455			LUMO-1→HOMO
30→33		0.34095	374.32	0.0491	LUMO-1→HOMO+1
30→35	3.3122	0.31834			LUMO-1→HOMO+3
30→46		0.17542			LUMO-1→HOMO+14
30→57		0.12150			LUMO-1→HOMO+25
31→32		0.10179			LUMO→HOMO
31→33		0.11528			LUMO→HOMO+1
31→35		0.13203			LUMO→HOMO+3

As for the numerical values, the calculated maximum absorption wavelengths (λ_{max}) for the molecule studied are found to be about 338 nm for the excited state 1, 273 nm for the excited state 2, and 269 nm for the excited state 3, respectively. The latter transition of 269 nm is associated with a π → π* transition because of the C=C bonds. Peak within the 273 nm of λ_{max} are associated with overlapping π → π* transitions in the benzene ring, affected by the oscillation effects. Additionally, a weak absorption peak observed between 338 and 360 nm is linked to an n → π* transition involving the heavy groups including nitro (NH) and bromine (C-Br) atoms. The values of oscillator strengths of 0.0000, 0.0164, and 0.0003 for the transitions are also presented in Table 2.

3.3.Thermodynamic Properties

Some thermodynamic quantities including total energy, zero-point vibrational energy, rotational constant, thermal energies, entropies and heat capacities with the translational, rotational, and vibrational modes, and dipole

moments (μ, μ_x, μ_y, μ_z, and μ) performed by B3LYP and HF with 6-31+G(d,p) level of theory are given in Table 3 for the 2,4,6-tribromoaniline molecule. As seen from table, total entropy is obtained to be about 92.988 and 90.223 cal.mol^{-1}K^{-1} at the B3LYP and HF calculation levels, respectively. Moreover, it is encountered that 2,4,6-tribromoaniline material has the total energy values of -360.02217337 a.u. and -357.74992498 a.u. at the B3LYP and HF level of theory. Similarly, the energy of zero-point vibrational system is also found to be about 56.32867 and 60.27843 a.u. The heat capacity parameter is calculated to as 33.622 and 31.951 cal.mol^{-1}K^{-1}. The dipole moment, a key factor in understanding a molecule's electronic properties, arises from the uneven distribution of charges across its atoms. It plays a significant role in analyzing intermolecular interactions, such as van der Waals dipole-dipole forces, with stronger interactions typically associated with larger dipole moments (Prasad, Sinha, Misra, Narayan, & Kumar, 2010). Therefore, it becomes straightforward to determine the biological properties of molecules, particularly in terms of their interactions with enzyme active sites. Likewise, the dipole moment can also give us the behavior of this material under a magnetic field. It has extensively been studied in numerous papers whether external magnetic field magnitudes affect in vitro regeneration, phenolic profiles, growth, antioxidant potential and defense enzyme activities of herbal and organic compounds or not (Ulgen, Yildirim, & Turker, 2020; Ulgen, Yildirim, Sahin, & Turker 2021). The dipole moment value is determined as about 3.6429 and 3.1754 Debye (Table 3) under DFT and HF methods, indicating polar (non-uniform atomic charge

distributions) structure of the compound. The obtained evidence is also confirmed by the simulation examinations. Besides, the findings can be used in composite and semiconductor materials (Haskul et al., 2020; Haskul, 2020; Al Hariri et al., 2022; Ekiz et al., 2023; Selimli et al.).

Table 3. Total energies (a.u.), Zero-point correction (a.u./Particle), zero-point vibrational energies (kcal mol^{-1}), entropies (cal $mol^{-1}K^{-1}$), thermal energies (kcal mol^{-1}), rotational constants (GHz), heat capacities (cal $mol^{-1}K^{-1}$), and dipole moment (Debye).

Parameter	DFT	HF
Total Energy	-360.02217337	-357.74992498
Zero-point vibrational Energy	56.32867	60.27843
Rotational Constant	2.13576	2.16583
	1.53905	1.54602
	0.89448	0.90209
Zero-point correction	0.089765	0.096060
Thermal correction to Energy	0.099077	0.104799
Thermal correction to Enthalpy	0.100021	0.105743
Thermal correction to Gibbs Free Energy	0.055840	0.062875
Entropy		
Total	92.988	90.223
Translational	40.337	40.337
Rotational	29.082	29.055
Vibrational	23.570	20.831
Heat capacity		
Total	33.622	31.951
Translational	2.981	2.981
Rotational	2.981	2.981
Vibrational	27.661	25.990
Thermal energy		
Total	73.622	65.762
Translational	0.889	0.889
Rotational	0.889	0.889
Vibrational	60.394	63.985
Total dipole moment	3.6429	3.1754
μ_x	3.6429	3.1754
μ_y	-0.0001	0.0000
μ_z	0.0033	0.0008

3.4.NMR Spectra Analyses

NMR analysis is one of the essential techniques to identify organic compounds. The difference between the ^{13}C and ^{1}H NMR spectra using HF/6-31+G(d,p) and

B3LYP/6-31+G(d,p) calculation techniques arises due to electron correlation effects. In the present work, the GIAO method is used to find the chemical shifts for the ^{13}C and ^{1}H NMR belonging to 2,4,6-tribromoaniline molecule with the results presented in Table 4. The B3LYP/6-311+G(d,p) calculations for the optimized molecular structure show a good correlation with experimental data. Experimentally, the 1H isotropic chemical shifts range from 4.560 to 7.497 ppm, while the calculated values are found to change from 3.9611 to 8.2442 ppm, indicating a close match between quantum calculation theory methods and experimental findings. Regarding the ^{13}C NMR chemical shifts relative to TMS (tetramethylsilane), the computed values fell within 125.300 (C_6) to 158.489 (C_2) ppm, while the experimental shifts range from 133.80 to 141.32 ppm. Besides, the chemical shifts for the bromine and nitrogenous atoms are provided in Table 4.

Table 4. Experimental and theoretical chemical shifts for 2,4,6-tribromoaniline molecule.

Label	DFT(B3LYP/6-31+(d,p))//			HF(B3LYP/6-31+(d,p))//			Experimental
	TMS HF/6-31G(d) GIAO	TMS B3LYP/6-311+G(2d,p) GIAO	CH4 HF/6-31G(d) GIAO	TMS HF/6-31G(d) GIAO	TMS B3LYP/6-311+G(2d,p) GIAO	CH4 HF/6-31G(d) GIAO	
C_2	158.489	140.969	157.603	155.714	138.194	154.829	141.32
C_3	157.942	140,422	157.057	155.420	137.901	154.535	
C_1	154.863	137.343	153.978	151.962	134.442	151.077	133.80
C_4	153.313	135.793	152.428	150.835	133.315	149.950	
C_5	127.874	110.354	126.989	128,921	111.401	128.035	
C_6	125.300	107.780	124.415	126.600	109,08	125.715	108.81
H_7	7.985	7.2695		8.5236	7.8081		7.497
H_8	8.2442	7.5287		8.2969	7.5814		
H_{13}	3.9611	3.2456		3.6606	2.9451		4.560
H_{14}	3.9611	3.2456		3.6606	2.9451		
	B2H6 B3LYP/6-311+G(2d,p)	HF(B3LYP/6-31+(d,p))//		B2H6 HF/6-31G(d) GIAO	B3LYP/6-311+G(2d,p) GIAO		
Br_9	202.069	225.169		228.877	205.777		
Br_{10}	213.639	236.740		230.09	206.990		
Br_{11}	223.704	246.804		244.379	221.279		
N_{12}	33,7029	36,1029		13.2247	10.8247		

3.5.Molecular Features of 2,4,6-Tribromoaniline Molecule

In this part, the fundamental properties of the frontier molecular orbitals, specifically the highest occupied molecular orbital (HOMO) and the lowest unoccupied molecular orbital (LUMO) are extensively examined. It is known that the inner orbitals represent the outermost orbital that contains electrons and acts as an electron donor. Conversely, the former orbitals are related to the innermost orbital with vacant spaces that can accept electrons. Correspondingly, orbitals are crucial for understanding the chemical reactivity and electronic properties of the organic molecule (Gece, 2008). According to molecular orbital theory, interactions between the HOMO and LUMO are associated with electronic transitions, such as π-π* type transitions, which influence directly the optical and electronic behavior of molecule (Fukui, 1987).

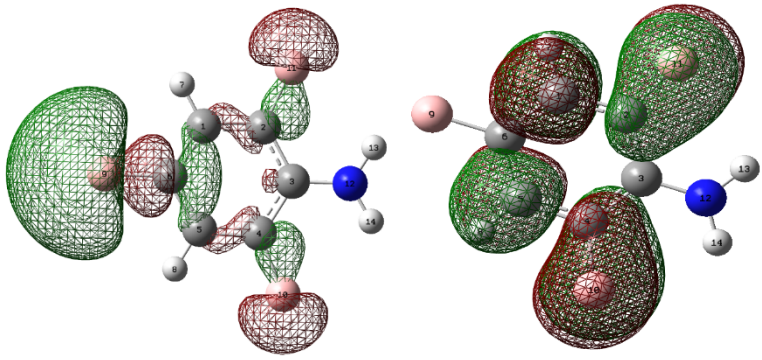

Fig. 2. 3D plots of a-) HOMO and b-) LUMO of the title compound. (Red/green regions reveal the positive/negative phases.

The energy level of the HOMO correlates with the ionization potential, indicating how easily the molecule can donate electrons. On the other hand, the LUMO energy relates to electron affinity, reflecting the ability of the molecule to accept electrons. The energy gap between the HOMO and LUMO, known as the band gap (ΔE), is a significant parameter that reveals the stability of the molecular structure. It is known that a smaller band gap represents higher chemical reactivity whereas a larger gap shows greater stability (Lewis, Ioannides, & Parke, 1994). In our calculations, the values for the frontier orbitals and band gap are summarized in Table 5, with 3D visualizations of the HOMO and LUMO displayed in Fig. 2.

The computed band gap at the B3LYP/6–31+G(d,p) level of theoryi approximately 0.1049 a.u. whereas at the HF/6–31+G(d,p) calculation level, the band gap is about 0.65121 a.u. Due to the lack of correlation in the HF calculation, relatively higher energy band gap is observed. As for the simulations, HOMO is predominantly localized in small pieces over all the molecule except for hydrogen atoms (positive charge) such as H_7, H_8, and amino group in the molecule, while the LUMO extends in rather larger pieces across the entire molecule except for Br9, amino group, C_3, and C_6 atoms. Furthermore, the lowest molecular orbital (MO) eigenvalue is found to be -14,42496 a.u. at the B3LYP/6–31+G(d,p) level and-15.64274 at the HF/6–31+G(d,p) level. In contrast, the highest MO eigenvalues are calculated to be 4,75958 a.u. for the B3LYP/6–31+G(d,p) level of theory and 5.20638 for the HF/6–31+G(d,p) basis level method. The findings

observed offer insight into the electronic structure of the compound, highlighting the variations in stability and reactivity based on the level of theory used in the calculations. One can see values of EA, IP, μ, ζ, χ, ψ, η, and ΔN_{max} parameters deduced from both modern computational chemistry models.

Table 5. The total electronic energies, energy gaps and molecular quantities for 2,4,6-Tribromoaniline molecule based on DFT and HF B3LYP/6-31+ G(d,p) levels of theory.

Molecular properties	DFT	HF
E_{HOMO} (a.u.)	-0.12122	0.01521
E_{LUMO} (a.u.)	-0.22612	-0.33600
$E_{HIGHEST}$ (a.u.)	4.75958	5.20638
E_{LOWEST} (a.u.)	-14.42496	-15.64274
Energy bandgap, ΔE $\lvert E_{HOMO} - E_{LUMO}$ (a.u.)$\rvert$	0.1049	0.65121
Ionization potential (IP = $-E_{HOMO}$)	0.12122	-0.01521
Electron affinity (EA = $-E_{LUMO}$)	0.22612	0.33600
Chemical hardness (η)	0.05245	0.325605
Chemical softness (ζ)	9.53288	1.535603
Electronegativity (χ)	0.17367	0.160395
Chemical potential (μ)	-0.17367	-0.160395
Electrophilicity index (ψ)	0.287524	0.03950577
Maximum charge transfer index ($\Delta N_{max} = -\mu/\eta$)	3.311153	0.49260607

3.6.Molecular Electrostatic Potential and Electrostatic Potential

In this part of paper, we focus extensively on ESP surface map over the electron density for the 2,4,6-Tribromoaniline molecule, illustrating its molecular size, shape, and charge distributions along the spatial chemical environment. As well known, the ESP mapping provides a valuable tool for analyzing molecular interactions, as information about ESP helps predict reactivity and highlights potential areas for intermolecular and intramolecular interactions, such as hydrogen bonding (Wang, Sun, Shen, Hou, & Zhai, 2008). Figure 3a displays the ESP map for the compound, supporting the findings of

the electron engagements, conjugative effect, and lone pairs discussed throughout the study. The map clearly identifies the most negatively charged regions, predominantly surrounding the nitrogen atom and some carbon atoms, indicating areas of electrophilic reactivity. This suggests that the π-electrons are extensively delocalized around these atoms, enhancing their potential for electrophilic interactions. Conversely, the map also shows that the carbon atoms in the rings and bromines are located in regions of nucleophilic reactivity, suggesting they may act as electron-rich sites within the molecule. These insights into the charge distribution and reactivity patterns not only favor the molecular findings from other parts of the paper but also provide a deeper understanding of the behavior of the title compound in various chemical and biological contexts.

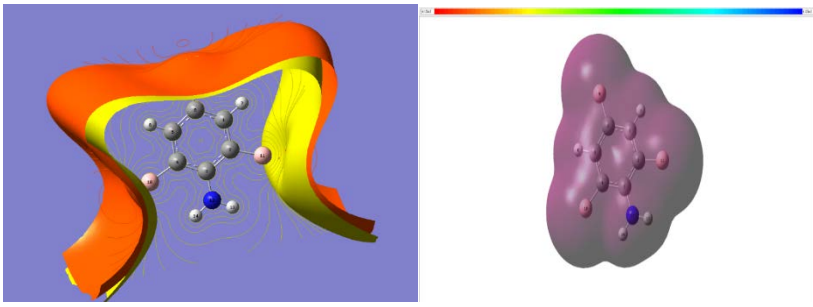

Fig. 3. 3D plots of a-) ESP picture and b-) MEP image of 2,4,6-Tribromoaniline compound

We also simulate MEP image (related to the interaction energy between the electron and nuclear charges with a hypothetical positive test charge (proton) at a given point in space) for the title compound in Fig. 3b. In this respect, the MEP serves as a valuable indicator for

understanding chemical reactivity. In more detail, the inspection of MEP map is closely linked to the electron density distribution and helps identify regions prone to electrophilic and nucleophilic interactions, as well as potential hydrogen-bonding sites (Politzer & Murray, 2002). That is exactly why the applied magnetic field strengths affect seriously the in vitro regeneration, phenolic profiles, growth, antioxidant potential and defense enzyme activities of herbal and organic compounds (Yildirim, Zalaoglu, Kirilmis, Koca, & Terzioglu, 2011; Ulgen, Yildirim, & Turker, 2017). As seen from the figure, the MEP map highlights areas of varying reactivity. The regions depicted in red correspond to sites favorable for electrophilic attack, contrariwise, the blue areas indicate regions suitable for nucleophilic reactivity. The map image indicates that the most negative potential, suggesting electrophilic reactivity, is concentrated around some carbon atoms and nitrogen atom. In contrast, the regions with a positive potential, which are more prone to nucleophilic behavior, are localized around the bromine and hydrogen atoms. The findings obtained indicate that the 2,4,6-Tribromoaniline molecule exhibits a versatile reactivity profile, with the ability to engage in both electrophilic and nucleophilic interactions. The distinct charge distribution also indicates potential for metallic bonding and various intermolecular interactions, making the compound a suitable candidate for diverse chemical applications.

4. CONCLUSION

In the present work, we present a comprehensive analysis of the 2,4,6-Tribromoaniline organic compound using quantum chemical methods of HF/6–31+G(d,p) and DFT-B3LYP/6–31+G(d,p). The investigation encompasses the atomic charge distributions-dipole moments, thermodynamic quantities, electronic properties, ^{13}C and ^{1}H NMR parameters, electronegativity, electrophilic index, softness, molecular charge transfer regions, chemical hardness, HOMO, MEP, LUMO, ESP, nucleophilic and electrophilic reactive regions. correspondingly, this work fills the gap in the literature. The results reveal significant ICT imbalances and electron-donating characteristics, influenced by substituent positions, electron distribution, electron engagements, lone pairs, π-π* interactions, ICT transfer, and intermolecular hydrogen bonding. The title compound exhibits pronounced regions of electrophilic and nucleophilic reactivity, confirming a serious potential as a candidate for antimicrobial, anticonvulsant, cytotoxic, antimalarial, and other pharmacological applications due to its strong interactions with biological targets. The characteristic behavior under external magnetic field strengths is also discussed.

REFERENCES

Al Hariri, A., Selimli, S., & Dumrul, H. (2022). Effectiveness of heat sink fin position on photovoltaic thermal collector cooling supported by paraffin and steel foam: An experimental study. *Applied Thermal Engineering*, *213*, 118784.

Al-Otaibi, J. S., Mary, Y. S., Mary, Y. S., Kaya, S., & Serdaroglu, G. (2022). DFT computational study of trihalogenated aniline derivative's adsorption onto graphene/fullerene/fullerene-like nanocages, X12Y12 (X= Al, B, and Y= N, P). Journal of Biomolecular Structure and Dynamics, 40(19), 8630-8643.

Alsabbagh, A. M., Aldous, K. M., Narang, R. S., & O'Keefe, P. W. (1992). Formation of brominated dioxins and brominated phenazines from pyrolyses of 2, 4, 6-tribromoaniline and N-(tribromophenyl) maleimide. Chemosphere, 24(11), 1625-1632.

Alsabbagh, A. M., Gierthy, J. F., Narang, R. S., Aldous, K. M., & O'Keefe, P. (1988). Formation of bromodioxin analogs from closed tube pyrolysis of 2, 4, 6-tribromoaniline (I). *Chemosphere*, *17*(12), 2391-2396.

Brillas, E. Costa, J.M. Pastor, E. (1983). Electrochemical Oxidation of 2,4,6-Tribromoaniline In Sulfuric-Acid, Anales De Quimica Serie A-Quimica Fisica Y Quimica Tecnica, 79 (2), 211-216.

Brillas, E. Costa, J.M. Pastor, E. (1984). Voltammetric study of the oxidation kinetics of 2,4,6,-tribromoaniline in

acid medium, Journal of Electroanalytical Chemistry and Interfacial Electrochemistry,160(1–2), 185-198.

Buyukuslu, H., Akdogan, M., Yildirim, G., & Parlak, C. (2010). Ab initio Hartree-Fock and density functional theory study on characterization of 3-(5-methylthiazol-2-yldiazenyl)-2-phenyl-1H-indole. Spectrochimica Acta Part A: Molecular and Biomolecular Spectroscopy, 75(4), 1362-1369.

Dennington, R., Keith, T., & Millam, J. (2009). GaussView, version 5, Semichem Inc., Shawnee Mission, KS, 2009.

Ekiz, A., Selimli, S., & Dumrul, H. (2023). An Experimental Study of the Effects of Heat-Sink Surface Form on PV Module Cooling and Electrical Performance. *Journal of Energy Engineering*, *149*(2), 04022062.

Foresman, J., & Frish, E. (1996). Exploring Chemistry with Electronic Structure Methods, 2nd ed., Gaussian Inc., Pittsburgh, PA, USA.

Frisch, M. J. E. A., Trucks, G. W., Schlegel, H. B., Scuseria, G. E., Robb, M. A., Cheeseman, J. R., Barone, V., Mennucci, B., Petersson, G. & Fox, D. J. (2009). gaussian 09, Gaussian. Inc., Wallingford CT, 121, 150-166.

Fukui, K. (1982). Role of frontier orbitals in chemical reactions, Science, 218, 747-754.

Furche, F., & Ahlrichs, R. (2002). Adiabatic time-dependent density functional methods for excited state

properties. The Journal of chemical physics, 117(16), 7433-7447.

Gece, G. (2008). The use of quantum chemical methods in corrosion inhibitor studies. Corrosion science, 50(11), 2981-2992.

Haruna, K., Saleh, T. A., Al Thagfi, J., & Al-Saadi, A. A. (2016). Structural properties, vibrational spectra and surface-enhanced Raman scattering of 2, 4, 6-trichloro-and tribromoanilines: a comparative study. Journal of Molecular Structure, 1121, 7-15.

Haskul, M., Ülgen, A. T., & Döner, A. (2020). Fabrication and characterization of Ni modified TiO_2 electrode as anode material for direct methanol fuel cell. International Journal of Hydrogen Energy, 45(7), 4860–4874.

Haskul, M. (2020). Elastic state of functionally graded curved beam on the plane stress state subject to thermal load. Mechanics Based Design of Structures and Machines, 48(6), 739–754.

Helgaker, T. U., Jensen, H. J. R. A., & Jorgensen, P. (1986). Analytical calculation of MCSCF dipole-moment derivatives. The Journal of chemical physics, 84(11), 6280-6284.

Jaiswal, R. M. P., Katon, J. E., & Tripathi, G. N. R. (1983). Polarized infrared spectra of oriented polycrystalline films. Intermolecular vibrational coupling in crystalline 2, 4, 6-tribromoaniline. The Journal of Chemical Physics, 79(1), 1-8.

Kádár, M., Nagy, Z., Karancsi, T., & Farsang, G. (2001). The electrochemical oxidation of 4-bromoaniline, 2, 4-dibromoaniline, 2, 4, 6-tribromoaniline and 4-iodoaniline in acetonitrile solution. Electrochimica acta, 46(22), 3405-3414.

Karabacak, M., Cinar, M., Kurt, M., & Sundaraganesan, N. (2013). Experimental and theoretical FTIR and FT-Raman spectroscopic analysis of 1-pyrenecarboxylic acid. Spectrochimica Acta Part A: Molecular and Biomolecular Spectroscopy, 114, 509-519.

Kohn, W., Becke, A. D., & Parr, R. G. (1996). Density functional theory of electronic structure. The journal of physical chemistry, 100(31), 12974-12980.

Kulakov, I. V., Il'in, A. I., Kabyl, Z. A., & Gazaliev, A. M. (2008). Synthesis of β-d-glucopyranosyl-and β-d-galactopyranosylamines from 4-bromo-3-methylaniline and 2-amino-5-bromopyridine. Russian Chemical Bulletin, 57(11), 2443-2445.

Lewis, D. F. V., Ioannides, C., & Parke, D. V. (1994). Interaction of a series of nitriles with the alcohol-inducible isoform of P450: Computer analysis of structure—activity relationships. Xenobiotica, 24(5), 401-408.

Milanović, Ž. B., Dimić, D. S., Avdović, E. H., Milenković, D. A., Marković, J. D., Klisurić, O. R., Trifunović, S.R., & Marković, Z. S. (2021). Synthesis and comprehensive spectroscopic (X-ray, NMR, FTIR, UV–Vis), quantum chemical and molecular docking investigation of 3-acetyl-4-hydroxy-2-oxo-2H-

chromen-7-yl acetate. Journal of Molecular Structure, 1225, 129256.

Milanović, Ž. B., Marković, Z. S., Dimić, D. S., Klisurić, O. R., Radojević, I. D., Šeklić, D. S., Živanovic, M. N., Markovic, J. D., Radulovic, M., & Avdović, E. H. (2021). Synthesis, structural characterization, biological activity and molecular docking study of 4, 7-dihydroxycoumarin modified by aminophenol derivatives. Comptes Rendus. Chimie, *24*(2), 215-232.

Olsen, J., & Jorgensen, P. (1985). Linear and nonlinear response functions for an exact state and for an MCSCF state. The Journal of chemical physics, 82(7), 3235-3264.

Pavlenko, N. I., & Rubailo, A. I. (1985). Hydrogen bonding in a 2, 4, 6-tribromoaniline crystal. J. Struct. Chem. (Engl. Transl.); (United States), 26(3).

Politzer, P., & Abu-Awwad, F. (1998). A comparative analysis of Hartree-Fock and Kohn-Sham orbital energies. Theoretical Chemistry Accounts, 99, 83-87.

Politzer, P., & Murray, J. S. (2002). The fundamental nature and role of the electrostatic potential in atoms and molecules. Theoretical Chemistry Accounts, 108, 134-142.

Prasad, O., Sinha, L., Misra, N., Narayan, V., Kumar, N., & Pathak, J. (2010). Molecular structure and vibrational study on 2, 3-dihydro-1H-indene and its derivative 1H-indene-1, 3 (2H)-dione by density functional

theory calculations. Journal of molecular structure: Theochem, 940(1-3), 82-86.

Selimli, S., Dumrul, H., Yilmaz, S., & Akman, O. (2021). Experimental and numerical analysis of energy and exergy performance of photovoltaic thermal water collectors. *Solar Energy*, *228*, 1-11.

Świderski, G., Kalinowska, M., Świsłocka, R., Wojtulewski, S., & Lewandowski, W. (2013). Spectroscopic (FT-IR, FT-Raman and 1H and 13C NMR) and theoretical in MP2/6-311++ G (d, p) and B3LYP/6-311++ G (d, p) levels study of benzenesulfonic acid and alkali metal benzenesulfonates. Spectrochimica Acta Part A: Molecular and Biomolecular Spectroscopy, 100, 41-50.

Ulgen, C., & Turker, A. (2024). Impacts of three different magnetic field applications on seed germination and seedling development of Melissa officinalis L. Biological Diversity and Conservation, 17(1), 18-25.

Ulgen, C., Yıldırım, A. B., & Turker, A. U. (2017). Effect of magnetic field treatments on seed germination of melissa officinalis L. International Journal of Secondary Metabolite, 4(3, Special Issue 1), 43-49.

Ulgen, C., Yıldırım, A., & Turker, A. (2020). Enhancement of plant regeneration in lemon balm (Melissa officinalis L.) with different magnetic field applications. International Journal of Secondary Metabolite, 7(2), 99-108.

Ulgen, C., Yıldırım, A., & Turker, A. (2023). Melissa officinalis: Antibacterial and antioxidant potential,

phenolic profile and enzyme activities. *Kahramanmaraş Sütçü İmam Üniversitesi Tarım ve Doğa Dergisi*, *26*(5), 1075-1085.

Ulgen, C., Yildirim, A. B., Sahin, G., & Turker, A. U. (2021). Do magnetic field applications affect in vitro regeneration, growth, phenolic profiles, antioxidant potential and defense enzyme activities (SOD, CAT and PAL) in lemon balm (Melissa officinalis L.). Industrial Crops and Products, 169, 113624.

Vashisth, A., & Nagarajan, S. (2008). Exposure of seeds to static magnetic field enhances germination and early growth characteristics in chickpea (Cicer arietinum L.). Bioelectromagnetics: Journal of the Bioelectromagnetics Society, The Society for Physical Regulation in Biology and Medicine, The European Bioelectromagnetics Association, 29(7), 571-578.

Wang, D. L., Sun, X. P., Shen, H. T., Hou, D. Y., & Zhai, Y. C. (2008). A comparative study of the electrostatic potential of fullerene-like structures of Au32 and Au42. Chemical Physics Letters, 457(4-6), 366-370.

Yildirim, G., Zalaoglu, Y., Kirilmis, C., Koca, M., & Terzioglu, C. (2011). A characterization study on 2, 6-dimethyl-4-nitropyridine N-oxide by density functional theory calculations. Spectrochimica Acta Part A: Molecular and Biomolecular Spectroscopy, 81(1), 104-110.

WEAKNESSES OF TRANSPORTATION INFRASTRUCTURE IN TURKEY AND FUTURE TARGETS TO BE ACHIEVED

Sedat OZCANAN[1]

1. INTRODUCTION

Transportation plays a critical role in the development of societies and the functioning of daily life. An effective transportation infrastructure is essential for economic growth, social integration, geopolitical advantages, and sustainability. Transportation systems can include various types, such as road, rail, air, sea, and pipeline networks, each offering distinct benefits to society. Transportation infrastructure, which holds strategic importance from geopolitical, economic, and social perspectives, is a fundamental building block for enhancing a nation's international competitiveness. In countries with vast territories like Turkey, the integration and harmonious operation of transportation systems are crucial.

It is evident that transportation holds significant importance in the economic development of nations. Numerous studies have examined the impact of transportation infrastructure on economic growth and regional development. Erdoğan (2016) analyzed

[1] Assoc. Prof. Dr., Sirnak University, Faculty of Engineering, Department of Civil Engineering, sozcanan@sirnak.edu.tr, ORCID: 0000-0002-8504-7611.

transportation sub-sectors from a technical perspective, while Maparu and Mazumder (2017) identified a long-term relationship between transportation infrastructure and urbanization, as well as a causality from development to transportation. Kara and Cigerlioglu (2018) confirmed the positive effect of road infrastructure on economic growth in Turkey using the Johansen cointegration test, and Logun and Tuzemen (2018) demonstrated the meaningful relationship between road and rail infrastructure and economic growth through the ARDL model. Alam et al. (2020) highlighted the positive impact of transportation infrastructure on development in Pakistan, although the statistical significance was found to be low. Magazzino and Mele (2020) revealed, through machine learning, that transportation investments influence development in China, while Telli (2020) emphasized the strong relationship between transportation infrastructure and human development in Turkey. Wang et al. (2021) identified a long-term relationship between maritime transportation infrastructure and economic development in China. Yurdakul (2022) analyzed the relationship between transportation infrastructure and economic development in Turkey using the ARDL bounds test, finding a statistically significant long-term relationship between economic development and road and maritime transportation infrastructure. These findings collectively underscore the critical role of transportation infrastructure in driving development.

The economic impact of transportation infrastructure is not independent of its social effects. The development of transportation infrastructure parallels

socio-economic development, as economic progress also triggers social advancement (Prus and Sikora, 2021). Moreover, transportation infrastructure is not only a tool for socio-economic development but also an indispensable element for national security and strategic superiority. Therefore, countries must design their transportation systems to support not only economic but also military and strategic objectives. In line with this, the transportation infrastructure of economically and militarily strong nations has developed in this direction (Lin, 2019).

In light of the evaluations above, the importance of transportation infrastructure has been emphasized. Considering its geographical position, socio-economic context, and military security, has Turkey's transportation infrastructure reached the required level? This study will address the current state of transportation infrastructure in Turkey and the future targets that need to be achieved.

2. CURRENT SITUATION

Transportation infrastructure in Turkey is diversified with various systems such as road, rail, air, and sea/ maritime transport. However, there are certain weaknesses in terms of the efficiency and sustainability of this infrastructure. Below, the current state and weaknesses of Turkey's transportation systems are examined.

As of 2022, Turkey's road network consists of 3,633 km of highways, 30,961 km of state roads, and 34,131 km of provincial roads, totaling 68,725 km (Figure 1). Of this network, 28,816 km consists of divided roads (UAB, 2022).

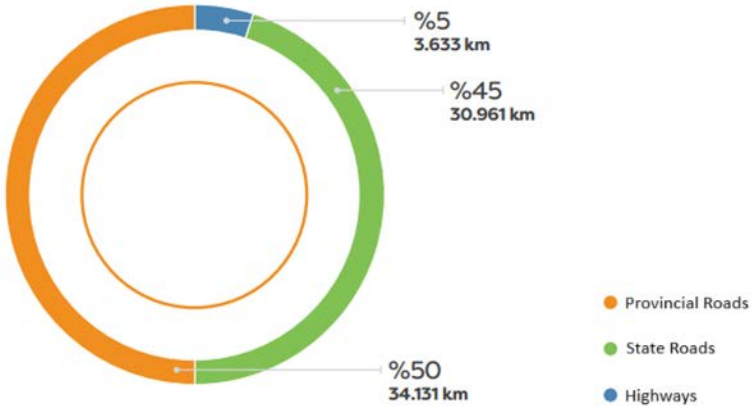

Figure 1. Status of Turkey's Road Network (UAB, 2022)

As shown in Figure 2, road transport is the most preferred mode of passenger and freight transportation in Turkey. As of 2021, 92.7% of domestic passenger transport and 89.4% of freight transport are carried out by road (UAB, 2022).

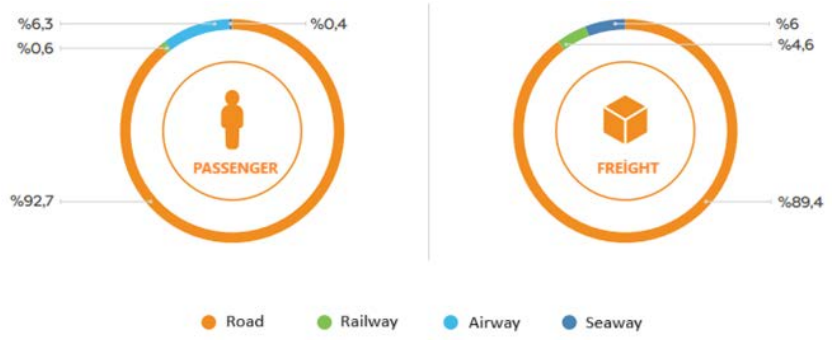

Figure 2. Domestic Passenger and Freight Transport Shares by Mode of Transportation in Turkey (UAB, 2022)

Road transport is the most commonly used mode of transportation for passengers across the EU. However, while 95.2% of passenger transportation in Turkey is by road, this figure is 89% in the US and around 79% in EU

countries. In freight transportation, there is a more balanced distribution between road, rail, and maritime transport. In EU countries, the share of road transport in freight transportation is approximately 45%. In Turkey, this share is 76.1%, and in the US, it is 69.5%. Especially when compared to the share in EU countries, road transport in Turkey dominates other modes of transportation. As shown in Figure 3, road infrastructure, having received more investment, has left other transportation modes relatively weak (Kuscu, 2012).

The EU's transportation policy aims to balance the modes of transportation and promote more sustainable transportation types. Within this framework, increasing the share of rail and maritime transport and reducing the environmental impacts of road transport have been targeted (Kuscu, 2012).

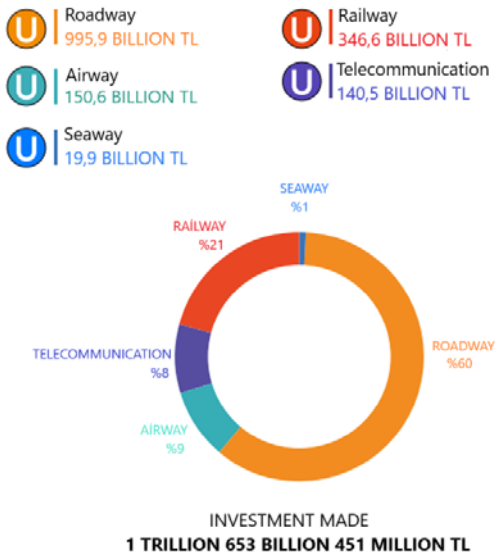

Figure 3. Distribution of Transportation and Communication Investments by Mode from 2003 to 2022 (UAB, 2022)

The EU, in line with its sustainable transportation goals, encourages modes of transport other than road transport to reduce carbon emissions, particularly investing in railway and maritime infrastructure. Additionally, through projects such as the Trans-European Transport Network (TEN-T), it aims to increase the use of environmentally friendly methods in transportation. In light of this data, it is expected that the transportation sector will evolve into a balanced and environmentally friendly structure in the future (Kuscu, 2012). When comparing the infrastructure, investment, and development status of transportation modes in Turkey with the current situation and goals of EU countries, it appears that Turkey is far from achieving these targets. Table 1 compares Turkey's transportation infrastructure status with the European average.

Table 1. Comparison of Total Length/Number of Transportation Modes in Turkey with the European Average

Transportation Mode	Turkey	European Average	Comparison
Road	68,526 km	~100,000 km	Turkey is below the European average.
Rail	13,021 km	~30,000 km	Below the European average.
Air	57 airports	80-100 airports	The number of airports lags behind Europe.
Sea/maritime	172 ports 172 ports Port capacities are insufficient.	200-250 ports High-capacity ports.	The port infrastructure is relatively developed.
Pipelines	~20,000 km	~15,000 km	Turkey is above the European average.

When comparing Turkey with the European average in terms of transportation infrastructure:

- **Road**: Turkey's road network is developing through modernization processes, but in terms of length, it remains below the European average.
- **Rail**: Turkey's railway network is limited, with fewer high-speed train lines compared to Europe.
- **Air**: Although the number of airports is lower than in Europe, Turkey is a significant transit hub for international flights.
- **Sea**: The port infrastructure is strong due to its strategic location, and although the capacity is lower, it is comparable to Europe.
- **Pipelines**: Turkey, being an important energy transportation hub, exceeds the European average.
- **Transportation systems**: When considered as a whole, Turkey lags behind Europe, particularly in terms of combined transport.

3. ACTIONS TO BE TAKEN

Technological innovations are needed to address the weaknesses of Turkey's transportation systems. Solutions such as autonomous vehicle technologies, smart transportation systems, and infrastructure modernization are of critical importance for achieving future transportation goals. Among the weaknesses of Turkey's transportation infrastructure, the lack of integration and inadequate technological infrastructure stand out. In the

future, equipping transportation systems with autonomous technologies and strengthening rail and maritime transport should be prioritized.

When comparing the total lengths of Turkey's transportation infrastructure with European averages, some areas fall short, though improvement efforts are ongoing in line with specific goals. In terms of road networks, Turkey's total length is 65,354 kilometers, of which 7,830 kilometers consist of highways. This highway density is below the European Union average (8.8 km/1,000 km^2), but new projects aim to close this gap.

For railways, Turkey's total network is approximately 13,022 kilometers, but this length is quite limited regarding modern high-speed train lines. While railway transportation plays a more active role in Europe, Turkey should invest in increasing capacity in this sector.

In maritime transportation, despite Turkey's strategic geographical position, efforts are needed to increase port capacity and ensure logistical efficiency. Turkey's current port infrastructure has less capacity compared to Europe's major ports; however, new projects aim to bridge this gap.

In the aviation sector, Turkey is in a more competitive position. Notably, Istanbul Airport's international freight and passenger capacity is comparable to that of Europe's major airports.

Comparative analyses with Europe highlight a lack of holistic and long-term planning in Turkey's transportation infrastructure. Addressing these

deficiencies requires viewing transportation projects not merely as economic tools but as a comprehensive development strategy that supports all sectors.

4. CONCLUSIONS AND RECOMMENDATIONS

The development of transportation infrastructure in Turkey is crucial for the country's economic growth and social cohesion. The increasing demand for transportation and logistics highlights the importance of combined transportation solutions and new international trade routes. Turkey, located at the crossroads of three continents and along historic trade and transportation corridors, holds a strategic position as a bridge. Its location between the production centers of the East and the markets of the West underscores the significance of transit transportation for the country. In this context, international transportation corridors such as Pan-European, TRACECA, and the Belt and Road Initiative should be carefully monitored and leveraged. However, for Turkey to effectively utilize this advantage, it requires a robust physical and legal transportation infrastructure.

Turkey's transportation strategy documents reveal a misalignment between goals and achievements, leading to frequent goal changes and a lack of cohesive planning. The transportation sector has been treated as an isolated field rather than integrated with other sectors, diminishing the efficiency of investments. Given the transportation sector's reciprocal impact on and from the economy, it is essential

to approach it with holistic planning to enhance benefits and maximize societal advantages.

To strengthen Turkey's transportation infrastructure, investments should focus not only on the road network but also on railway, maritime, and air transportation. Addressing the deficiencies compared to Europe would be a significant step toward achieving sustainable development.

Based on the current situation and the necessary actions discussed in this report, it is recommended that Turkey modernize, integrate, and transform its transportation systems into a sustainable structure.

REFERENCES

Alam K.M., Li X, Baig S. Vd. (2020). Causality between transportation infrastructure and economic development in Pakistan: An ARDL analysis, Research in Transportation Economics, 1-12. https://doi.org/10.1016/j.retrec.2020.100974

Erdoğan, H. T. (2016). Ulaşım hizmetlerinin ekonomik kalkınma üzerine etkisi. İstanbul Gelişim Üniversitesi Sosyal Bilimler Dergisi, 3 (1), 187-215. DOI: 10.17336/igusbd.05060.

Kara, M. A. ve Ciğerlioğlu, O. (2018). Türkiye ekonomisinde ulaşım altyapısının ekonomik büyümeye etkisi, Gaziantep University Journal of Social Sciences, 17 (2), 577-591. DOI: 10.21547/jss.382949.

Kuscu, S, 2012. Avrupa Birliği, Avrasya Ulaştırma Politikaları ve Bölge Ekonomilerine Muhtemel Yansımaları. International Conference On Eurasian Economies, Almaty, Kazakhstan.

Lin, W. (2019) Transport geography and geopolitics: Visions, rules and militarism in China's belt and road initiative and beyond. Transport Geography, 81, 102436. Available from: https://doi.org/10.1016/j.jtrangeo.2019.05.001.

Löğün, A., Tüzemen, A. (2018). Türkiye'deki ulaştırma altyapılarının ekonomik büyümeye etkisi: ARDL Sınır Testi Yaklaşımı. Social Sciences Studies Journal (SSSJournal), 27, 5935-5941. DOI : http://dx.doi.org/10.26449/sssj.1046.

Magazzino, C. ve Mele M. (2020). On the relationship between transportation infrastructure and economic development in China, Research in Transportation Economics, 88. https://doi.org/10.1016/j.retrec.2020.100947.

Maparu, T. ve Mazumder, T. (2017). Transport infrastructure, economic development and urbanization in India (1990–2011): ıs there any causal relationship?, Transportation Research Part A, 319-336. https://doi.org/10.1016/j.tra.2017.04.033.

Prus P, and Sikora M., (2021). The Impact of Transport Infrastructure on the Sustainable Development of the Region—Case Study. Agriculture 11(4):279. https://doi.org/10.3390/agriculture11040279.

Telli, R. (2020). Türkiye'de ulaşım altyapısının bölgesel kalkınmaya etkileri, Türk Sosyal Bilimler Araştırmaları Dergisi, 5(1), 53-69. http://tursbad.hku.edu.tr/tr/pub/issue/54074/674254.

Ulaştırma ve Altyapı Bakanlığı (UAB), 2022. "Ulaşan ve Erişen Türkiye 2002-2022", Ankara, Türkiye. https://www.uab.gov.tr/uploads/pages/bakanlik-yayinlari/ulasan-ve-erisen-turkiye-2021.pdf

Wang, C, vd. (2021). Causality between logistics infrastructure and economic development in China, Transport Policy, 100, 49-58. https://doi.org/10.1016/j.tranpol.2020.10.005.

Yurdakul, Elif Meryem. (2022). The Relationship Between the Transportation Infrastructure and Economic

Development of Turkey: ARDL Bound Test, Kent Akademisi Dergisi, 15(2):666-680 https://doi.org/10.35674/kent.105816.

WEIGHT MINIMIZATION OF STEEL SPACE FRAMES USING RAO-1 ALGORITHM

İbrahim Behram UĞUR[1]

1. INTRODUCTION

With the rise in population and rapid urbanization over time, advancements in technology and industry have led to increased demand for diverse structural forms. Structures such as factory buildings, bridges, industrial facilities, sports complexes, aircraft hangars, large warehouses, and workshops have evolved to meet these demands. In the construction of such structures, steel systems are frequently favored due to their homogeneous and isotropic properties, capacity to span wide areas, ease of fabrication, recyclability, and lightweight characteristics.

As structural density continues to increase, optimizing steel systems has become essential to reduce material usage and minimize project costs. Mathematical optimization is the process of finding the maximum or minimum value of a function under specified conditions. Broadly, optimization techniques fall into two categories: classical and heuristic methods. Classical methods typically address problems with continuous variables, but because practical design challenges often involve discrete variables,

[1] Şırnak University, Engineering Faculty, Civil Engineering Department, behramugur@sirnak.edu.tr, ORCID: 0000-0002-0950-4876

heuristic optimization methods inspired by biological processes, evolutionary mechanisms, and natural phenomena are widely applied (Dorigo, Maniezzo, & Colorni, 1996; Goldberg, 1989; Karaboga & Basturk, 2007; Kennedy & Eberhart, 1995; R. V Rao, Savsani, & Vakharia, 2011).

In civil engineering, heuristic optimization methods have proven effective across various domains, including hydraulic structures, retaining walls, water transmission lines, roadway planning, and structural design (Abdelmohsen & El-Rayes, 2018; Chong, Lai, Ahmed, Wan Jaafar, & El-Shafie, 2021; Hasancebi, Carbas, Dogan, Erdal, & Saka, 2009; Shakeel, Azam, Riaz, & Shihata, 2022). In steel structures, achieving optimal design involves selecting the smallest feasible cross-sectional dimensions for structural elements. These dimensions must ensure that the structure can withstand external loads, maintain stability, and adhere to allowable displacement limits. However, optimizing full-scale steel structures presents significant challenges due to the need to comply with regulatory standards, meet strength constraints, and achieve the lightest possible design without compromising safety or functionality.

This study investigates the optimization of steel frame systems subjected to static loads while satisfying all relevant design constraints. The RAO-1 algorithm, a recent metaheuristic optimization technique, was utilized for this purpose. Structural analysis and validation of the optimized designs were performed using SAP2000, a widely used structural analysis software.

2. RAO-1 ALGORITHM

Rao (R. V. Rao, 2020) introduced the RAO algorithm series as a framework to address optimization problems without relying on metaphor-based concepts or algorithm-specific parameters. These algorithms provide a simple and effective approach by iteratively improving solutions based on the best and worst candidates within the population. In this study, the first one (RAO-1) is utilized for the optimization process.

Initially, a random set of candidate solutions is generated to form an initial population. For each iteration, the best and worst candidates are identified based on their performance in meeting the objective. Solutions are iteratively refined by generating new candidate solutions based on random adjustments around the best and worst solutions. The optimization continues until a specified number of iterations or another stopping condition is met.

The formula for updating candidate solutions is:

$$X'_{j,k,i}=X_{j,k,i}+r_1,j,X_{j,best,i}-X_{j,worst,i} \quad (1)$$

where $Xj,best,i$ and $Xj,$worst,i are the best and worst solutions for the j-th variable at iteration i, $X'j,best,i$ represents the refined candidate solution, is a randomly generated coefficient between 0 and 1, ensuring variation in candidate updates. $r1,j$ is randomly generated coefficient between 0 and 1, ensuring variation in candidate updates (R. V. Rao, 2020).

This method effectively directs solutions towards feasible regions in the design space, optimizing with a

balance of exploration and exploitation without the need for additional control parameters.

3. OPTIMUM DESIGN OF SPACE STEEL FRAMES

Structural optimization seeks to identify the lightest feasible design for a space steel frame while ensuring compliance with all design constraints. The optimization problem is framed by grouping members into categories based on structural symmetry, with each group sharing the same cross-sectional properties. The objective is to minimize the total weight of the structure (W), which depends on the material density (γ), cross-sectional areas (A), and member lengths (L) across all groups (NG) as given below:

$$\text{Minimize} \quad W = \sum_{i=1}^{N_g} \left(\gamma_i \cdot A_i \cdot \sum_{j=1}^{N_m} L_j \right) \tag{1}$$

$$\text{Subjected to} \quad g_k \leq 0 \qquad k = 1,2,3 \ldots, N_c \tag{2}$$

The design variables comprise steel profiles selected from a predefined list, and constraints are imposed to ensure structural safety and performance. These constraints include normalized strength criteria for axial and flexural behavior, derived from the Load and Resistance Factor Design (LRFD) (AISC, 2022) specifications as given below:

$$g_{(i,j)} = \frac{P_u}{\phi_c P_n} + \frac{8}{9}\left(\frac{M_{ux}}{\phi_b M_{nx}} + \frac{M_{uy}}{\phi_b M_{ny}}\right) - 1 \leq 0 \text{ for } \frac{P_u}{\phi_c P_n} \geq 0.2 \quad (3)$$

$$g_{(i,j)} = \frac{P_u}{2\phi_c P_n} + \left(\frac{M_{ux}}{\phi_b M_{nx}} + \frac{M_{uy}}{\phi_b M_{ny}}\right) - 1 \leq 0 \text{ for } \frac{P_u}{\phi_c P_n} > 0.2 \quad (4)$$

Strength limits account for axial forces (P_u) and moments along major and minor axes (M_{ux}, M_{uy}), incorporating resistance factors for compression, tension, and bending ($\phi_c, \phi_t\ \phi_b$)

Additionally, structural members must satisfy shear strength requirements, which are governed by the ratio of applied to nominal shear strength (V_n), adjusted with a shear resistance factor (ϕ_v), as given below:

$$g_{(i,j)} = \left(\frac{V_u}{\phi_v V_n}\right) - 1 \leq 0 \quad (5)$$

Beyond strength-based constraints, the design must comply with inter-story drift limits and maximum lateral displacement criteria, ensuring stability and serviceability under loading conditions

$$g_{isd} = \frac{\delta_{isd}}{\delta_{isd,lim}} - 1 \leq 0 \quad (6)$$

$$g_d = \frac{\Delta_{roof}}{\Delta_{r,lim}} - 1 \leq 0 \quad (7)$$

This optimization framework ensures the resulting steel frame designs are both efficient and structurally robust, adhering to established engineering standards.

3.1.SAP2000 Software for Structural Analysis

SAP2000 (Computers & Structures Inc, 2019) is a powerful tool for structural analysis and design, widely used for its advanced capabilities in modeling and simulating structures under static and dynamic loads. Its parametric modeling tools simplify defining and adjusting structural components to meet project needs. The software's Open Application Programming Interface (OAPI) enables seamless integration with programming environments like MATLAB or Python, automating tasks such as model creation, analysis, and result extraction. With its robust analytical tools and user-friendly interface, SAP2000 is a versatile and indispensable resource in modern structural engineering.

3.2.Optimal Design of Space Steel Frames Using the RAO-1 Algorithm

A 135-member braced space frame model from the literature was optimized to assess the performance of heuristic algorithms in designing space steel frames. Structural analyses were conducted using SAP2000, while the optimization process was executed via a MATLAB-based program. Each method was tested 10 times to ensure reliable comparisons, and the results, including the lightest design and the corresponding number of structural analyses, were recorded. Additional metrics such as average weight, worst-case weight, standard deviation, and constraint violation percentages were also

evaluated. The space frame had material properties of an elastic modulus of 20 GPa and a yield strength of 248.2 MPa (Azad, 2014) . Design constraints were based on AISC-LRFD (AISC, 2022) specifications, with geometric constraints for beam-column connections included for further refinement. The optimization process was terminated after a maximum of 625 iterations.

3.3.Three Story 135-Bar Space Frame

The three-story, 135-bar braced space frame, adapted from Azad (Azad, 2014) was used as the initial example for the optimal design of space steel frames. The frame consists of 10 groups of structural members, categorized based on their roles, such as corner columns, edge columns along the *xz* and *xy* planes, interior columns, floor beams, and bracing members. To enhance lateral stiffness, V-shaped braces were included along the *xz* plane.

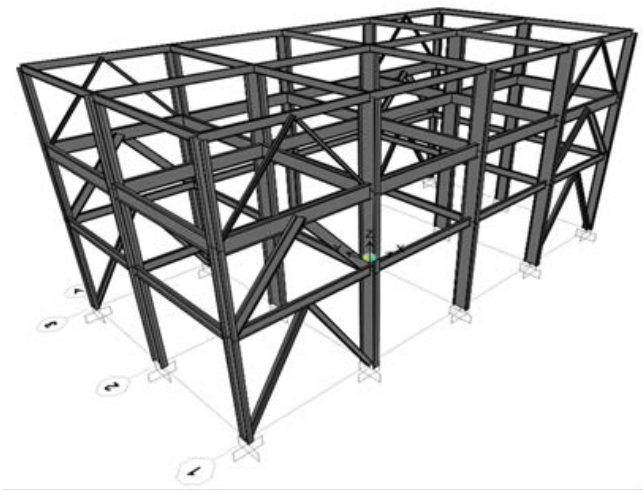

Figure 1. Three Storey 135-bar Steel Frame

The frame was analyzed under 10 load combinations, including dead, live, and seismic loads as follows:

1. 1.4D
2. 1.2D + 1.6 L
3. 1.2D + 1.0E_x +0.5L
4. 1.2D + 1.0E_{ex}+0.5L
5. 1.2D + 1.0E_y+0.5L
6. 1.2D + 1.0E_{ey}+0.5L
7. 0.9D + 1.0Ex
8. 0.9D + 1.0Eex
9. 0.9D + 1.0Ey
10. 0.9D + 1.0Eey

Dead loads for regular and roof beams were set at 20 kN/m and 15 kN/m, respectively, while live loads were 12 kN/m and 7 kN/m. Seismic loads were determined using the equivalent static method outlined in ASCE 7-98, with the base shear distributed across floors based on the structural weight and importance factor. The fundamental period of the frame was estimated using the ASCE 7-98 guidelines, with adjustments made to the structural parameters through linear interpolation. Seismic loads were dynamically updated during optimization to reflect changes in the frame's weight caused by varying design variables. To ensure stability, the effective length factors were set at 1.0 for beams and braces. For columns, these factors were adjusted based on their strong and weak axes as per standard guidelines. Maximum allowable

displacements included a roof displacement limit of 0.03 m and an inter-story drift limit of one-fourth the story height. A rigid diaphragm assumption was applied, ensuring uniform lateral displacements across nodes on the same floor (Azad, 2014).

Table 1. Optimum Design Results for the 135-Bar Braced Space Steel Frame Using RAO -1

	Group	RAO-1
1	KL1	W12×35
2	KL2	W24×68
3	KL3	W24×84
4	KL4	W24×68
5	KR1	W21×44
6	KR2	W21×44
7	KR3	W12×16
8	ÇR1	W8×28
9	ÇR2	W6×15
10	ÇR3	W4×13
Best weight (ton)		**36.92**
Number of Analysis		24852
Mean weight (ton)		43.58
Worst weight (ton)		50.17
Std (ton)		3.97
Constraint Violation (%)		0

The optimization results for the 135-bar braced space steel frame using the RAO-1 algorithm are summarized in Table 1. The RAO-1 algorithm achieved an optimum design with a minimum structural weight of 36.92 tons after performing 24,852 structural analyses. Statistical outcomes derived from 10 independent optimization runs are also presented, including the best, mean, worst weights, and the standard deviation of the resulting designs. The mean structural weight was determined to be 43.58 tons, while the worst case reached 50.17 tons. The standard deviation of 3.97 tons indicates a moderate level of variability in the

optimization outcomes, which reflects the algorithm's robustness in consistently identifying near-optimal solutions across multiple runs.

It is noteworthy that the design achieved by the RAO-1 algorithm adhered strictly to all predefined strength and displacement constraints. The absence of any constraint violations, as shown in Table 1, underscores the reliability of the algorithm in producing feasible designs that satisfy structural performance requirements. To further validate the accuracy of the obtained solution, the optimal design was implemented in SAP2000 software, with results demonstrating full compliance with strength constraints. This is visually confirmed through the color map representation of the strength ratio, as illustrated in Fig. 2.

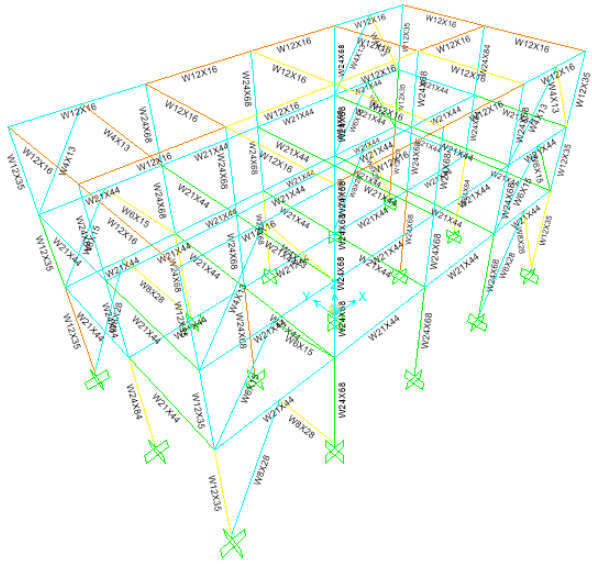

Figure 2. Design verification of the 135-bar steel frame model in SAP2000

The convergence behavior of the RAO-1 algorithm is depicted in Fig. 3, which illustrates the variation in structural weight as a function of the number of structural analyses performed. An initial rapid reduction in weight is observed during the first 3,000 analyses, indicating the algorithm's efficiency in identifying promising design regions early in the optimization process. Beyond this point, the reduction in weight progresses more gradually as the algorithm refines the design, converging steadily toward the global optimum.

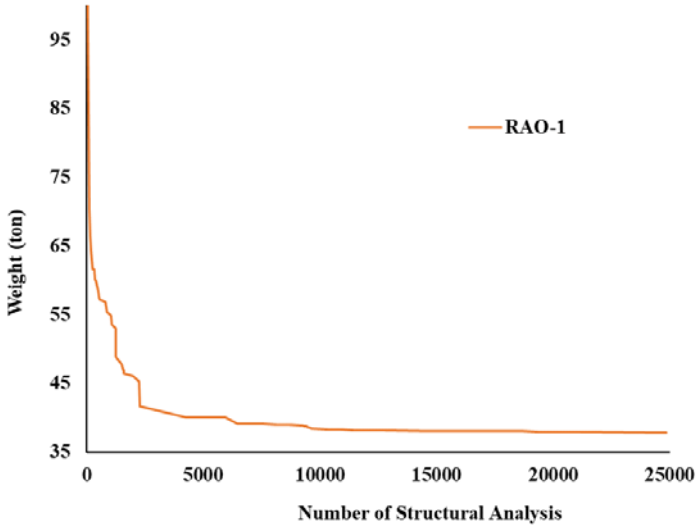

Figure 3. Convergence curve of 135-bar steel frame using RAO-1 algorithm

4. CONCLUSION

This manuscript demonstrates the effective application of the RAO-1 algorithm for the optimal design of a 135-bar braced space steel frame, emphasizing its

simplicity, efficiency, and effectiveness. As a parameterless algorithm, RAO-1 eliminates the need for tuning algorithm-specific parameters, making it easy to implement. The optimization process integrated SAP2000's Open Application Programming Interface (OAPI) with MATLAB, facilitating seamless interaction between structural analysis and optimization tasks. This integration enabled automated structural analysis, design validation, and iterative updates, improving computational efficiency and ensuring accurate results. The RAO-1 algorithm's fast convergence, reliable performance, and straightforward implementation make it a useful tool for structural optimization. Future studies could expand on this research by applying the algorithm to larger structures, exploring multi-objective optimization, and comparing its performance with other emerging metaheuristic algorithms to assess its broader applicability in structural engineering.

5. ADKNOWLEDGEMENT

This study was funded by Sirnak University Scientific Research Projects Coordination Unit (Grant No. 2022.FNAP.06.06.01).

REFERENCES

Abdelmohsen, A. Z., & El-Rayes, K. (2018). Optimizing the Planning of Highway Work Zones to Maximize Safety and Mobility. *Journal of Management in Engineering*, 34(1). Retrieved from https://doi.org/10.1061/(asce)me.1943-5479.0000570

AISC. (2022). American Institute of Steel Construction. *United States of America*.

Azad, S. K. (2014). *Computationally enhanced techniques for practical optimum design of steel structures*. Middle East Technical University.

Chong, K. L., Lai, S. H., Ahmed, A. N., Wan Jaafar, W. Z., & El-Shafie, A. (2021). Optimization of hydropower reservoir operation based on hedging policy using Jaya algorithm. *Applied Soft Computing*. Retrieved from https://doi.org/10.1016/j.asoc.2021.107325

Computers & Structures Inc. (2019). Sap 2000. *Sap 2000*.

Dorigo, M., Maniezzo, V., & Colorni, A. (1996). Ant system: Optimization by a colony of cooperating agents. *IEEE TRANSACTIONS ON SYSTEMS MAN AND CYBERNETICS PART B-CYBERNETICS*, 26(1), 29–41. Retrieved from https://doi.org/10.1109/3477.484436

Goldberg, D. E. (1989). Genetic Algorithms in Search, Optimization, and Machine Learning, Addison-Wesley, Reading, MA, 1989. *NN Schraudolph and J..*, 3.

Hasancebi, O., Carbas, S., Dogan, E., Erdal, F., & Saka, M. P. (2009). Performance evaluation of metaheuristic search techniques in the optimumdesign of real size pin jointed structures. *COMPUTERS & STRUCTURES*, 87(5–6), 284–302. Retrieved from https://doi.org/10.1016/j.compstruc.2009.01.002

Karaboga, D., & Basturk, B. (2007). A powerful and efficient algorithm for numerical function optimization: Artificial bee colony (ABC) algorithm. *Journal of Global Optimization*, 39(3). Retrieved from https://doi.org/10.1007/s10898-007-9149-x

Kennedy, J., & Eberhart, R. (1995). Particle swarm optimization. In *IEEE International Conference on Neural Networks - Conference Proceedings* (Vol. 4). Retrieved from https://doi.org/10.4018/ijmfmp.2015010104

Rao, R. V. (2020). Rao algorithms: Three metaphor-less simple algorithms for solving optimization problems. *International Journal of Industrial Engineering Computations*, 11(1). Retrieved from https://doi.org/10.5267/j.ijiec.2019.6.002

Rao, R. V, Savsani, V. J., & Vakharia, D. P. (2011). Teaching-learning-based optimization: A novel method for constrainedmechanical design optimization problems. *COMPUTER-AIDED DESIGN*, 43(3), 303–315. Retrieved from https://doi.org/10.1016/j.cad.2010.12.015

Shakeel, M., Azam, R., Riaz, M. R., & Shihata, A. (2022). Design Optimization of Reinforced Concrete

Cantilever Retaining Walls: A State-of-the-Art Review. *Advances in Civil Engineering*. Retrieved from https://doi.org/10.1155/2022/4760175

3D PRODUCTION TECHNOLOGIES

Mete Han BOZTEPE[1]

1. INTRODUCTION

A wide variety of structures and complex shapes can be produced in three dimensions with 3D printing. This process involves stacking successive layers of material on top of each other. The origins of this technology began with a technique discovered by Charles Hull in 1986. This technique, known as stereolithography (SLA), was later followed by later developments such as powder bed blending, fused deposition systems (FDM), inkjet printing, and contour machining (CC). 3D technologies have come a long way over the years. The additive manufacturing technique is widely used in different industries, especially construction, prototyping, and biomechanics. It has significantly reduced the waste of waste materials, especially in the construction sector (Ngo et al., 2018).

In other words, 3D printing technology has emerged as a versatile technology platform for computer-aided design (CAD) and rapid production. Thanks to this technique, unlike older production methods, it allows production from metals, polymers, and ceramics without the need for molding or machining. Today, since the prices

[1] Dr.Öğr.Üyesi, Şırnak Üniversitesi Mühendislik Fakültesi Makine Mühendisliği Bölümü, metehanboztepe@sirnak.edu.tr, ORCID: 0000-0001-8418-1352

of 3D printers have fallen, it is possible to produce even on the desktop at home. Just as the development of digital 2D printing together with desktop publishing revolutionized communication and information technology, the development of AM technologies together with the "internet of things" has revolutionized the computer-guided production of both complex objects and multifunctional material systems. Additive manufacturing is inherently much faster than traditional manufacturing and enables rapid prototyping (Ligon et al., 2017).

3D manufacturing technology is built on three main principles: universal, practical, and efficient. The ability to print from anywhere in the world with 3D printing is a testament to how universal it is. It is now possible to 3D print anything you desire. Seeing your food come out of a printer is not a far-fetched scenario (Bandyopadhyay & Heer, 2018).

This innovative technology has the potential to change the way we both design and consume products. The ability to design a part anywhere and everywhere using 3D printing equipment can be interpreted as the realization of this assumption (Babu et al., 2015).

Three-dimensional additive manufacturing has fundamentally transformed the landscape of manufacturing, thereby facilitating the emergence of novel solutions across a multitude of sectors. With prospective advancements on the horizon, it appears likely that the production of increasingly intricate and functionally sophisticated structures will become feasible.

2. METHODS

2.1. Principles and Technologies of 3D Printers

3D printers add materials layer by layer to create a physical object from a digital model. Each layer can be thought of as a thin slice of the object. These printers usually operate using a thermoplastic extruder and a Cartesian XYZ platform. With materials such as PLA filament, they can produce physical objects with high precision (100 microns or 0.1 mm) and at low cost (Mishra & Srivastava, 2021; Pathade et al., 2015; Shahrubudin et al., 2019).

3D printer technologies create objects using a variety of methods and materials. These technologies include;

2.1.1. Vat Photopolymerization

Vat photopolymerization (VP) is one of the 3D printing techniques and the desired product is obtained by curing liquid polymers with light. The biggest advantages of this method are high precision and printing speed. In this way, it has found its place in both industrial applications and academic fields. There are different techniques for vat photopolymerization. These include stereolithography (SLA), digital light processing (DLP) and continuous digital light processing (CDLP). The basis of these production technologies is based on the technique of UV light hardening the resin used. In this way, layer-by-layer structures are created and the final product is obtained. Among these, DLP has become the most preferred technology (Andreu et al., 2021; Pagac et al., 2021). The

schematic view of a 3D printer with SLA technology is shown in Figure 1.

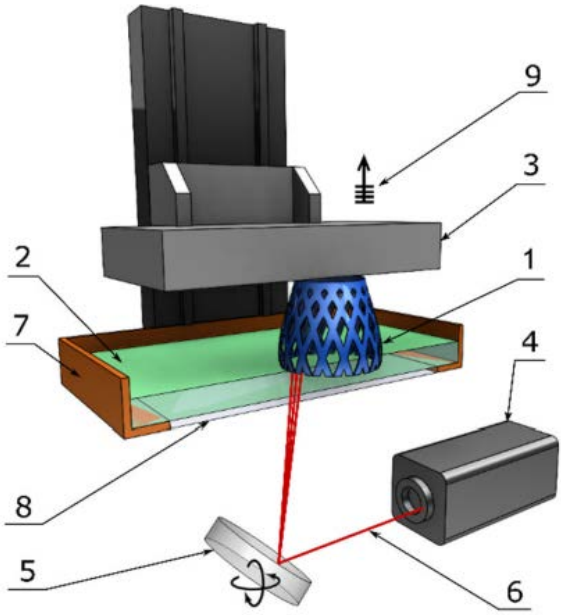

Figure 1. Components of a typical SLA machine: 1-printed part, 2-iquid resin, 3-building platform, 4-UV laser source, 5-XY scanning mirror, 6-laser beam, 7-resin tank, 8-window, and 9-layer-by-layer elevation (Pagac et al., 2021)

The following sections summarize the advantages and disadvantages of this technology.

- **Advantages of Vat Photopolymerization**

High Resolution and Speed: The use of VP facilitates the accelerated production of complex architectures characterized by intricate details required in medical contexts, including tissue engineering and prosthetic development (Li et al., 2024).

Material Versatility: The technology accommodates a wide range of materials, encompassing biocompatible and bio-functional compounds that can be tailored to meet specific medical requirements (Timofticiuc et al., 2024).

Complex Geometries: VP technology can manufacture structures with complex geometries that are difficult to produce (Shebeeb et al., 2023).

- **Disadvantages of Vat Photopolymerization**

Material Limitations: The limited choice of biocompatible materials that can be used in VP complicates the application of this technology in the pharmaceutical field (Graça et al., 2024).

Mechanical Weakness: Structures produced with VP may require the addition of graphene as a filler material because they have a wrinkled structure (Shebeeb et al., 2023).

Process Challenges: Problems such as high viscosity, generally encountered in ceramic material production, cause low printing speeds and dimensional errors.

2.1.2. Powder Bed Fusion

Powder Bed Fusion (PBF) is an additive manufacturing technology that produces 3D objects. Here, powder materials are combined layer by layer with the help of an energy source to obtain the final product. This technology is widely used in the production of materials such as metals, ceramics and polymers. Thanks to this technique, it allows the use of different materials to create 3D structures. It is ideal for industrial applications and is open to development. However, studies in this area are still in their early stages and many fundamental questions

remain unanswered. (Dzogbewu & de Beer, 2023; Mehrpouya et al., 2022). A schematic view of powder bed fusion is given in Figure 2 (web).

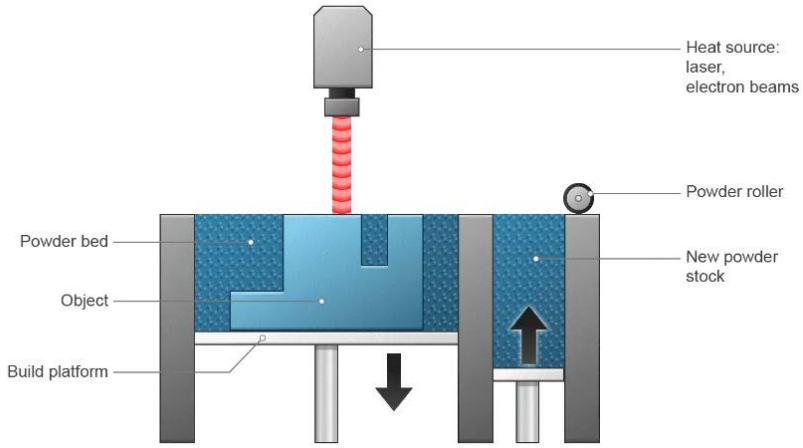

Figure 2. A schematic image of PBF

Powder Bed Fusion (PBF) is used in various industrial applications. While it stands out with its design flexibility and efficiency, high initial installation costs are still a problem.

- **Advantages of Powder Bed Fusion**

Design Flexibility: With the Powder Bed Fusion (PBF) technique, structures with complex geometries can be achieved (Bernsmann et al., 2023).

Precision and Quality: In parallel with the developments in laser technology, the precision and accuracy of PBF technologies have increased (Hedric, 2024).

Reduced Material Waste: In this technology, unused powder materials are reused, contributing to cost reduction (Nichols, 2021)

- **Disadvantages of Powder Bed Fusion**

High Costs: Initial investment costs are high (Bernsmann et al., 2023).

Thermal Stress and Cracks: Thermal differences between different materials can cause cracks (Dzogbewu & de Beer, 2023).

Mechanical Limitations: Ceramic materials, such as alumina, exhibit lower mechanical performance (Abdelmoula et al., 2024).

Although Powder Bed Fusion (PBF) is a method that offers high flexibility in production, its implementation costs are quite high. Future studies can focus on strategies to reduce costs and make processes more efficient so that this technology can be used more widely in different industrial sectors.

2.1.3. Material Extrusion (FDM)

Fused Deposition Modeling (FDM) is one of the additive manufacturing methods. It is a technique of combining a meltable material, such as thermoplastic, layer by layer by passing it through a nozzle. This method uses a variety of materials, from fiber-reinforced cementitious materials to polymers and metals. Screw and piston extrusion methods are commonly used for cementitious materials. For polymers, techniques such as Material Extrusion (ME) or Fused Deposition Modeling® (FDM) create objects by depositing molten polymer filaments layer by layer onto a surface (Mackay, 2018; Perrot et al., 2019). The basic components of material extrusion are given in Figure 3 (Shah et al., 2019).

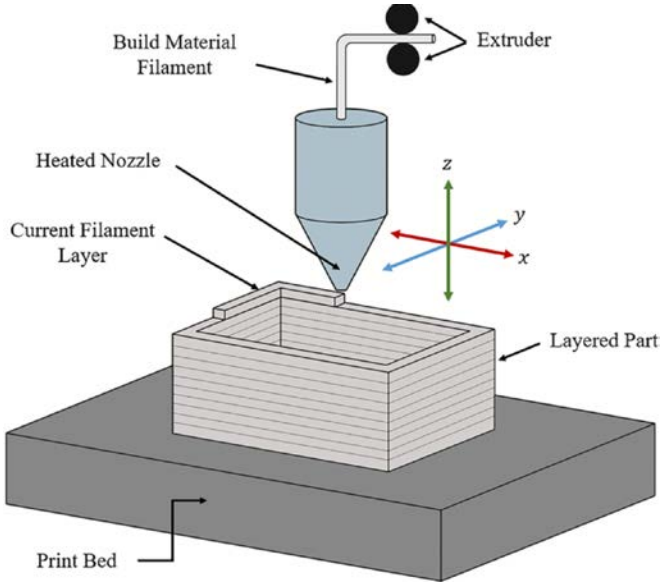

Figure 3. Basic working principle of material extrusion printing

FDM is additive manufacturing and has some advantages and disadvantages. Some of them are as follows.

- **Advantages of Material Extrusion**

Cost Effectiveness: This technique is more economical than other joint manufacturing methods. Therefore, it has a wide range of applications (Al-Tamimi et al., 2023; Boulaala et al., 2020).

Design Flexibility: This method allows for structures with complex designs, especially in aerospace and medical (Jiang et al., 2020).

Material Diversity: This method can also use biodegradable materials such as PLA (Tümer & Erbil, 2021).

- **Disadvantages of Material Extrusion**

Mechanical Limitations: They have lower mechanical properties than products obtained by traditional methods (Tümer & Erbil, 2021).

Material Limitations: Printable polymer materials are limited (Jiang et al., 2020).

Porosity: Pores may occur during the consolidation of the material. This may negatively affect the mechanical properties (Al-Tamimi et al., 2023).

Although this method of production offers significant advantages, it needs research and development due to reasons such as low mechanical properties and poor surface quality

2.1.4. Material Jetting

Another 3D additive manufacturing technology is material jetting. This production method enables production through the polymerization of liquid photopolymers. This innovative production method provides perfect dimensional accuracy and minimal surface roughness. Due to these superior properties, it is suitable for use in sectors such as biomedical, dentistry, manufacturing, and aerospace

In this technique, liquid material jetting and UV curing are performed in a single process. This allows multi-component materials to be produced. It can also be produced with both rigid and flexible photopolymers (Tee et al., 2020). This allows for the production of complex geometries at micro scales (Sun et al., 2022). The material jetting technique is an environmentally friendly

technology. It minimizes material waste in the creation of complex structures (Nagarajan et al., 2018).

This technique develops dental solutions and provides specific requirements for each patient. It is also used in microelectronic packaging and ceramic manufacturing areas (Salmi, 2021; Sun et al., 2022).

The mechanical properties of the parts produced vary depending on the reinforcement materials and components. Rigid reinforcement elements increase the strength, while flexible reinforcement elements act as a site for crack initiation. The printing parameters have an impact on both the dimensional accuracy and mechanical properties of the final product. The direction of the printing and the alignment of the reinforcement elements affect the durability of the material (Tee et al., 2020; Yap et al., 2017). A general schematic representation of material jetting is given in Figure 4 (Gülcan et al., 2021).

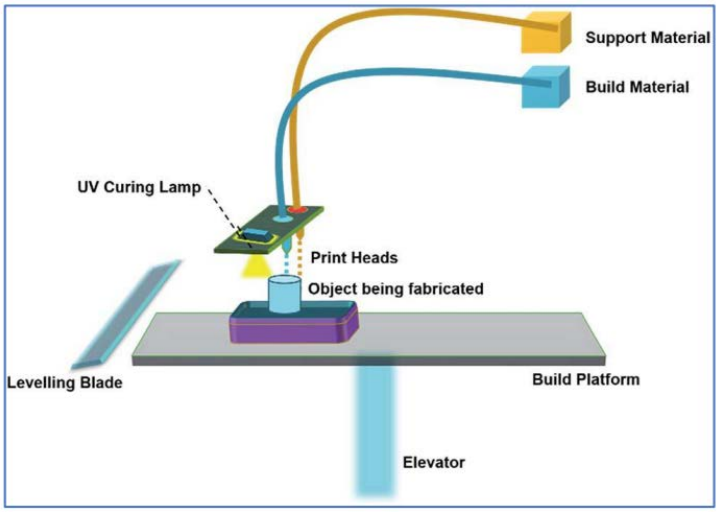

Figure 4. A schematic representation of MJ

Material spraying, a 3D manufacturing method, has distinct advantages and disadvantages that have significant impacts in different industries. This technology has the potential to make manufacturing processes more efficient and improve material performance. However, various challenges can be encountered in terms of material adhesion and compatibility. The positive and negative aspects of this method can be summarized as follows.

- **Advantages of Metarial Jetting**

Economic Viability: Deposition of metals on 3D printed polymers facilitates rapid fabrication of complex geometries, thus offering a cost-effective alternative to traditional direct metal printing (Ramaraju & Chandra, 2022).

Wide Range of Materials: It has the ability to interact with a range of alloys and composites (Li et al., 2018).

Design Flexibility: The application of additive manufacturing methodologies facilitates the realization of complex designs while simultaneously minimizing waste, thus making it highly suitable for various applications, including energy conversion systems (Hüner et al., 2022)

- **Disadvantages of Metarial Jetting**

Material Restrictions: Compatibility of sprayed materials with underlying substrates may limit the scope of application and require extensive testing (Hüner et al., 2022).

Surface Roughness: The resulting surface roughness after spraying can exhibit high levels, potentially requiring additional processing (Vo & Martin, 2017).

Limited Part Geometry: There are constraints in the production of components, especially those characterized by thin walls or complex geometric configurations.

3. CONCLUSION

Additive manufacturing technologies have revolutionized manufacturing processes, offering advantages such as design freedom, speed and efficiency. While Vat Photopolymerization stands out for its high resolution and the production of complex geometries, it also has disadvantages such as limited material diversity and mechanical durability challenges. Powder Bed Fusion is ideal for high performance materials such as metals and ceramics, but energy density and surface quality issues are problems that need to be improved. Material Extrusion offers low-cost production, but has structural strength limitations due to anisotropic properties. Material Spraying offers advantages in terms of multi-material production and high precision, but adhesion issues and material limitations are obstacles to be solved.

All these technologies are important building blocks of the modern manufacturing industry, with features that address different needs. In the future, advances in materials science, software algorithms and energy use are expected to make these methods more efficient, environmentally friendly and accessible. This flexible nature of manufacturing processes will continue to provide innovative solutions in a wide range of applications, from personalized products to large-scale industrial applications.

REFERENCES

Abdelmoula, M., Küçüktürk, G., Juste, E., & Petit, F. (2024). Enhancing powder bed fusion of alumina ceramic material: a comprehensive study from powder tailoring to mechanical performance evaluation. The International Journal of Advanced Manufacturing Technology, 131(3), 1745-1767. https://doi.org/10.1007/s00170-024-13158-x

Al-Tamimi, A. A., Tlija, M., Abidi, M. H., Anis, A., & Abd Elgawad, A. E. E. (2023). Material Extrusion of Multi-Polymer Structures Utilizing Design and Shrinkage Behaviors: A Design of Experiment Study. Polymers, 15(12).

Andreu, A., Su, P.-C., Kim, J.-H., Ng, C. S., Kim, S., Kim, I., Lee, J., Noh, J., Subramanian, A. S., & Yoon, Y.-J. (2021). 4D printing materials for vat photopolymerization. Additive Manufacturing, 44, 102024. https://doi.org/https://doi.org/10.1016/j.addma.2021.102024

Babu, S. S., Love, L., Dehoff, R., Peter, W., Watkins, T. R., & Pannala, S. (2015). Additive manufacturing of materials: Opportunities and challenges. MRS Bulletin, 40(12), 1154-1161. https://doi.org/10.1557/mrs.2015.234

Bandyopadhyay, A., & Heer, B. (2018). Additive manufacturing of multi-material structures. Materials Science and Engineering: R: Reports, 129, 1-16.

https://doi.org/https://doi.org/10.1016/j.mser.2018.04.001

Bernsmann, J.-S. L., Hillebrandt, S., Rommerskirchen, M., Bold, S., & Schleifenbaum, J. H. (2023). On the Use of Metal Sinter Powder in Laser Powder Bed Fusion Processing (PBF-LB/M). Materials, 16(16), 5697. https://www.mdpi.com/1996-1944/16/16/5697

Boulaala, M., Elmessaoudi, D., Buj-Corral, I., El Mesbahi, J., Ezbakhe, O., Astito, A., El Mrabet, M., & El Mesbahi, A. (2020). Towards design of mechanical part and electronic control of multi-material/multicolor fused deposition modeling 3D printing. The International Journal of Advanced Manufacturing Technology, 110(1), 45-55. https://doi.org/10.1007/s00170-020-05847-0

Dzogbewu, T. C., & de Beer, D. (2023). Powder Bed Fusion of Multimaterials. Journal of Manufacturing and Materials Processing, 7(1), 15. https://www.mdpi.com/2504-4494/7/1/15

Graça, A., Bom, S., Martins, A. M., Ribeiro, H. M., & Marto, J. (2024). Vat-based photopolymerization 3D printing: From materials to topical and transdermal applications. Asian Journal of Pharmaceutical Sciences, 19(4), 100940. https://doi.org/https://doi.org/10.1016/j.ajps.2024.100940

Gülcan, O., Günaydın, K., & Tamer, A. (2021). The State of the Art of Material Jetting—A Critical Review. Polymers, 13(16).

Hedric, W. (2024). Laser Powder Bed Fusion: Exploring Recent Technological Breakthroughs and Alloy Utilization. In Preprints: Preprints.

Hüner, B., Kıstı, M., Uysal, S., Uzgören, İ. N., Özdoğan, E., Süzen, Y. O., Demir, N., & Kaya, M. F. (2022). An Overview of Various Additive Manufacturing Technologies and Materials for Electrochemical Energy Conversion Applications. ACS Omega, 7(45), 40638-40658. https://doi.org/10.1021/acsomega.2c05096

Jiang, Z., Diggle, B., Tan, M. L., Viktorova, J., Bennett, C. W., & Connal, L. A. (2020). Extrusion 3D Printing of Polymeric Materials with Advanced Properties. Advanced Science, 7(17), 2001379. https://doi.org/https://doi.org/10.1002/advs.202001379

Li, W., Yang, K., Yin, S., Yang, X., Xu, Y., & Lupoi, R. (2018). Solid-state additive manufacturing and repairing by cold spraying: A review. Journal of Materials Science & Technology, 34(3), 440-457. https://doi.org/https://doi.org/10.1016/j.jmst.2017.09.015

Li, Y., Sheng, P., Lin, L., Wang, L., Lu, D., Lin, K., Wu, H., & Wu, S. (2024). Vat Photopolymerization versus Conventional Colloidal Processing Methods in Structural Ceramics: Progress, Challenges, and Future Perspectives. Additive Manufacturing Frontiers, 3(1), 200110. https://doi.org/https://doi.org/10.1016/j.amf.2024.200110

Ligon, S. C., Liska, R., Stampfl, J., Gurr, M., & Mülhaupt, R. (2017). Polymers for 3D Printing and Customized Additive Manufacturing. Chemical Reviews, 117(15), 10212-10290. https://doi.org/10.1021/acs.chemrev.7b00074

Mackay, M. E. (2018). The importance of rheological behavior in the additive manufacturing technique material extrusion. Journal of Rheology, 62(6), 1549-1561. https://doi.org/10.1122/1.5037687

Mehrpouya, M., Tuma, D., Vaneker, T., Afrasiabi, M., Bambach, M., & Gibson, I. (2022). Multimaterial powder bed fusion techniques. Rapid Prototyping Journal, 28(11), 1-19. https://doi.org/10.1108/RPJ-01-2022-0014

Mishra, A., & Srivastava, V. (2021, 2021//). Effect and Use of 3D Printers Technologies. Advances in Mechanical Engineering, Singapore.

Nagarajan, B., Eufracio Aguilera, A. F., Wiechmann, M., Qureshi, A. J., & Mertiny, P. (2018). Characterization of magnetic particle alignment in photosensitive polymer resin: A preliminary study for additive manufacturing processes. Additive Manufacturing, 22, 528-536. https://doi.org/https://doi.org/10.1016/j.addma.2018.05.046

Ngo, T. D., Kashani, A., Imbalzano, G., Nguyen, K. T. Q., & Hui, D. (2018). Additive manufacturing (3D printing): A review of materials, methods, applications and challenges. Composites Part B:

Engineering, 143, 172-196. https://doi.org/https://doi.org/10.1016/j.compositesb.2018.02.012

Nichols, M. R. (2021). The pros & cons of powder bed fusion. Metal Powder Report, 76(2), 90-91. https://doi.org/10.1016/j.mprp.2020.04.004

Pagac, M., Hajnys, J., Ma, Q.-P., Jancar, L., Jansa, J., Stefek, P., & Mesicek, J. (2021). A Review of Vat Photopolymerization Technology: Materials, Applications, Challenges, and Future Trends of 3D Printing. Polymers, 13(4), 598. https://www.mdpi.com/2073-4360/13/4/598

Pathade, H., Kulkarni, P. C., & Thokale, M. (2015). 3D printing technology. International Journal of Multidisciplinary Research and Development, 2, 351-358.

Perrot, A., Rangeard, D., Nerella, V. N., & Mechtcherine, V. (2019). Extrusion of cement-based materials - an overview. RILEM Technical Letters, 3(0), 91-97. https://doi.org/10.21809/rilemtechlett.2018.75

Ramaraju, R. g. v., & Chandra, S. (2022). Additive Manufacturing by Thermal Spray Deposition of Metals on 3D-Printed Polymer Substrates. https://doi.org/10.31399/asm.cp.itsc2022p0607

Salmi, M. (2021). Additive Manufacturing Processes in Medical Applications. Materials, 14(1).

Shah, J., Snider, B., Clarke, T., Kozutsky, S., Lacki, M., & Hosseini, A. (2019). Large-scale 3D printers for additive manufacturing: design considerations and

challenges. The International Journal of Advanced Manufacturing Technology, 104, 1-15. https://doi.org/10.1007/s00170-019-04074-6

Shahrubudin, N., Lee, T. C., & Ramlan, R. (2019). An Overview on 3D Printing Technology: Technological, Materials, and Applications. Procedia Manufacturing, 35, 1286-1296. https://doi.org/https://doi.org/10.1016/j.promfg.2019.06.089

Shebeeb, C. M., Afif, M. B., Jacob, L., Choi, D., & Butt, H. (2023). Vat photopolymerisation 3D printing of graphene-based materials. Virtual and Physical Prototyping, 18(1), e2276250. https://doi.org/10.1080/17452759.2023.2276250

Sun, C., Chu, X., Chen, J., Chen, D., Ren, J., & Yuan, S. (2022). The jetting process and spreading characteristics of the power-law fluids for material jetting process. Smart Materials and Structures, 31(11), 115029. https://doi.org/10.1088/1361-665X/ac9bad

Tee, Y. L., Tran, P., Leary, M., Pille, P., & Brandt, M. (2020). 3D Printing of polymer composites with material jetting: Mechanical and fractographic analysis. Additive Manufacturing, 36, 101558. https://doi.org/https://doi.org/10.1016/j.addma.2020.101558

Timofticiuc, I.-A., Călinescu, O., Iftime, A., Dragosloveanu, S., Caruntu, A., Scheau, A.-E., Badarau, I. A., Didilescu, A. C., Caruntu, C., & Scheau, C. (2024).

Biomaterials Adapted to Vat Photopolymerization in 3D Printing: Characteristics and Medical Applications. Journal of Functional Biomaterials, 15(1), 7. https://www.mdpi.com/2079-4983/15/1/7

Tümer, E. H., & Erbil, H. Y. (2021). Extrusion-Based 3D Printing Applications of PLA Composites: A Review. Coatings, 11(4).

Vo, P., & Martin, M. (2017). Layer-by-Layer Buildup Strategy for Cold Spray Additive Manufacturing. ITSC2017,

web powder bed fusion. https://www.3ds.com/make/guide/process/powder-bed-fusion.

Yap, Y. L., Wang, C., Sing, S. L., Dikshit, V., Yeong, W. Y., & Wei, J. (2017). Material jetting additive manufacturing: An experimental study using designed metrological benchmarks. Precision Engineering, 50, 275-285. https://doi.org/https://doi.org/10.1016/j.precisioneng.2017.05.015

NON-TRADITIONAL MACHINING METHODS

Mete Han BOZTEPE[1]

1. INTRODUCTION

With the developing technology, non-traditional production methods have emerged and found a place for themselves in industrial applications. The process that accelerated the development of non-traditional production was the limits encountered in traditional production. Traditional manufacturing techniques generally face problems such as low flexibility and high costs. On the other hand, non-traditional production methods have some advantages such as very flexible production and low costs (Berman, 2012).

Non-traditional manufacturing methods have high sustainability. They provide environmentally friendly production by significantly reducing material waste compared to traditional methods. For example, products are built layer by layer in a 3D printer, using only the necessary materials. This significantly reduces waste (Ford & Despeisse, 2016).

Non-traditional manufacturing methods mainly include mechanical, chemical, electrochemical and thermal

[1] Dr.Öğr.Üyesi, Şırnak Üniversitesi Mühendislik Fakültesi Makine Mühendisliği Bölümü, metehanboztepe@sirnak.edu.tr, ORCID: 0000-0001-8418-1352

manufacturing techniques. This provides flexibility and high precision in the production of complex geometry parts (Brasil, Moura, & Rocha Neto, 2019; Ikumapayi et al., 2023; Snoeys, Staelens, & Dekeyser, 1986)

2. METHODS

2.1. Mechanical Processes

2.1.1. Ultrasonic Machining (USM)

One of the traditional manufacturing methods is the ultrasonic machining (USM) method. With this method, it has become possible to process brittle and hard materials such as ceramics, glass and titanium. Since high temperatures are not released in this method, there is no damage or permanent stress on the part. Due to these superior features, it is frequently preferred in industrial applications (K, Kuriachen, & Mathew, 2021; Kumar, 2013; Singh & Khamba, 2006).

In this method of production, abrasive particles are used and the chip is removed by direct impact on the workpiece. These particles strike the workpiece under the action of the tool moving with ultrasonic vibrations, creating micro-cracks and causing the material to break off in small pieces (K et al., 2021; Kataria & Kumar, 2016). This method makes it possible to remove material without thermal damage or permanent stress to the workpiece (Goswami & Chakraborty, 2015; Singh & Khamba, 2006). Figure 1 shows the basic elements of an USM (Singh & Khamba, 2006)

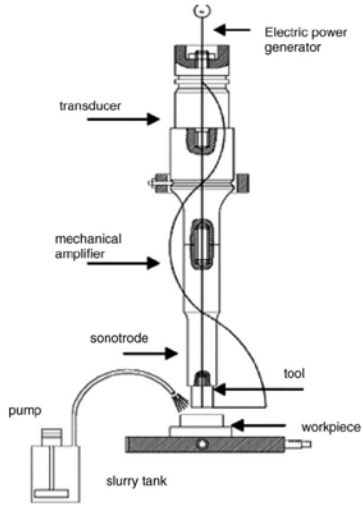

Figure 1. Basic elements of an USM

In the USM method, material removal rate (MRR) and tool wear rate depend on various parameters used. In addition, these parameters affect the surface quality of the workpiece. These important process parameters include ultrasonic vibration amplitude, vibration frequency, the size of the abrasive particles used, the static load exerted by these particles on the workpiece, etc.(Das, Kumar, Kibria, Doloi, & Bhattacharyya, 2020; Lalchhuanvela, Doloi, & Bhattacharyya, 2012). For example, increasing the vibration amplitude and frequency can increase the material removal rate by enabling faster and higher material removal. However, the diameter of the abrasive particles and their concentration in the abrasive fluid used also play an important role, as larger particle sizes and a more concentrated abrasive content can positively or negatively affect the final surface finish remaining on the surface of the workpiece. By optimizing MRR and tool wear problems,

surface quality can be improved (Lalchhuanvela et al., 2012).

During the USM process, tools are worn due to abrasive slurry and high frequency. This wear increases the processing time and costs. The wear rate depends on the material structure of the tool used, the strength of the abrasive slurry and ultrasonic vibration. Tools made of more durable materials have better wear resistance and higher process efficiency. The size of the abrasive particles used is another factor affecting wear. For all the reasons, appropriate material and abrasive slurry should be selected to increase the durability of the tools used in the USM process (K et al., 2021; Singh & Khamba, 2009).

Since high heat is not released in the USM method, there is no thermal damage on the part and no residual stress is created. This feature is a feature that is superior to traditional methods. It is advantageous to process especially sensitive and brittle parts with this method (Goswami & Chakraborty, 2015; Singh & Khamba, 2006). However, USM also has some limitations. For example, the processing time is longer than other methods. Because the material removal process is a slow process. In addition, wear may occur on the tool due to abrasive slurry and ultrasonic vibrations. This requires more frequent tool changes and increases costs (Kumar, 2013; Sabareesan, Vasudevan, Sridhar, Kannan, & Sankar, 2021).

In summary, USM is a very good method for processing hard and brittle materials. During chip removal, factors such as process parameters and tool wear determine

the quality and efficiency of the process. It is also preferred because there is no thermal damage during the process

2.1.2. Water Jet Machining (WJM)

Another non-traditional production method is water jet machining (WJM) technology. In this process, the material is processed with the help of pressurized water. This technique offers many advantages over traditional processing methods. Material processing with this technique is used in many sectors.

The working principle of WJM is based on the principle of passing high-pressure water through a narrow nozzle. The water gains high speed as it passes through this nozzle and hits the material at high speed. This ensures that the material is cut by erosion (Jagadish & Gupta, 2020).

The parameters used during the WJM process affect the precision and efficiency of cutting. These parameters include; water pressure, nozzle exit speed, amount of abrasive particles and distance between the nozzle and the workpiece. Optimizing these parameters are the basic factors that determine efficiency (Gostimirovic, Pucovsky, Sekulic, Rodic, & Pejic, 2019; Ozcan, Tunc, Kopacka, Cetin, & Sulitka, 2021). Figure 2 shows the WJM system and the main parts of which it is composed (El-Hofy, 2005).

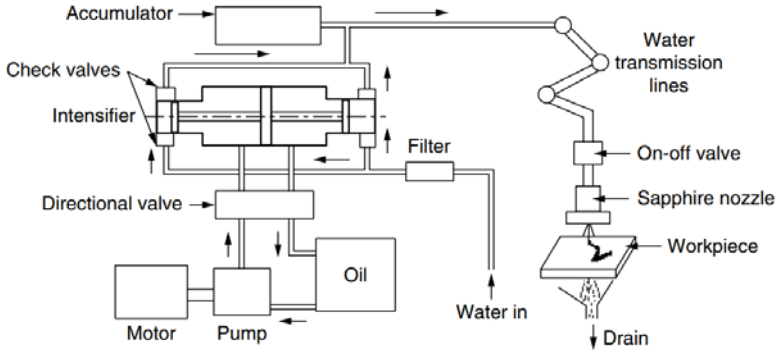

Figure 2. Schematic illustration of WJM system

AWJM is a variation of WJM and works by adding abrasive particles to the water. In this way, the particles gain momentum in the water and enable cutting of much harder materials. With the AWJM technique, operations such as drilling and surface cleaning can be performed on the material (Rao, 2011).

In the WJM process, there is no physical contact with the material during the cutting process. Thanks to this feature, both the risk of deformation in the material is reduced and thermal damage does not occur. It allows the processing of delicate parts compared to traditional manufacturing methods. However, WJM has some disadvantages. For example, the drilling process does not occur instantly, which can increase the processing time. In addition, the initial installation costs of this system can be high for small and medium-sized businesses (Geren, Bayramoğlu, & Eşme, 2007).

Both WJM and AWJM are used in many areas such as aerospace and automotive. This is because this method offers greater flexibility to process high-quality materials

compared to traditional manufacturing methods (Gostimirovic et al., 2019; Ozcan et al., 2021).

In conclusion, WJM technology is a technology that uses high-pressure water. It is possible to process harder materials by adding abrasive particles to water. This system has a wide range of applications, especially in engineering fields such as aerospace and automotive.

2.2. Chemical Processes

2.2.1. Chemical Milling (CM)

Chemical milling is one of the non-traditional production methods and the process is carried out chemically. This process starts with a controlled chemical reaction acting on the surface of the material and unwanted material is removed from the surface. This method is especially suitable for parts requiring precise shaping. Minimum stress occurs compared to mechanical methods. It is also an effective method for obtaining complex geometries and fine details.

Chemical milling is a method in which mechanical energy initiates chemical reactions. In this way, the chemical reaction on the material accelerates and ensures the removal of unwanted parts (McCormick & Froes, 1998). Figure 3 shows the chemical milling system and the main parts of which it is composed (El-Hofy, 2005).

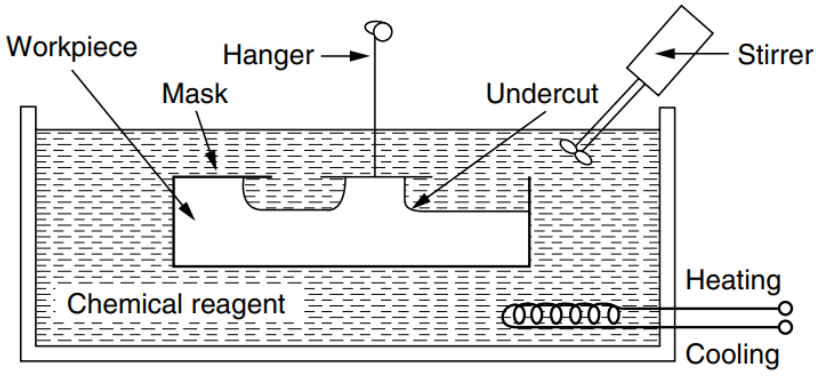

Figure 3. Schematic illustration of chemical milling system

In the chemical milling process, more chemical reactions take place to remove the material. This process accelerates solid state diffusion. In addition, various reactions can occur between chemical liquids and the material (Lukin et al., 2019).

In this process, reaction parameters must be controlled. In particular, control of values such as temperature and pressure affects reaction rate. In new devices, mechanochemical reactivity is increased using controlled heating programs, thus reducing energy and time costs (Cindro, Tireli, Karadeniz, Mrla, & Užarević, 2019).

Real-time monitoring of chemical milling reactions helps to understand the mechanism in more detail. Techniques such as high-energy X-ray diffraction can directly monitor reaction profiles, formation of intermediates, and structure transformations. This plays a critical role in better understanding the dynamic nature of mechanochemical processes and reaction rates (Friščić et al., 2013).

This method is especially used to improve the solubility of poorly soluble drugs. This makes drugs more useful by changing their particle size, surface area and shape. It is also an effective method for the production of advanced materials such as metal-organic frameworks (Friščić et al., 2013; Loh, Samanta, & Sia Heng, 2015).

Electrochemical milling is similar to chemical milling. The only difference is that electric current is used throughout the process. This method is especially used for machining complex and delicate parts (Hinduja & Pattavanitch, 2016).

As a result, chemical milling is a production method that combines mechanical energy and chemical reactions. Real-time monitoring, heat, pressure control, electrochemical methods ensure that this process is efficient. It is also used in many areas from the pharmaceutical industry to the production of advanced products.

2.2.2. Photochemical Milling (PCM)

Photochemical milling (PCM) is a method in which parts are removed from the surfaces of materials using light and chemical reactions. With this process, thin, delicate and complex structures can be processed. Unlike traditional milling methods, the material is processed by light and chemical methods.

Thanks to this method, unwanted parts can be removed from the surfaces of materials such as aluminum, copper, steel, titanium, ceramics and some plastics and processed. It also allows the processing of thin and complex parts. PCM is widely used in industries such as electronics,

automotive, aviation, and medicine. It is ideal for high hardness or brittle materials and produces less stress and heat than conventional machining methods. Photochemical machining allows for low cost, fast delivery and flexible design changes. In addition, since the tools are produced by photographic techniques, it is a great advantage that patterns can be easily reproduced (El-Hofy, 2005). Figure 4 shows the main steps of photochemical machining.

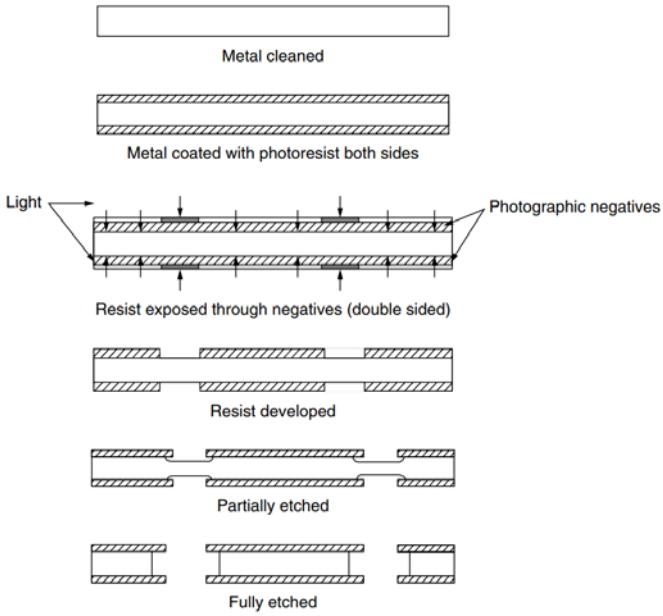

Figure 4. Photochemical milling process

2.3. Electrochemical Processes

2.3.1. Electrochemical Machining (ECM)

Electrochemical machining (ECM) is a processing technique that allows material to be removed by electrolytic dissolution. This process involves anodic dissolution of the material using high current densities. ECM works based on

Faraday's law, which states that the material is dissolved by electrolysis at the atomic level. In this processing method, by applying an electrical current to the surface of the material, the metal atoms dissolve in the electrolyte and the desired shape is obtained. In the ECM process, it allows the processing of hard, complex geometry precision parts with low thermal properties. The current used during the process is generally around 100 A/cm², which allows the workpiece to be shaped anodicly in a controlled manner. In the ECM process, aqueous NaNO3 solutions are generally used. The electrolyte removes material from the surface by continuously passing current through the gap between the workpiece and the tool. In the ECM process, the interaction of factors such as current density, temperature, pressure and viscosity determines the process efficiency. In addition, these parameters directly affect the material removal rate (Cole, 1965; "Electro-chemical machining," 1978; Lohrengel, Rataj, & Münninghoff, 2016).

The ECM process takes place in an electrochemical cell where the workpiece acts as an anode. During the process, an oxide layer and a meta-stable product film are formed on the surface of the workpiece, which is continuously removed by the electrolyte flow. The first stage is the formation of an electrolyte solution between the workpiece and the electrode. In the electrolyte, metal ions produced by the dissolution of the workpiece are transported towards the cathode under the influence of an electric field. In the final stage of the ECM process, these metal ions accumulate at the cathode and form dendritic structures. This process allows the desired shape to be

obtained on the surface of the workpiece (Lee et al., 2023; Lohrengel et al., 2016).

Figure 5 shows the basic components of the ECM machine: feed control system, electrolyte supply system, power supply unit and workpiece holding device. As shown in Figure 6, the feed control system keeps the tool moving at a constant speed during machining. The power supply provides the machining current at a constant direct current (continuous or pulsed) voltage. The electrolyte supply unit supplies the electrolyte solution at a given speed, pressure and temperature. There are also installations for filtering the electrolyte, temperature control and sludge disposal. ECM machines are capable of a range of operations such as replication, immersion and drilling. Semi-automatic and fully automatic systems are used for large size operations such as deburring, especially in the automotive industry. Unlike conventional machining machines, ECM machines are built with non-metallic materials to resist the effects of corrosion (El-Hofy, 2005).

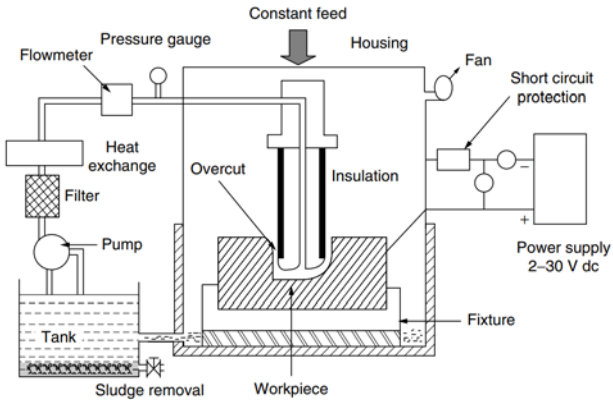

Figure 5. ECM elements

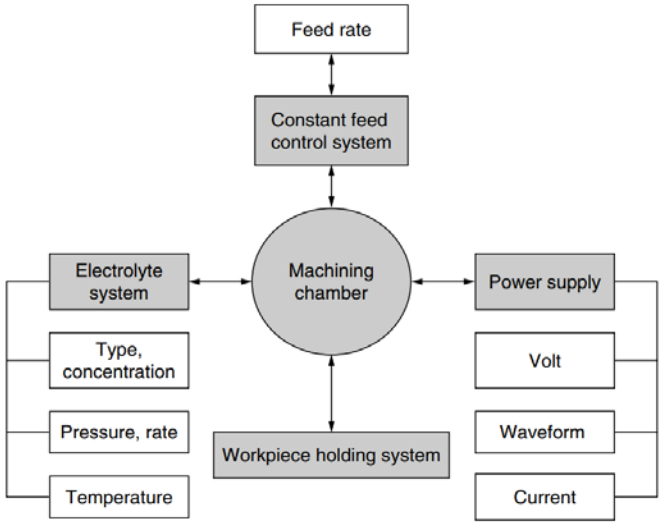

Figure 6. ECM system components

ECM is a widely used machining method in the aerospace industry. In this field, ECM is preferred in the production of aircraft engine components made of complex and difficult-to-machine materials. One of the key advantages of ECM is the absence of tool wear and high machining efficiency, which makes applications in this industry more efficient. Furthermore, the electro-chemical dissolution properties of ECM provide a significant benefit in machining new and hard materials that are difficult to machine with conventional cutting methods. Thanks to these properties, ECM continues to be favored in the production of critical components in the aerospace industry (Rajurkar, Zhu, McGeough, Kozak, & De Silva, 1999; "Recent Research and Developments in Electrochemical Machining," 2003; Xu & Wang, 2021).

In summary, Electrochemical Machining (ECM) is a method used in various industrial applications that

performs material removal by anodic dissolution at high current densities. ECM also plays an important role in micro- and nanoscale processing techniques and can be combined with hybrid processing techniques to increase its efficiency. The process is based on fundamental principles such as electrolytic dissolution, current density, electrodes, electrolyte utilization and heat-mass transfer.

2.4. Thermal Processes

2.4.1. Electrodischarge Machining (EDM)

Non-traditional manufacturing methods are used when it is necessary to machine materials with particularly high hardness and durability, or when complex shapes need to be obtained. Conventional machining methods can be limited in dealing with such challenging materials and shapes. This is where electrodischarge machining (EDM) comes into play, enabling the processing of almost any electrically conductive material. EDM is also notable for providing high precision and surface quality (Rajurkar & Wang, 1993).

EDM (Electrical Discharge Machining) performs material removal by means of electrical discharges between the workpiece and the electrode. During this process, significant topographical changes and metallurgical transformations occur on the surface of the workpiece. The plasma channel formed in the space between the workpiece and the electrode causes the material to melt and vaporize with high temperature and energy, thus achieving the desired shape and size. This process is particularly effective for machining hard and sensitive materials (Chu, Zhu, Wang, Hu, & Zhang, 2016; Gangadhar, Shunmugam, &

Philip, 1991). Figure 7 shows the schematic representation of the EDM device (El-Hofy, 2005).

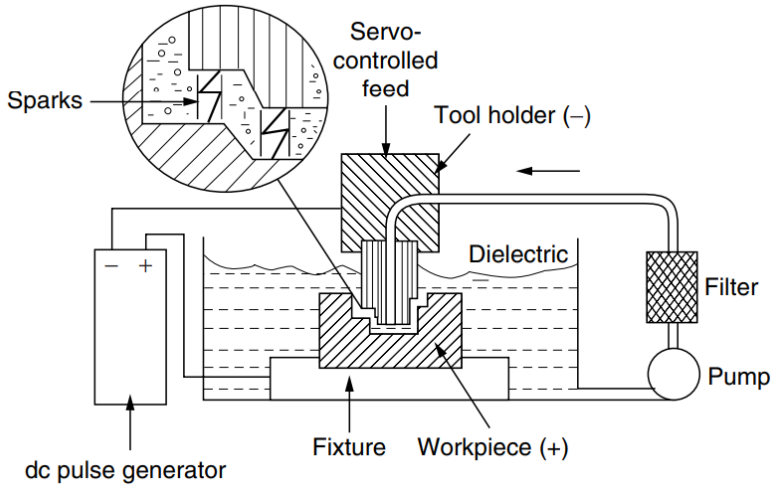

Figure 7. EDM schematic

Wire EDM (WEDM) is a method that performs cutting using a thin wire electrode. This technology is preferred to optimize energy consumption in the most efficient way, especially for difficult-to-machine materials such as super alloys (Gamage, DeSilva, Chantzis, & Antar, 2017). Micro EDM is a derivative of conventional EDM and enables machining on a micro scale. This process performs high precision machining using narrow-width pulse power generators that can operate in smaller cavities and at low energy levels (Chu et al., 2016).

EDM plays a critical role in machining difficult-to-machine materials such as superalloys and ceramics. For example, EDM is almost single-handedly the preferred method for machining materials such as REFEL silicon carbide (SiC), which has high hardness and wear resistance.

These properties make EDM particularly advantageous when precision machining and complex shapes are required (Mahdavinejad, Mehraban, & Mahdavinejad, 2006). EDM is also widely used in the mold and die making industry, where it plays an important role in producing high precision and complex designs (Gamage, DeSilva, Harrison, & Harrison, 2016).

The EDM process leads to significant changes in the surface properties of the workpiece. Selecting the appropriate process parameters allows the surface of the workpiece to be modified to achieve the desired functional properties. This surface modification can improve the mechanical properties, wear resistance and overall performance of the material (Gangadhar et al., 1991). Furthermore, careful optimization of the process parameters is necessary to ensure that the EDM process can be efficiently applied to electrically non-conductive materials, such as ZrO2 ceramics. Since such materials lack direct electrical conductivity, it is critical to manage the energy transfer and plasma channel correctly in the EDM process. This enables precision machining even on such challenging materials (Chen, Lin, Lin, Chen, & Hsu, 2010).

In conclusion, Electro-Erosion Machining (EDM) is an important technology for high precision machining of difficult-to-machine materials. This technology enables complex shapes and precise details to be achieved, while environmental impact and energy consumption can be optimized to create more sustainable production processes. The various types of EDM and its wide range of applications allow the technology to be used effectively in

different industries and material types. This diversity makes EDM an indispensable method, especially in industries with high precision and demanding material processing requirements.

2.4.2. Laser Beam Machining

Laser Beam Machining (LBM) is a non-contact machining method based on thermal energy, where the laser beam is focused on the material, melting and vaporizing the unwanted material. This technology is particularly ideal for precision machining such as cutting geometrically complex shapes and drilling fine holes. LBM offers high accuracy and fast process times in applications such as miniaturized hole making, surface forming and cutting in metals and other materials (Dubey & Yadava, 2008).

Cutting, Carving, Turning, Milling and Drilling: LBM is used for common machining methods such as cutting, carving, turning, milling and drilling. These processes have variable quality characteristics depending on material type and system parameters, and each can be customized for specific applications (Bakhtiyari, Wang, Wang, & Zheng, 2021).

Surface Treatment: Laser surface treatment is widely preferred for applying corrosion and wear resistant coatings and for repairing engine and machine parts. This process improves surface quality and ensures the longevity of products (Meijer, 2004).

Micro Machining: Short and ultrashort laser pulses enable precision machining at the nanometer level,

minimizing thermal damage to the material. This technology enables high accuracy processing at the micro level, opening up new application areas and avenues (Meijer, 2004).

Laser Beam Machining (LBM) excels thanks to compact systems that deliver short laser pulses with high precision and low cost. This technology can be applied to almost all types of materials and the most widely used laser types in industry are CO2 and Nd:YAG lasers. Furthermore, artificial intelligence techniques are effectively used in modeling, optimization, monitoring and control of the LBM process. Artificial neural networks, fuzzy logic, metaheuristic optimization algorithms and hybrid approaches are used to predict and improve the quality characteristics of laser machined workpieces, improving process efficiency and result quality (Bakhtiyari et al., 2021; Dubey & Yadava, 2008; Meijer, 2004). Figure 8 shows the schematic representation of the LBM device (El-Hofy, 2005).

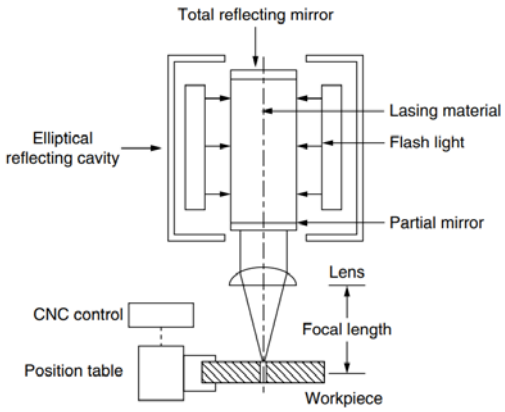

Figure 8. LBM schematic

3. CONCLUSION

Non-conventional manufacturing methods offer significant advantages in terms of precision, quality and production efficiency for materials with complex geometries or difficult-to-machine materials. These methods transform the material processing process by utilizing thermal, chemical, electrical or acoustic principles without the need for mechanical contact.

Methods such as EDM, LBM, ECM and, WJM have been successfully applied in various industries such as automotive, aerospace, medical and electronics, providing processing possibilities that are not accessible with conventional methods. In addition, these methods are also gaining attention in terms of energy savings, environmental sustainability and processing flexibility.

In the future, the efficiency and accuracy of these methods can be further improved with the integration of AI, IoT and digital manufacturing technologies. In this context, it is clear that non-traditional manufacturing methods will become an indispensable part of modern production processes.

REFERENCES

Bakhtiyari, A. N., Wang, Z., Wang, L., & Zheng, H. (2021). A review on applications of artificial intelligence in modeling and optimization of laser beam machining. Optics & Laser Technology, 135, 106721. doi:https://doi.org/10.1016/j.optlastec.2020.106721

Berman, B. (2012). 3-D printing: The new industrial revolution. Business Horizons, 55(2), 155-162. doi:https://doi.org/10.1016/j.bushor.2011.11.003

Brasil, B. S., Moura, L. B., & Rocha Neto, A. R. (2019). Non-traditional machining: a review on methods employed in advanced materials treatment. Journal of Mechatronics Engineering, 2(1), 8 - 34. doi:10.21439/jme.v2i1.24

Chen, Y.-F., Lin, Y.-J., Lin, Y.-C., Chen, S.-L., & Hsu, L.-R. (2010). Optimization of electrodischarge machining parameters on ZrO2 ceramic using the Taguchi method. Proceedings of the Institution of Mechanical Engineers, Part B: Journal of Engineering Manufacture, 224(2), 195-205. doi:10.1243/09544054jem1437

Chu, X., Zhu, K., Wang, C., Hu, Z., & Zhang, Y. (2016). A Study on Plasma Channel Expansion in Micro-EDM. Materials and Manufacturing Processes, 31(4), 381-390. doi:10.1080/10426914.2015.1059445

Cindro, N., Tireli, M., Karadeniz, B., Mrla, T., & Užarević, K. (2019). Investigations of Thermally Controlled Mechanochemical Milling Reactions. ACS

Sustainable Chemistry & Engineering, 7(19), 16301-16309. doi:10.1021/acssuschemeng.9b03319

Cole, R. R. (1965). BASIC RESEARCH IN ELECTROCHEMICAL MACHINING—PRESENT STATUS AND FUTURE DIRECTIONS. International Journal of Production Research, 4(2), 75-85. doi:10.1080/00207546508919966

Das, S., Kumar, S., Kibria, G., Doloi, B., & Bhattacharyya, B. (2020). Advancement in Ultrasonic Machining for 3D Profile Cutting. In S. Das, G. Kibria, B. Doloi, & B. Bhattacharyya (Eds.), Advances in Abrasive Based Machining and Finishing Processes (pp. 29-51). Cham: Springer International Publishing.

Dubey, A. K., & Yadava, V. (2008). Laser beam machining—A review. International Journal of Machine Tools and Manufacture, 48(6), 609-628. doi:https://doi.org/10.1016/j.ijmachtools.2007.10.017

El-Hofy, H. A. G. (2005). Advanced Machining Processes: Nontraditional and Hybrid Machining Processes: McGraw Hill LLC.

Electro-chemical machining. (1978). Production Engineer, 57(6), 27-30. doi:doi:10.1049/tpe.1978.0114

Ford, S., & Despeisse, M. (2016). Additive manufacturing and sustainability: an exploratory study of the advantages and challenges. Journal of Cleaner Production, 137, 1573-1587. doi:https://doi.org/10.1016/j.jclepro.2016.04.150

Friščić, T., Halasz, I., Beldon, P. J., Belenguer, A. M., Adams, F., Kimber, S. A. J., . . . Dinnebier, R. E. (2013). Real-time and in situ monitoring of mechanochemical milling reactions. Nature Chemistry, 5(1), 66-73. doi:10.1038/nchem.1505

Gamage, J. R., DeSilva, A. K. M., Chantzis, D., & Antar, M. (2017). Sustainable machining: Process energy optimisation of wire electrodischarge machining of Inconel and titanium superalloys. Journal of Cleaner Production, 164, 642-651. doi:https://doi.org/10.1016/j.jclepro.2017.06.186

Gamage, J. R., DeSilva, A. K. M., Harrison, C. S., & Harrison, D. K. (2016). Process level environmental performance of electrodischarge machining of aluminium (3003) and steel (AISI P20). Journal of Cleaner Production, 137, 291-299. doi:https://doi.org/10.1016/j.jclepro.2016.07.090

Gangadhar, A., Shunmugam, M. S., & Philip, P. K. (1991). Surface modification in electrodischarge processing with a powder compact tool electrode. Wear, 143(1), 45-55. doi:https://doi.org/10.1016/0043-1648(91)90084-8

Geren, N., Bayramoğlu, M., & Eşme, U. (2007). Improvement of a low-cost water jet machining intensifier using reverse engineering and redesign methodology. Journal of Engineering Design, 18(1), 13-37. doi:10.1080/09544820600650928

Gostimirovic, M., Pucovsky, V., Sekulic, M., Rodic, D., & Pejic, V. (2019). Evolutionary optimization of jet lag

in the abrasive water jet machining. The International Journal of Advanced Manufacturing Technology, 101(9), 3131-3141. doi:10.1007/s00170-018-3181-5

Goswami, D., & Chakraborty, S. (2015). Parametric optimization of ultrasonic machining process using gravitational search and fireworks algorithms. Ain Shams Engineering Journal, 6(1), 315-331. doi:https://doi.org/10.1016/j.asej.2014.10.009

Hinduja, S., & Pattavanitch, J. (2016). Experimental and numerical investigations in electro-chemical milling. CIRP Journal of Manufacturing Science and Technology, 12, 79-89. doi:https://doi.org/10.1016/j.cirpj.2015.07.003

Ikumapayi, O. M., Omietimi, B. H., Onu, P., Ogedengbe, T. S., Oluwafemi, J. R., Afolalu, S. A., & Akinlabi, E. T. (2023). Non-Traditional Machining Techniques in Manufacturing Industries – An Overview. E3S Web Conf., 430, 01213. Retrieved from https://doi.org/10.1051/e3sconf/202343001213

Jagadish, & Gupta, K. (2020). Introduction to Abrasive Water Jet Machining. In Jagadish & K. Gupta (Eds.), Abrasive Water Jet Machining of Engineering Materials (pp. 1-11). Cham: Springer International Publishing.

K, V., Kuriachen, B., & Mathew, J. (2021). Chapter 13 - An insight on ultrasonic machining technology. In K. Gupta & A. Pramanik (Eds.), Advanced Machining and Finishing (pp. 451-478): Elsevier.

Kataria, R., & Kumar, J. (2016). Ultrasonic Machining: A Review. Advanced Materials Research, 1137, 61-78. doi:10.4028/www.scientific.net/AMR.1137.61

Kumar, J. (2013). ULTRASONIC MACHINING—A COMPREHENSIVE REVIEW. Machining Science and Technology, 17(3), 325-379. doi:10.1080/10910344.2013.806093

Lalchhuanvela, H., Doloi, B., & Bhattacharyya, B. (2012). Enabling and Understanding Ultrasonic Machining of Engineering Ceramics Using Parametric Analysis. Materials and Manufacturing Processes, 27(4), 443-448. doi:10.1080/10426914.2011.585497

Lee, E. L., Goh, Y. S., Haseeb, A. S. M. A., Wong, Y. H., Mohd Sabri, M. F., & Low, B. (2023). Review—Electrochemical Migration in Electronic Materials: Factors Affecting the Mechanism and Recent Strategies for Inhibition. Journal of The Electrochemical Society, 170. doi:10.1149/1945-7111/acb61a

Loh, Z. H., Samanta, A. K., & Sia Heng, P. W. (2015). Overview of milling techniques for improving the solubility of poorly water-soluble drugs. Asian Journal of Pharmaceutical Sciences, 10(4), 255-274. doi:https://doi.org/10.1016/j.ajps.2014.12.006

Lohrengel, M. M., Rataj, K. P., & Münninghoff, T. (2016). Electrochemical Machining—mechanisms of anodic dissolution. Electrochimica Acta, 201, 348-353. doi:https://doi.org/10.1016/j.electacta.2015.12.219

Lukin, S., Tireli, M., Stolar, T., Barišić, D., Blanco, M. V., di Michiel, M., . . . Halasz, I. (2019). Isotope Labeling Reveals Fast Atomic and Molecular Exchange in Mechanochemical Milling Reactions. Journal of the American Chemical Society, 141(3), 1212-1216. doi:10.1021/jacs.8b12149

Mahdavinejad, R., Mehraban, M., & Mahdavinejad, D. (2006). The behaviour of REFEL SiC under electrodischarge machining. Proceedings of the Institution of Mechanical Engineers, Part B: Journal of Engineering Manufacture, 220(10), 1635-1646. doi:10.1243/09544054jem284

McCormick, P. G., & Froes, F. H. (1998). The fundamentals of mechanochemical processing. JOM, 50(11), 61-65. doi:10.1007/s11837-998-0290-x

Meijer, J. (2004). Laser beam machining (LBM), state of the art and new opportunities. Journal of Materials Processing Technology, 149(1), 2-17. doi:https://doi.org/10.1016/j.jmatprotec.2004.02.003

Ozcan, Y., Tunc, L. T., Kopacka, J., Cetin, B., & Sulitka, M. (2021). Modelling and simulation of controlled depth abrasive water jet machining (AWJM) for roughing passes of free-form surfaces. The International Journal of Advanced Manufacturing Technology, 114(11), 3581-3596. doi:10.1007/s00170-021-07131-1

Rajurkar, K. P., & Wang, Z. Y. (1993). EDM Fundamentals and Practices. Society of Manufacturing Engineers.

Rajurkar, K. P., Zhu, D., McGeough, J. A., Kozak, J., & De Silva, A. (1999). New Developments in Electro-Chemical Machining. CIRP Annals, 48(2), 567-579. doi:https://doi.org/10.1016/S0007-8506(07)63235-1

Rao, R. V. (2011). Modeling and Optimization of Modern Machining Processes. In R. V. Rao (Ed.), Advanced Modeling and Optimization of Manufacturing Processes: International Research and Development (pp. 177-284). London: Springer London.

Recent Research and Developments in Electrochemical Machining. (2003). International Journal of Electrical Machining, 8, 1-14. doi:10.2526/ijem.8.1

Sabareesan, S., Vasudevan, D., Sridhar, S., Kannan, R., & Sankar, V. (2021). Response analysis of ultrasonic machining process under different materials – Review. Materials Today: Proceedings, 45, 2340-2342. doi:https://doi.org/10.1016/j.matpr.2020.10.695

Singh, R., & Khamba, J. S. (2006). Ultrasonic machining of titanium and its alloys: A review. Journal of Materials Processing Technology, 173(2), 125-135. doi:https://doi.org/10.1016/j.jmatprotec.2005.10.027

Singh, R., & Khamba, J. S. (2009). Mathematical modelling of surface roughness in ultrasonic machining of titanium using Buckingham-Π approach: a review. International Journal of Abrasive Technology, 2(1), 3-24. doi:10.1504/ijat.2009.021635

Snoeys, R., Staelens, F., & Dekeyser, W. (1986). Current Trends in Non-Conventional Material Removal Processes. CIRP Annals, 35(2), 467-480. doi:https://doi.org/10.1016/S0007-8506(07)60195-4

Xu, Z., & Wang, Y. (2021). Electrochemical machining of complex components of aero-engines: Developments, trends, and technological advances. Chinese Journal of Aeronautics, 34(2), 28-53. doi:https://doi.org/10.1016/j.cja.2019.09.016

DAMAGES TO THE SOIL BY MINING AND IMPROVEMENT WORKS

Görkem ERTUĞRUL[1]

Fatih ARLI[2]

1. INTRODUCTION

Mining is one of the most critical sectors that guide societies to reach the level of economic and technical welfare on a global scale. Mining can meet countries' industrial raw material needs from the past to the future. As in ancient times, the minerals used by mining traders and the minerals used by modern humans have a common denominator because they are formed from sediments scattered worldwide. (Hustrulid, Kuchta, and Martin 2013). However, a wide range of environmental problems arise during and after mining. These problems can be classified as open pit mining and underground mining, which are the methods used to recover precious metals from the earth and their effects on the environment. The works carried out with the open pit method directly affect the land's topography negatively. In underground mining, it is the effects of cracks and collapses in the soil. For this reason, both environmental and legal examination and analysis of

[1] Instructor., Karamanoğlu Mehmet Bey University, Kazim Karabekir Vocational School, Medical Services and Techniques Department, Environmental Health Program, 70600 Karaman-Turkey, ORCID: 0000-0002-7840-713X.

[2] Asst. Prof. Dr., Şırnak University, Engineering Faculty, Energy System Engineering Department, 73000 Şırnak-Turkey, ORCID: 0000-0002-0899-3460.

mining activities are remarkable studies. Within the framework of the reclamation template obtained when the ecological planning of the mining sites whose activities have been completed, positive contributions are provided in social activities such as sports fields and museums, as well as economic evaluation such as agriculture and fish farms (Ertuğrul 2010; Jain and Domen 2016). In this study, the application of Open Pit and Underground mining methods are explained, and the damages to the soil structure and the improvement of these damages are discussed. In addition, in this research, studies on the deterioration of soil structure (such as physical and chemical) during and after mining activities were evaluated thematically. In this evaluation, different variables (soil pollutant types) taken into account by the researchers were discussed in terms of their quantitative and qualitative characteristics in the soil.

2. OPEN MINE MINING AND ITS IMPACTS ON SOIL

Open pit mining consists of creating slope(s) in the upper rock mass of these ores and removing this material by blasting or digging machines in order to recover valuable ores close to the earth. These studies are implemented in two ways. In the Figure 1, if the precious ore is very close to the soil surface or on a mountain, production is carried out by creating a single slope.

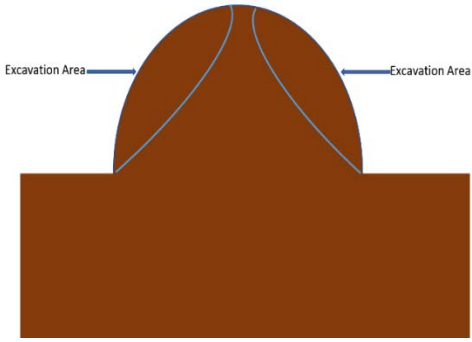

Figure 1. Surface mining (Hustrulid et al. 2013)

In the Figure 2, if the reserve is on a flat area and hundreds of meters below the surface, several steps are formed depending on the amount of ore mass, and mining activities are carried out (Hustrulid et al. 2013). It is estimated that more than 70% of all materials excavated in mining operations worldwide are waste. It is estimated that about 80% of mine waste rock is due to unnecessary excavation. This inefficient operation creates negativity in terms of mine waste management. Mining wastes mostly do not contain industrial materials. Therefore, they are not crucial in terms of recovery processes.

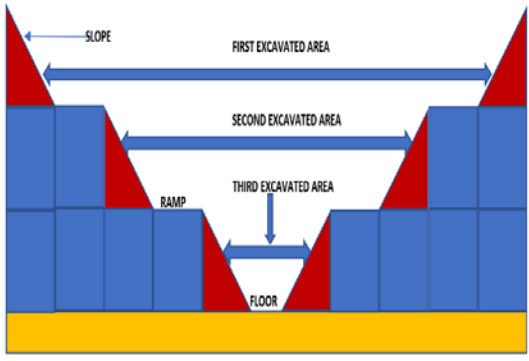

Figure 2. Open pit mining (Hustrulid et al. 2013)

There are different criteria for separating the country rock from the ore in mining. In these criteria, the geometry of the open pit (depth and step height) is considered, depending on the thickness of the country rock material (waste) covering the ore surface. The waste rock material's thickness and the waste amount show a direct proportion. Mining wastes are generally heterogeneous geological materials. These materials include sedimentary, metamorphic, igneous rocks, soils and loose sediments. The particle sizes of these waste materials vary from micron to meter. The physical and chemical properties of the mine waste material vary according to the mineralogy, geochemistry, geotechnics, climatic conditions of the region and the type of machinery and equipment operated in the operating region. In open pit mining, in addition to waste rock material, mine wastewater and atmospheric emissions (particulate matter and greenhouse Mineral Water, one of the mining wastes, is called meteoric water, which undergoes chemical changes due to the reactions of the minerals found in the mining activity areas and the water and chemical compounds used in the processes. This water is released due to open mining and underground mining operations (removing, separating and processing ore from the ground). Depending on its content, mineral water is removed from the environment or disposed of, or if there are valuable minerals in this water, it is evaluated by using recovery methods. In mining terminology, Mineral Water (Table 1) is generally accepted as any body of water, including surface water and groundwater (Amos and Younger 2003; Banks et al. 1997; Impacts 2008; Johnson and Younger 2005; Morin, K.A., & Hutt 1997).

Table 1. Terminology of mine water released from mining activities (open pit mining or underground mining) (Impacts 2008)

Mine Water Types	Explanation
Mine Water	ground or surface waters existing at the mine site
Mining Water	water released from mining operations
Mill Water	water is used in ore dressing units to crush and size the mineral
Mine Drainage Water	surface or groundwater that occurs at the mine site that actually or potentially flows into the area outside the mine site
Acid Mine Drainage (AMD) Water	surface or groundwater that has acidic properties (Low pH) that formed as a result of the reaction of sulfide minerals with water and oxygen that actually or potentially flows into the area outside the mine site

In his study, (Pichtel 2003) states that mineral water is a potential environmental hazard. He underlined that if uncontrolled discharge flow and drainage of this water is made, it infiltrates the soil and water resources and dramatically deteriorates the soil and water quality since the mineral water contains pH value, heavy metal content and toxic compounds. In the study of (Younger 2000), mineral water that does not leak into the soil and water resources completely evaporates due to the heat in the environment, and the particles left from the mineral water body (such as suspended solids, acidic or basic materials, heavy metals and salts) are released into the atmosphere over time. leaking and triggering further increases in air pollution. Brown meat. AMD is a sign of a special chemical process formed by the oxidation of sulfide minerals (such

as iron and copper minerals) and low pH mineral water. (Munk, Faure, and Koski 2006).

The problem of soil degradation caused by mining activities intersects at a common point globally. At this point, soil pollution gradually increases in areas used for purposes such as agriculture and animal husbandry, and its quality has decreased within the framework of the perspectives provided according to the information obtained by considering this pollution both locally and worldwide. It is necessary to develop practices for the effective recovery of soil masses Soil improvement studies stated in their study that, thanks to these applications, degraded soils that cannot fulfil their long-term duties will be healed. In addition, showed common findings about applications showed that degraded soil-borne pollutants will be prevented from penetrating into the biosphere, hydrosphere, and atmosphere. Concentrations of organic and inorganic materials in soil vary considerably, especially according to open pit mining activities. However, some elements (such as Hg and As) and compounds (such as HCN, H_2SO_4 and NaOH) found in these organic and inorganic materials are seriously harmful to the soil mass. These often exceed the permissible concentration limits and worsen ecological functions due to the interference of mining activities with the natural balance. The accumulation of hazardous mining wastes (especially heavy metals and compounds with ion concentrations) gradually destroys the ecological system (Jain and Domen 2016). The presence of Hg, which is among the heavy metals, in the soil directly changes the physical mobility of the soil, material solubility and

chemical reaction equations in a harmful way to the environment. Among these changes are important factors such as pH level, redox potential, cation exchange capacity and organic matter content of soil masses (O'Connor et al. 2019). The physical and chemical activities of Hg negatively affect the toxin level in the soil and the chemical-specific mobility systems (such as isotopic composition, complex molecular structure changes and oxidation state) of living things in the soil (Templeton and Fujishiro 2017). Under natural conditions, Hg exists in elemental form, as an oxide (HgO), sulfurous (HgS) compound, or in alkaline form. It has been observed that mercury derivatives are not very stable chemically in highly polluted soils due to anthropogenic activities. Therefore, the pollutant level is high (Nieder, Benbi, and Reichl 2018). Especially Hg compounds in oxide form can pass into the atmosphere due to their high volatility. In soil, Hg derivatives are inorganic and become organometallic if methylation occurs. Although these organic Hg compounds are found in very low amounts in soil, they are among the most toxic Hg derivatives. Even in very small amounts, these compounds accumulate easily in living organisms and therefore, the level of harm is relatively high (Hudson-Edwards, Jamieson, and Lottermoser 2011; Rodríguez et al. 2009). Therefore, soils with Hg content are hazardous for living things, and if the Hg issue is not taken into account, a high risk for environmental health arises (Lottermoser 2007). It is common for soil degradation to occur in mine sites with sulfide minerals. According to industry planning, the level of damage to soil by sulfide mining operations may increase. Ecological processes are not observed in such

industrially degraded areas (Gascó et al. 2019; Paz-Ferreiro et al. 2014). Soil pollution in mining areas is a significant environmental problem. In these areas, due to the properties of pollutants other than heavy metals that reduce soil quality and pH, the desired level cannot be achieved in the classical phytoremediation method used to remove heavy metals from the soil. Instead, the auxiliary phytoremediation method is preferred, and its use for improving degraded soil gradually increases (Houben, Evrard, and Sonnet 2013; Kabata-Pendias and Pendias 2000). Auxiliary phytoremediation helps plant growth by preventing soil erosion, infiltration of polluted water, and removing heavy metals (such as Cu, Pb, Zn, Ni, Cr, and As) from the soil. Applying this method with natural fertilizers (such as rabbit manure), especially in soils contaminated by heavy metals, significantly increases soil fertility (Novak et al. 2018; Park, Kim, and Kim 2012). Thus, natural life re-emerges. The metal concentration in the soil varies depending on human activities and natural processes. However, the severity of some of these metals depends on the concentration level. This harmful severity often exceeds the permissible limits, causing adverse effects on the biological functions of organisms. Mining activities are one of the most critical factors threatening the ecosystem. The accumulation of hazardous waste from these activities adversely affects soils and crops and threatens surrounding populations and human health as polluting metals enter the food chain through plants and contaminated water. Especially in agriculture, animal husbandry and toxicology, Hg has an important place in environmental health. Contaminated soils due to Hg are hazardous for

living things. Hg has been identified as one of the ten main chemicals threatening human health by the World Health Organization (WHO 2016). If the Hg factor is not considered, it poses a high risk to health and the environment. In studies to protect human health and the environment from the negative effects of Hg and to reduce Hg pollution, in Hg mining, in mining sites where Hg is used. In order to control air emissions containing Hg, in industries where chlor-alkali processes are used, environmental regulations have been introduced. With these regulations, it becomes easier to control Hg in the environment (Selin et al. 2018; UNEP 2002).

3. UNDERGROUND MINING AND ITS IMPACT ON SOIL

Underground mining is the preferred mining method when the mining of valuable minerals by open pit method is costly and excessive workload. Extracting ore by an underground mining method involves the creation of different types of openings with a significant range of functions. It consists of various openings to an operating underground mining operation. Includes main shaft, straight drives and crosscuts, ore haulages, ventilation shafts and airways, mine access, and service openings. (Darling 2001). In underground mining, depending on the underground tectonic conditions, the potential to cause physical and chemical (such as AMD formation) effects on the soil structure is quite high. Due to these effects, biomass is degraded. Large-scale destruction of vegetation is observed due to the chemical composition of rock waste

masses, such as the effects of wastes from underground mining, which are likely to damage the soil, and wastes from open-pit mining. In addition, most underground mining also releases toxic compounds into the air and water. These released components turn water bodies into polluting structures. These water bodies can contaminate the area surrounding the mine and beyond (Impacts 2008; Jain and Domen 2016; Lottermoser 2007). In underground mining, Hg is widely used to facilitate the recovery of precious ores. However, due to improper disposal methods, Hg waste becomes a major concern and damages the atmosphere and water bodies (Mcneill and Vrtis 2019; Schor and Gray 2008). Most underground mining operations use pumps to drain, and polluted water from these pumps triggers sedimentation and contamination of nearby streams. Therefore, it complicates the development of vegetation dependent on the stream. Underground mining indirectly causes deforestation, degradation of beneficial microorganisms and formation of erosion. Whether it is open pit mining or underground mining, chemical-resistant cement sets should be used in order to prevent harmful factors from entering the soil, and humic acid and natural animal fertilizers should be used for soil improvement (Guo et al. 2021; Jain and Domen 2016; TAŞKESEN et al. 2022). Another effect of underground mining is the depressions it will create on the earth if the underground operation does not work with filled methods. After underground productions, the rock mass on the cavity is defeated by the effect of gravity over time and moves to fill the void formed due to production. As a result, there may be a displacement in the rock mass up to the

surface layer above the underground cavity. This vertical displacement is called subsidences in mining (Darling 2001). The same event can occur not only in the mining area but also during the creation of any underground structure or overtime after its creation. These subsidences physically damage sensitive areas such as settlements, agricultural lands and forest lands, and this damage is difficult to repair. To control the leash, seismic activity above ground should be constantly examined. Keeping the stresses occurring in the underground cavities in balance prevents the movement of the rock mass and to ensure this, supporting the existing fortification and filling the cavity with filling material are among the critical points. Thus, there will be no displacement of the rock mass originating from the subsidences above ground and no environmental damage will occur.

4. RESULT AND DISCUSSION

Many studies on the environmental impacts of mining have underlined it. Restoration of mining-damaged soil is essential in terms of soil quality and the quality of water resources (Pacetti et al. 2020). Evaluation of this restoration effectiveness, 3D solid modelling of the investigated soil mass in the computer environment (Wang, Qin, and Bai 2018) and investigating the estimation of soil heavy metal concentration by hyper-spectral methods (such as Aerial photogrammetry and Remote Sensing) for soil heavy metal monitoring and evaluation. It can be seen as a good tool to improve soil quality. Defining the soil quality indicator of the site before and after mining

has an important role in soil degradation repair works. Evaluation of site-specific factors such as pH, NH_4^+, NO_3, P, K, organic matter, and electrical conductivity of the soil lead to optimal soil quality (Levi et al. 2021). The formation and growth processes of vegetation indicate that the soil has healed over time. It emerges as quantitative evidence of a good soil level and vegetation recovery over the years, thanks to the analysis of activities in the vegetation using soil biological index methods. Damage to vegetation due to mining can indirectly increase CO_2 emissions, which are among the sources of the global warming problem. Another factor in CO_2 emissions is fossil-based mining activities. This spontaneous and uncontrolled coal combustion creates a severe greenhouse gas in the atmosphere (Soria et al. 2021). Soil macropore systems of soil physically degraded by open pit mining can be considered a measure of the damage level of the soil ecosystem. Soil macroporous properties (such as width, number and depth) indicate the quality level of soil recovered in open pit mining areas. Determination of the properties of macropore systems by in situ studies is not preferred due to negative factors such as time consumption and excessive workload. Instead, information on soil macropores should be provided using a high-resolution, non-destructive computed tomography (CT) technique. With the 3D solid model of the soil containing numerical information, the quantitative properties of the soil macropores can be determined by analyzing the number and volume of the macropores. Thus, the soil's visual and numerical models are obtained (Wang et al. 2018). According to this model, soil improvement plans are

directed. Open pit mining has many negative consequences on land resources and puts dramatic pressure on the ecological environment. In mining, stripping, digging, transporting and unloading the soil requires important planning in terms of the environment. In these plans, landscaping works are restructured, and the heterogeneity of the soil (decreased quality of the soil and increased pollutant content) factor is taken into consideration (Feng et al. 2019). The importance of detailed and long-term implementation of mine soil reclamation should be emphasized as concerns about the negative consequences of mining are growing. Limestone (Pihlap et al. 2019), humic acid (Portillo Miranda et al. 2021), sewage sludge, biochar and compressed food residues can be used to remove adverse soil changes in soil improvement works at mining sites. Characterizing the chemical composition and structural, and morphological properties of these materials has an important role in ensuring the systematicity of soil improvement studies. In addition, thanks to these materials, phytonutrient levels such as Cd, Cr, As, Zn, and Pb, which cause soil pH and soil improvement studies, have reached (Azeem et al. 2021; Liu et al. 2021; Martins et al. 2018). Mixing wood ash and biological sludge can give a new direction to soil reclamation studies. The ash's dissolved salts and chloride content limit the potential toxicity levels, and the biological sludge regulates the release of soluble salts and chloride in the ash, providing organic matter and alkalinity. Limestone strongly influences the aggregation (breaking, crumbling and pulverizing) property of loose soil as it acts as a strong cementing agent and optimizes the photo-availability of

heavy metals, causing a significant change in pH value. In addition, limestone is important in developing microbial biomass as it does not limit the N uptake of the soil (Martins et al. 2018; Pihlap et al. 2019). On the other hand, in terms of soil fertility, it helps both the increase of useful materials (such as N and C) in the soil, the proliferation of beneficial microorganisms, the low cost of soil improvement, the reduction of heavy metals such as Cd, As, Hg, and Pb in the soil, thus also in plants. It contributes positively to the reduction of heavy metal accumulation, the improvement of plant growth parameters (such as fresh, dry biomass, root and shoot lengths) and the performance of breeding studies. The accumulation of heavy metals and sulphurous compounds in organisms, their movement in the soil, the tendency of microbial and phytotoxic parameters, and their density and chemical change factors guide soil improvement studies. For example, a quantitative measure of the effects of the presence of Mn heavy metal in the soil to be reclaimed can be examined. In order to reduce the impact of Mn heavy metal, compounds with a long C chain are used. This compound increases biological factors such as plant biomass, height and photosynthetic pigment mobility. Using organic materials to improve the chemical and biological properties of degraded soils (especially carbonate-based minerals) from the mines accelerates the improvement processes because it increases biological activities. In this sense, the success of organic sewage sludge and composted domestic waste in soil improvement is evaluated over the long term (Rodríguez-Berbel et al. 2020). In reclamation studies using rock wool and lignite dust, only the physical properties of degraded soil (air

permeability, porosity and bulk density of the soil) are improved (Kołodziej, Bryk, and Otremba 2020). Landscape studies using P focus directly on plant growth. In soils contaminated by heavy metals, the nutrients required for plant growth are inadequate. Therefore, P reduces oxidative stress, improves plant growth, composition, and cellular structure, and facilitates the phytoremediation potential of fibrous crop plant species. Due to acid and heavy metal, it is planned to use lime and biopile repair methods in the contaminated soils at the mine sites' borders. With these methods, due to the increase in pH and organic matter content, the solubility of heavy metals such as Cu, Zn, As, Mn and Pb, which have a high accumulation potential in plants (Wang et al. 2021), decreases in the soil. As biochemical activities increase in the soil, acids are broken down. Elements such as C and N released from these decomposed acids allow vegetation to develop (Brasil Neto et al. 2021; Ezeokoli et al. 2021; Jiang et al. 2022; Paniagua-López et al. 2021). Soil thickness, which forms the life cycle, is decreasing due to mining activities. The decrease in the thickness of the soil causes serious damage to the ecosystem (Malone and Searle 2020). In this sense, using mushrooms creates a new direction in improving the soil whose thickness has decreased. In soil reclamation studies, the use of fungal communities has an essential role in the emergence of organic C fractions and vegetation development. These fungi increase plants' resistance to environmental conditions. Thanks to these plants and fungi with increasing resistance, C, N and S ratios reach an environmentally friendly level, the solubility of organic C, which is necessary for life, increases, and the pH in the soil

reaches ideal levels. It is important to preserve the polluted soil in the areas where mining activity continues and ends. Pollution zones expand as this soil mass is easily transported to areas outside the mine site in the form of sediment depending on climatic conditions. This expansion poses a threat to public health as well as widely disrupting geological and hydrological systems. Whether it is large-scale or small-scale mining activities, the effects of soil improvement work on the sediment yield are discussed on the samples taken from the soil and water resources, taking into account the geochemical and hydrological components. Accordingly, regulatory and environmental management plans are prepared for the uncontrolled flow of polluted sediment caused by the mining sector (Awotwi et al. 2021; Bond et al. 2019). Although mining and reclamation operations are complex and regionally specific, achieving a sequential systematic with coherent plans is possible. Thus approaching the goal of sustainable mining with minimal environmental destruction. It includes a holistic reclamation approach that restores ecosystem function to its original extent through sustainable mining, In order to increase ecosystem productivity, mining and reclamation processes should be taken into account simultaneously when investigating the effects of mining on soil properties (Figure 3). The complexity of mining on soil properties results not only from the interactions of mining systems but also from man-made systems such as human communities and land use types and from natural processes. Recovering soil damaged by mining is a key element in ecosystem restoration. Research on soil recovery offers better aspects of reclamation practices. Studies

examining soil's chemical and biological properties provide special guidance in soil improvement. However, the comprehensive application of new technologies in reclamation areas is impossible in all terrain conditions. More advanced applications will emerge if environmental restoration is detailed based on the basic components of the improvement studies (Figure 4). However, rehabilitation studies are limited due to establishing a database of environmental factors and the lack of integration and large-scale studies on the mine soil information system and other nature restoration systems of mining areas.

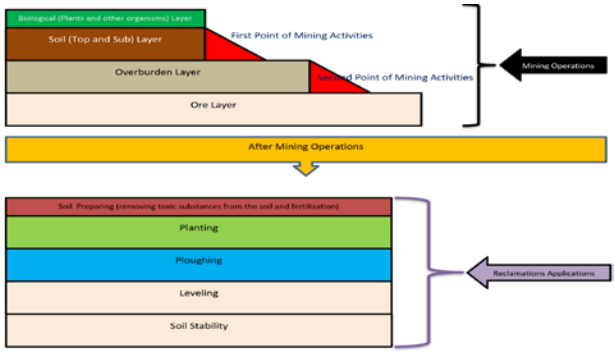

Figure 3. Core of reclamation applications in mining

Figure 4. Reclamation system principles in mining

5. CONCLUSIONS

Mining activities have significant physical, chemical, and biological effects on soil properties and cause serious effects in terms of the lack of vegetation. In this context, it is necessary to consider improving vegetation and soil as an environmentally friendly approach. If landfills and pit pits are left to their own devices as a result of mining operations, it is almost impossible for these areas to repair themselves and become usable again. However, it is possible to improve these areas, whose natural structure is deteriorated, with the repair works to be done. These recovery works cover a wide period of time, starting from the site selection stage for mining activities to the completion of the repair works. In this period of time, in terms of both the optimal operation of the mine and the sustainable use of resources;

- Performing planned excavation works and improvement works simultaneously,
- Consideration of existing land use plans, local development, construction plans and designated landscape protection areas,
- Combining landscape structuring plans with regional development plans,
- Ensuring optimal coordination between industry, site structure and landscape planning,
- Determining the type of land use to be made after mining before operation,
- Ecological data related to the area should be evaluated before operation and

- A combination of plans for restoration and sustainable use, ecosystem management, and rational use of natural land will lead to successful mining-related sustainable environmental practices.

Soil degradation and reduction of agricultural uses is a global problem. This global problem leads to deepening concerns about food supply in the future. For this reason, it is critical that agricultural studies focus on the recovery of soils. The most important factor affecting soil degradation is the mining sector. Due to the wide working scope of the mining sector, it affects soil degradation to a large extent compared to other sectors. As a result of this deterioration, the lands are closed to agricultural production for many years. Degraded soils damage these layers by penetrating pollutants into the biosphere, hydrosphere and atmosphere. The level of environmental pollution is gradually increasing as the degraded soil does not fulfil functions such as filtration and buffering. Anthropogenic environmental impacts pose problems such as global land degradation and increased waste generation. In particular, open pit mining causes environmental damage that cannot be ignored, and it is an important issue to apply nature restoration works to the site in order to eliminate this damage. In this direction, calcium carbonate-containing rock wastes and plant-derived organic wastes, which can contribute to the restoration of nature, can be used after mining to prevent soil erosion, improve soil and protect it from external pollutants. However, changes in soil structure take a long time. In order to accelerate this process, the use of soil strengtheners (such as humic acid) rich in materials that can be more effective in soil improvement and productivity should be taken into account. Thanks to these

boosters, biochemical processes beneficial to the soil are accelerated. In order to make optimal use of these processes, it is necessary to obtain detailed information about the pollutants in the soil (such as their components, amount and reaction tendency) and to organize studies according to this information. Addition of animal manure (such as rabbit and worm manure) to soil contaminated with many heavy metals (such as Co, Cr, Cu, Ni, Zn, Pb, Hg and As) and coal causes an increase in beneficial microorganisms.

REFERENCES

Amos, Philip W., and Paul L. Younger. 2003. "Substrate Characterisation for a Subsurface Reactive Barrier to Treat Colliery Spoil Leachate." *Water Research* 37(1):108–20. doi: 10.1016/S0043-1354(02)00159-8.

Awotwi, Alfred, Geophrey K. Anornu, Jonathan Arthur Quaye-Ballard, Thompson Annor, Isaac Kwadwo Nti, Samuel N. Odai, Emmanuel Arhin, and Charles Gyamfi. 2021. "Impact of Post- Reclamation of Soil by Large-Scale, Small-Scale and Illegal Mining on Water Balance Components and Sediment Yield: Pra River Basin Case Study." *Soil and Tillage Research* 211(March):105026. doi: 10.1016/j.still.2021.105026.

Azeem, Muhammad, Amjad Ali, Parimala G. S. Arockiam Jeyasundar, Saqib Bashir, Qaiser Hussain, Fazli Wahid, Esmat F. Ali, Hamada Abdelrahman, Ronghua Li, Vasileios Antoniadis, Jörg Rinklebe, Saby M. Shaheen, Gang Li, and Zenqqiang Zhang. 2021. "Effects of Sheep Bone Biochar on Soil Quality, Maize Growth, and Fractionation and Phytoavailability of Cd and Zn in a Mining-Contaminated Soil." *Chemosphere* 282(May). doi: 10.1016/j.chemosphere.2021.131016.

B. H. G. Brady, E. T. Brown. 1979. *Rock Mechanics for Underground Mining*. Vol. 24. Third edit.

Banks, David, Paul L. Younger, Rolf Tore Arnesen, Egil R. Iversen, and Sheila B. Banks. 1997. "Mine-Water Chemistry: The Good, the Bad and the Ugly."

Environmental Geology 32(3):157–74. doi: doi.org/10.1007/s002540050204.

Bond, William Edward, Kevin M. Yeager, Christopher D. Barton, and Andrea M. Erhardt. 2019. "The Forestry Reclamation Approach: Measuring Sediment Mass Accumulation Rates in Reclaimed Mine Lands and Naturally Regenerated Logged Forests of Eastern Kentucky." doi: 10.1130/abs/2019se-326711.

Brasil Neto, Alberto Bentes, Gustavo Schwartz, Norberto Cornejo Noronha, Marcos André Piedade Gama, and Gracialda Costa Ferreira. 2021. "Natural Regeneration for Restoration of Degraded Areas after Bauxite Mining: A Case Study in the Eastern Amazon." *Ecological Engineering* 171(July). doi: 10.1016/j.ecoleng.2021.106392.

Darling, Peter. 2001. *Underground Mining Methods*. Edited by. Society for Mining, Metallurgy, and Exploration, Inc. (SME).

Ertuğrul, Görkem. 2010. "Madencilik Faaliyetlerinin Çevresel Etkilerinin ve Doğa Onarım Çalışmalarının Coğrafi Bilgi Sistemi (CBS) Ile Belirlenmesi ve Modellenmesi." *Dokuz Eylül Üniversitesi* .

Ezeokoli, Obinna T., Oluwatosin G. Oladipo, Carlos C. Bezuidenhout, Rasheed A. Adeleke, and Mark S. Maboeta. 2021. "Assessing the Ecosystem Support Function of South African Coal Mining Soil Environments Using Earthworm (Eisenia Andrei) Bioassays." *Applied Soil Ecology* 157(May 2020):103771. doi: 10.1016/j.apsoil.2020.103771.

Feng, Yu, Jinman Wang, Zhongke Bai, and Lucy Reading. 2019. "Effects of Surface Coal Mining and Land Reclamation on Soil Properties: A Review." *Earth-Science Reviews* 191(February):12–25. doi: 10.1016/j.earscirev.2019.02.015.

Gascó, G., M. L. Álvarez, J. Paz-Ferreiro, and A. Méndez. 2019. "Combining Phytoextraction by Brassica Napus and Biochar Amendment for the Remediation of a Mining Soil in Riotinto (Spain)." *Chemosphere* 231:562–70. doi: 10.1016/j.chemosphere.2019.05.168.

Guo, Jing, Yuxiu Zhang, Hai Huang, and Fan Yang. 2021. "Deciphering Soil Bacterial Community Structure in Subsidence Area Caused by Underground Coal Mining in Arid and Semiarid Area." *Applied Soil Ecology* 163(January):103916. doi: 10.1016/j.apsoil.2021.103916.

He, Feng, Jie Gao, Eric Pierce, P. J. Strong, Hailong Wang, and Liyuan Liang. 2015. "In Situ Remediation Technologies for Mercury-Contaminated Soil." *Environmental Science and Pollution Research* 22(11):8124–47. doi: 10.1007/s11356-015-4316-y.

Houben, David, Laurent Evrard, and Philippe Sonnet. 2013. "Beneficial Effects of Biochar Application to Contaminated Soils on the Bioavailability of Cd, Pb and Zn and the Biomass Production of Rapeseed (Brassica Napus L.)." *Biomass and Bioenergy* 57:196–204. doi: 10.1016/j.biombioe.2013.07.019.

Hudson-Edwards, Karen A., Heather E. Jamieson, and Bernd G. Lottermoser. 2011. "Mine Wastes: Past, Present, Future." *Elements* 7(6):375–80. doi: 10.2113/gselements.7.6.375.

Hustrulid, W., M. Kuchta, and R. Martin. 2013. *Open Pit Mine Planning & Design 3rd Edition*.

Impacts, Environmental. 2008. *Mine Wastes: Characterization, Treatment, Environmental Impacts*. Vol. 45.

Jain, Ravi K., and Jeremy K. Domen. 2016. *Environmental Impact of Mining and Mineral Processing*.

Jiang, Shaojun, Guangling Dai, Jie Zhou, Jie Zhong, Junguang Liu, and Yuehong Shu. 2022. "An Assessment of Integrated Amendments of Biochar and Soil Replacement on the Phytotoxicity of Metal(Loid)s in Rotated Radish-Soya Bean-Amaranth in a Mining Acidy Soil." *Chemosphere* 287(P1):132082. doi: 10.1016/j.chemosphere.2021.132082.

Johnson, Karen L., and Paul L. Younger. 2005. "Rapid Manganese Removal from Mine Waters Using an Aerated Packed-Bed Bioreactor." *Journal of Environmental Quality* 34(3):987–93. doi: 10.2134/jeq2004.0300.

Kabata-Pendias, Alina, and Henryk Pendias. 2000. *Trace Elements in Soils and Plants: Third Edition*.

Kołodziej, Beata, Maja Bryk, and Krzysztof Otremba. 2020. "Effect of Rockwool and Lignite Dust on Physical State of Rehabilitated Post-Mining Soil." *Soil and*

Tillage Research 199(January). doi: 10.1016/j.still.2020.104603.

Levi, Nathan, Noa Hillel, Eli Zaady, Guy Rotem, Yaron Ziv, Arnon Karnieli, and Tarin Paz-Kagan. 2021. "Soil Quality Index for Assessing Phosphate Mining Restoration in a Hyper-Arid Environment." *Ecological Indicators* 125(March):107571. doi: 10.1016/j.ecolind.2021.107571.

Liu, Xingwang, Siyuan Chen, Xiulan Yan, Tao Liang, Xiao Yang, Ali El-Naggar, Jie Liu, and Hongbo Chen. 2021. "Evaluation of Potential Ecological Risks in Potential Toxic Elements Contaminated Agricultural Soils: Correlations between Soil Contamination and Polymetallic Mining Activity." *Journal of Environmental Management* 300(July):113679. doi: 10.1016/j.jenvman.2021.113679.

Lottermoser, B. G. 2007. *Bernd G. Lottermoser Mine Wastes*. Berlin Heidelberg New York: Springer.

Malone, Brendan, and Ross Searle. 2020. "Improvements to the Australian National Soil Thickness Map Using an Integrated Data Mining Approach." *Geoderma* 377(July):114579. doi: 10.1016/j.geoderma.2020.114579.

Martins, Gabriel Caixeta, Evanise Silva Penido, Ingrid Fernanda Santana Alvarenga, Jéssica Cristina Teodoro, Maria Lucia Bianchi, and Luiz Roberto Guimarães Guilherme. 2018. "Amending Potential of Organic and Industrial By-Products Applied to Heavy Metal-Rich Mining Soils." *Ecotoxicology and*

Environmental Safety 162(July):581–90. doi: 10.1016/j.ecoenv.2018.07.040.

Mcneill, J. R., and George Vrtis. 2019. *Mining North America*.

Morin, K.A., & Hutt, N. M. 1997. *Environmental Geochemistry of Mine Site Drainage, Practical Theory and Case Studies. MDAG Publishing,, 333p*.

Munk, Lee Ann, Gunter Faure, and Randolph Koski. 2006. "Geochemical Evolution of Solutions Derived from Experimental Weathering of Sulfide-Bearing Rocks." *Applied Geochemistry* 21(7):1123–34. doi: 10.1016/j.apgeochem.2006.04.003.

Nagels, L. J., and I. Poels. 2000. "The Role of Spéciation in Analytica Chemistry." *Trends in Analytical Chemistry* 19(7):410–17.

Nieder, Rolf, Dinesh K. Benbi, and Franz X. Reichl. 2018. *Soil Components and Human Health*.

Novak, Jeffrey M., James A. Ippolito, Thomas F. Ducey, Donald W. Watts, Kurt A. Spokas, Kristin M. Trippe, Gilbert C. Sigua, and Mark G. Johnson. 2018. "Remediation of an Acidic Mine Spoil: Miscanthus Biochar and Lime Amendment Affects Metal Availability, Plant Growth, and Soil Enzyme Activity." *Chemosphere* 205:709–18. doi: 10.1016/j.chemosphere.2018.04.107.

O'Connor, David, Deyi Hou, Yong Sik Ok, Jan Mulder, Lei Duan, Qingru Wu, Shuxiao Wang, Filip M. G. Tack, and Jörg Rinklebe. 2019. "Mercury Speciation, Transformation, and Transportation in Soils, Atmospheric Flux, and Implications for Risk

Management: A Critical Review." *Environment International* 126(March):747–61. doi: 10.1016/j.envint.2019.03.019.

Pacetti, Tommaso, Marco Lompi, Claudio Petri, and Enrica Caporali. 2020. "Mining Activity Impacts on Soil Erodibility and Reservoirs Silting: Evaluation of Mining Decommissioning Strategies." *Journal of Hydrology* 589(March):125107. doi: 10.1016/j.jhydrol.2020.125107.

Paniagua-López, M., M. Vela-Cano, D. Correa-Galeote, F. Martín-Peinado, F. J. Martíne. Garzón, C. Pozo, J. González-López, and M. Sierra Aragón. 2021. "Soil Remediation Approach and Bacterial Community Structure in a Long-Term Contaminated Soil by a Mining Spill (Aznalcóllar, Spain)." *Science of the Total Environment* 777:145128. doi: 10.1016/j.scitotenv.2021.145128.

Park, Jiyeon, Ju Yong Kim, and Kyoung Woong Kim. 2012. "Phytoremediation of Soil Contaminated with Heavy Metals Using Brassica Napus." *Geosystem Engineering* 15(1):10–18. doi: 10.1080/12269328.2012.674428.

Paz-Ferreiro, J., H. Lu, S. Fu, A. Méndez, and G. Gascó. 2014. "Use of Phytoremediation and Biochar to Remediate Heavy Metal Polluted Soils: A Review." *Solid Earth* 5(1):65–75. doi: 10.5194/se-5-65-2014.

Pichtel, John. 2003. *Mine Water*. Vol. 32.

Pihlap, Evelin, Miljenka Vuko, Maik Lucas, Markus Steffens, Michael Schloter, Doris Vetterlein, Manuel

Endenich, and Ingrid Kögel-Knabner. 2019. "Initial Soil Formation in an Agriculturally Reclaimed Open-Cast Mining Area - the Role of Management and Loess Parent Material." *Soil and Tillage Research* 191(March):224–37. doi: 10.1016/j.still.2019.03.023.

Portillo Miranda, Gricel Alcira, José Tavares Araruna Júnior, Eduardo de Albuquerque Brocchi, and Hongtao Wang. 2021. "Humic Substances Reduce the Erodibility of Soils in Mining Areas." *Journal of Cleaner Production* 279. doi: 10.1016/j.jclepro.2020.123700.

Rodríguez-Berbel, N., R. Ortega, M. E. Lucas-Borja, A. Solé-Benet, and I. Miralles. 2020. "Long-Term Effects of Two Organic Amendments on Bacterial Communities of Calcareous Mediterranean Soils Degraded by Mining." *Journal of Environmental Management* 271(February). doi: 10.1016/j.jenvman.2020.110920.

Rodríguez, L., E. Ruiz, J. Alonso-Azcárate, and J. Rincón. 2009. "Heavy Metal Distribution and Chemical Speciation in Tailings and Soils around a Pb-Zn Mine in Spain." *Journal of Environmental Management* 90(2):1106–16. doi: 10.1016/j.jenvman.2008.04.007.

Schor, Horst J., and Donald H. Gray. 2008. *Landforming: An Environmental Approach to Hillside Development, Mine Reclamation and Watershed Restoration*.

Selin, Henrik, Susan Egan Keane, Shuxiao Wang, Noelle E. Selin, Kenneth Davis, and Dominique Bally. 2018. "Linking Science and Policy to Support the

Implementation of the Minamata Convention on Mercury." *Ambio* 47(2):198–215. doi: 10.1007/s13280-017-1003-x.

Soria, R., N. Rodríguez-Berbel, R. Ortega, M. E. Lucas-Borja, and I. Miralles. 2021. "Soil Amendments from Recycled Waste Differently Affect CO_2 Soil Emissions in Restored Mining Soils under Semiarid Conditions." *Journal of Environmental Management* 294:112894. doi: 10.1016/j.jenvman.2021.112894.

Taşkesen, Edip, Şükrü Acar, Görkem Ertuğrul, Fatih Arli, Hakan Dumrul, and Saban Bulbul. 2022. "Şırnak-Uludere Bölgesinde Yaygın Olarak Bulunan Asfaltitlerden Doğal Hümik Asit Elde Edilebilirliğinin İncelenmesi." *Politeknik Dergisi* 25(2):691–97. doi: 10.2339/politeknik.766461.

Templeton, Douglas M., and Hitomi Fujishiro. 2017. *Terminology of Elemental Speciation – An IUPAC Perspective*. Vol. 352. Elsevier B.V.

UNEP. 2002. "Global Mercury Assessment." 270.

Wang, Jinman, Qian Qin, and Zhongke Bai. 2018. "Characterizing the Effects of Opencast Coal-Mining and Land Reclamation on Soil Macropore Distribution Characteristics Using 3D CT Scanning." *Catena* 171(October 2017):212–21. doi: 10.1016/j.catena.2018.07.022.

Wang, Quan, Sabry M. Shaheen, Yahui Jiang, Ronghua Li, Michal Slaný, Hamada Abdelrahman, Eilhann Kwon, Nanthi Bolan, Jörg Rinklebe, and Zengqiang Zhang. 2021. "Fe/Mn- and P-Modified Drinking

Water Treatment Residuals Reduced Cu and Pb Phytoavailability and Uptake in a Mining Soil." *Journal of Hazardous Materials* 403(March 2020). doi: 10.1016/j.jhazmat.2020.123628.

WHO. 2016. "Artisanal and Small-Scale Gold Mining and Health-Technical Paper #1: Environmental and Occupational Health Hazards Associated With Artisanal and Small-Scale Gold Mining." *Department of Public Health, Environmental and Social Determinants of Health (PHE), World Health Organization* 1–36.

Younger, Paul L. 2000. "Nature and Practical Implications of Heterogeneities in the Geochemistry of Zinc-Rich, Alkaline Mine Waters in an Underground F-Pb Mine in the UK." *Applied Geochemistry* 15(9):1383–97. doi: 10.1016/S0883-2927(00)00010-X.

PERFORMANCE ANALYSIS OF biSTMD WITH MR DAMPER FOR STRUCTURAL VIBRATION CONTROL

Hüseyin AGGÜMÜŞ[1]

1. INTRODUCTION

The study of vibrations in engineering systems represents a critical area of research, offering valuable insights into the dynamic behavior of structures and mechanisms. The intensity of the vibrations occurring in these systems may cause damage to the system. Vibrations in structures can cause partial or complete damage to the structure (Haskul & Kisa, 2021, Aggumus et al. 2022, 2022) or the entire structure (Aggumus et al. 2024). Furthermore, the collapse of the structure holds significant importance both in terms of human safety and material losses. Consequently, controlling structural vibrations remains a prominent research topic that garners significant attention from scholars.(Aggumus & Cetin, 2018; Aggumus & Guclu, 2020a; Guclu & Yazici, 2007; Turan & Aggumus, 2022.; Wang & Dyke, 2013).

Tuned mass dampers (TMD) are effective control elements used to suppress structural system vibrations (Hadi & Arfiadi, 1998a; Warburton, 1982). In passive

[1] Assist. Prof. Dr., Şırnak University, Şırnak Vocational School, Department of Machinery and Metal Technologies, haggumus@sirnak.edu.tr, ORCID: 0000-0002-7158-677X.

control applications their performance depends only on the correct setting of parameters. (Den Hartog, 1947; Leung & Zhang, 2009). By selecting the damping or spring element or both with variable characteristics, these control applications can be converted to semi-active, thereby improving their performance further.

Semi-active control devices are notable for achieving a balance between high performance and cost-effectiveness in mitigating vibrations. MR dampers are control elements that can generate variable damping force. They are effective control devices due to their ability to meet requirements such as durability, applicability, and performance with ease. (Dyke et al., 1996; Terasawa et al., 2004a). They can make passively tuned mass dampers semi-active (STMD). Thus, they have a higher performance than in the passive control case (TMD).

TMDs can be placed individually in the structure (Aggumus & Guclu, 2020b; Guclu & Yazici, 2009; Hadi & Arfiadi, 1998b; Y. Kim et al., 2008; Paksoy & Aggümüş, 2022) or they can be installed in multiple locations (MTMD) to enable semi-active control applications (Ahmad et al., 2019). MTMDs have different applications (MSTMD). One approach involves installing two mass dampers on the top floor of the structure. (biTMD) (Ok et al., 2008, 2009). Like MTMDs, The effectiveness of biTMDs can be enhanced by optimizing their parameters and implementing semi-active control methods.

This study examines the effectiveness of semi-active biTMD applications in suppressing structural vibrations. The system performance of a biTMD consisting of two

TMDs with MR dampers added to each of the two TMDs (biSTMD) is investigated. The semi-active MR damper control force is obtained by determining the voltages for each MR damper in the biSTMD separately.

2. SYSTEM MODELING

Figure 1 presents the structural model analyzed in this study, alongside the biSTMD configuration used for vibration mitigation. The system's lateral vibrations under harmonic excitation at its critical frequency are analyzed. The equation of motion of the building model is given in Eq.1.

$$M_s\ddot{x}(t) + C_s\dot{x}(t) + K_s x(t) = -H_s f(t) - M_s L\ddot{x}_g \quad (1)$$

Here M_s, C_s ve K_s $\in R^{12x12}$ are the matrices of mass, damping, and stiffness, respectively. $\ddot{X}(t)$, $\dot{x}(t)$ ve $x(t)$ $\in R^{12x1}$ are acceleration, velocity, and displacement vectors, respectively.

x, L and H_s $\in$ R^{12x1}, the displacement vector x, the disturbance input vector L and the location of the controller H are given below.

$$x = [x_1 \quad x_2 \quad x_3 \quad \dots \quad x_{10} \quad x_{11} \quad x_{12}]^T \quad (2)$$

$$H_{s1} = [0 \quad 0 \quad \dots \quad 0 \quad 0 \quad 1]^T \quad (3)$$

$$H_{s2} = [0 \quad 0 \quad \dots \quad 0 \quad 1 \quad 0]^T \quad (4)$$

where H_{s1} and H_{s2} denote the location of the control element applied to the 1. and 2. STMD respectively.

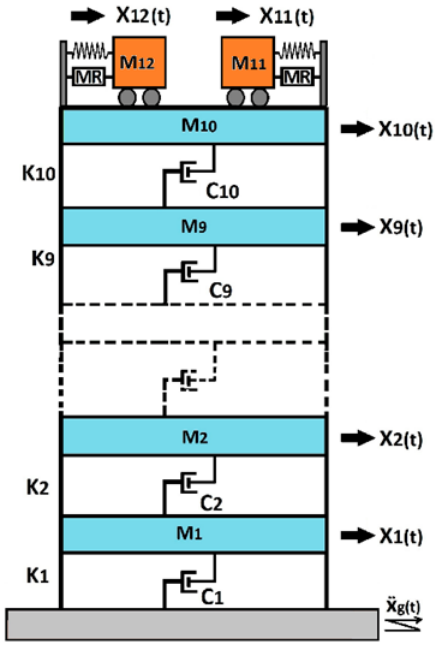

Figure 1. The building model with biSTMD

The mass of the building model, $m_{1\ldots10} = 7.2 * 10^4$ kg, rigidity, $k_{1\ldots10} = 1.3 * 10^8 \frac{N}{m}$, damping, $c_{1\ldots10} = 1.24 * 10^6 \frac{Ns}{m}$.

The frequency of the excitation applied to the system is 1.0108 Hz, and the amplitude of the acceleration is 0.002g m/s^2. The biTMD parameters, each obtained at a mass ratio of 0.015. The optimum frequency (Eq. 8 and 9) and optimum damping ratios (Eq. 10 and 11), which are necessary to calculate the optimum biTMD parameters are calculated for each TMD as follows (Ok et al., 2009).

$$f_{opt1} = \sqrt{\frac{1}{1.0737+2.2593\mu}} \quad (8)$$

$$f_{opt2} = \sqrt{\frac{1}{0.9895+0.4418\mu}} \quad (9)$$

$$\xi_{opt1} = 0.2623\mu^{0.3386} \quad (10)$$

$$\xi_{opt2} = 0.4054\mu^{0.4600} \quad (11)$$

Table 1 summarizes the calculated biTMD parameters, including mass, damping, and rigidity values.

Table 1. biTMD parameters

Mass (kg)	Damping (Ns/m)	Rigidity (N/m)
$m_{11} = 10800$	$c_{11} = 7.8366 * 10^3$	$k_{11} = 3.5508 * 10^5$
$m_{12} = 10800$	$c_{12} = 8.0883 * 10^3$	$k_{12} = 4.3899 * 10^5$

3. CONTROL ALGORITHM AND THE MR DAMPER MODEL

For each of the two MR dampers used in BiSTMD, the Lugre model is used and the force generated is as follows (Terasawa et al., 2004b).

$$f = \sigma_a z + \sigma_0 z v + \sigma_1 \dot{z} + \sigma_2 \dot{x}_1 + \sigma_b \dot{x}_1 v \quad (12)$$

$$\dot{z} = \dot{x}_1 - a_0 |\dot{x}_1| z \quad (13)$$

Here, σ_0, σ_1, and σ_a represent, respectively, the stiffness, damping coefficient, and stiffness of the internal state variable z(t). σ_b refers to the viscous damping influenced by v(t), and σ_2 denotes the viscous damping coefficient. a_0 is a constant value, and f represents the MR damper force (Sakai et al., 2003).

The application of voltage to the MR damper is governed by the groundhook control algorithm, which is described as follows (H.-S. Kim & Kang, 2012; Koo et al., 2004).

$$V_{MR1} = \begin{cases} V_{max} & \rightarrow & x_{10}(\dot{x}_{10} - \dot{x}_{11}) \leq 0 \\ V_{min} & \rightarrow & x_{10}(\dot{x}_{10} - \dot{x}_{11}) > 0 \end{cases} \quad (14)$$

$$V_{MR2} = \begin{cases} V_{max} & \rightarrow & x_{10}(\dot{x}_{10} - \dot{x}_{12}) \leq 0 \\ V_{min} & \rightarrow & x_{10}(\dot{x}_{10} - \dot{x}_{12}) > 0 \end{cases} \quad (15)$$

V_{MR1} represents the MR damper added to 1. STMD and V_{MR2} represents the MR damper added to 2. STMD. Where V_{max} and V_{min} are voltage values ranging from 10v to 0v.

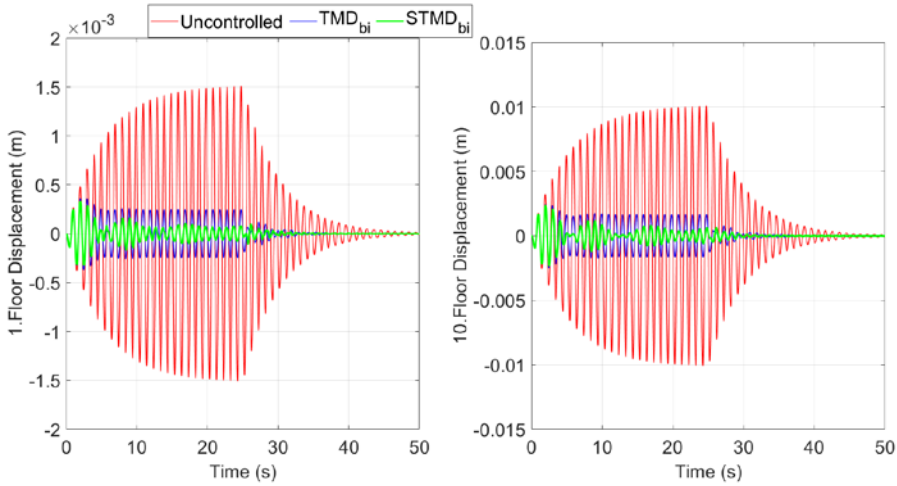

Figure 2. 1st and 10th floor displacement time responses

4. SIMULATIONS

This study investigates displacement and acceleration time responses to evaluate the effectiveness of biSTMD in suppressing vibrations in a ten-story building. Both the maximum and root mean square (RMS) values of these responses are evaluated. The system performance is evaluated by comparing the no control case with the biTMD and biSTMD control cases.

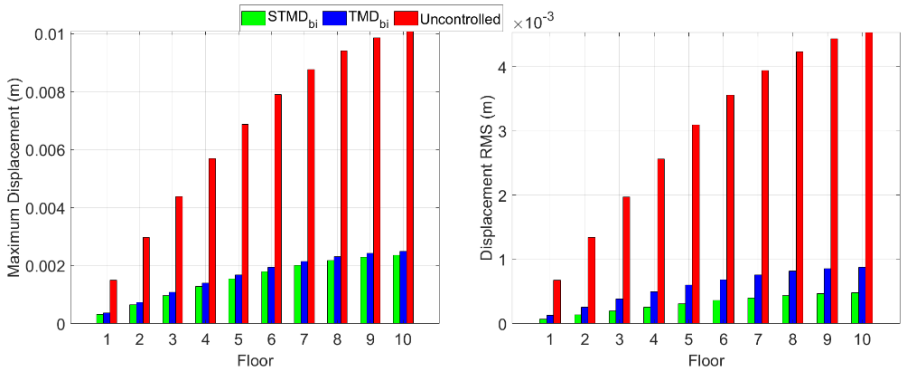

Figure 3. Maximum displacement and displacement rms responses

Figure 2 shows the displacements of the 1st and 10th floors of the system under the effect of external disturbance input. Figure 3 shows the maximum and rms values of the displacement responses. Across all levels, the biSTMD control configuration demonstrates superior performance compared to the biTMD system.

Figure 4 depicts the acceleration-time curves of the 1st and 10th floors of the system subjected to external disturbance inputs. Figure 5 shows the maxima and rms values of the acceleration responses. As in the displacement responses, there is a decrease in the system responses in both control cases. Although the biSTMD control case performs better than the biTMD control case, this is the opposite in the first two floors for the maximum responses

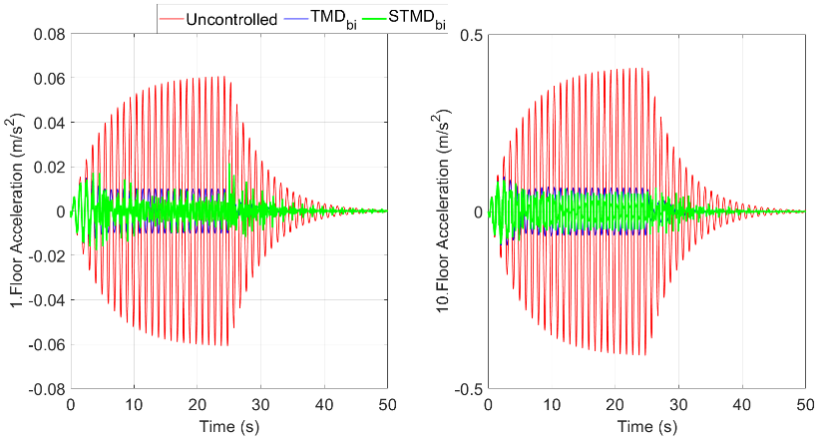

Figure 4. 1st and 10th floor acceleration time responses

In general, biTMD and biSTMD applied to the system suppressed the system responses in performance values. However, biSTMD showed a superior performance. For acceleration responses, in the first two stories, the biSTMD control responses were similar to the biTMD case but slightly worse. However, this is acceptable considering the displacement response improvements.

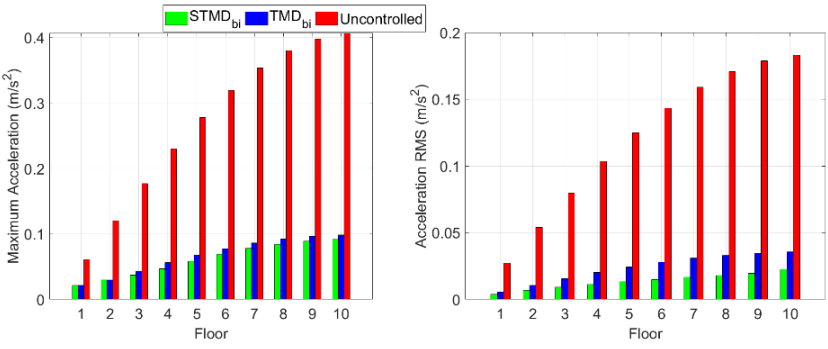

Figure 5. Maximum acceleration and acceleration rms responses

5. CONCLUSIONS

In this study, the performance of a semi-active multi-mass damper is investigated to suppress the vibrations of a ten-story building under harmonic excitation. The semi-activity is achieved by using MR damper controller. The groundhook control algorithm is used for the MR damper voltage. The installation of two mass dampers at the top floor of the building enables a performance comparison between biSTMD and biTMD systems. Simulation results demonstrate that biSTMD provides superior suppression of system vibrations compared to biTMD.

REFERENCES

Aggümüş, H., Haskul, & M, Turan, A. (2022b, December 25). Deprem etkisindeki tek serbestlik dereceli bir binanın kolonlardaki çatlakların sistem cevaplarına etkisi. *Doğa ve Mühendislik Bilimlerinde Güncel Tartışmalar 7, 285-291.*

Aggümüş, H., Turan, A., & Haskul, M. (2022, December 20). Harmonik ve deprem uyarımı altındaki bir binada bulunan çatlakların sistem cevaplarına etkisi. 1st *International Conference on Engineering, Natural and Social Sciences*, 404-407.

Aggumus, H., & Cetin, S. (2018). Experimental investigation of semiactive robust control for structures with magnetorheological dampers. *Journal of Low Frequency Noise, Vibration and Active Control*, *37*(2), 216–234. https://doi.org/10.1177/0263092317711985

Aggumus, H., Daskin, M., Haskul, M., & Turan, A. (2024). The Effect of the Crack-Stiffness Relationship on the System Response in Columns of an SDOF Steel Structure Model under Harmonic and Earthquake Excitations. *Shock and Vibration*, *2024*(1), 9278849.

Aggumus, H., & Guclu, R. (2020a). Robust H∞ Control of STMDs Used in Structural Systems by Hardware in the Loop Simulation Method. *Actuators*, *9*(3), 55. https://doi.org/10.3390/act9030055

Ahmad, A. Z., Abu, A., Quen, L. K., Aâ, N., & In, F. C. (2019). Numerical Modelling of Multiple Tuned Mass Damper Equipped with Magneto Rheological

Damper for Attenuation of Building Seismic Responses. *Jurnal Teknologi*, *81*(6).

Den Hartog, J. P. (1947). *Mechanical vibrations* (3rd ed). New York, N.Y. : McGraw-Hill. https://trove.nla.gov.au/version/21341052

Dyke, S. J., Spencer, B. F., Sain, M. K., & Carlson, J. D. (1996). Modeling and control of magnetorheological dampers for seismic response reduction. *Smart Materials and Structures*, *5*(5), 565–575. https://doi.org/10.1088/0964-1726/5/5/006

Guclu, R., & Yazici, H. (2007). Fuzzy Logic Control of a Non-linear Structural System against Earthquake Induced Vibration. *Journal of Vibration and Control*, *13*(11), 1535–1551. https://doi.org/10.1177/1077546307077663

Guclu, R., & Yazici, H. (2009). Seismic-vibration mitigation of a nonlinear structural system with an ATMD through a fuzzy PID controller. *Nonlinear Dynamics*, *58*(3), 553–564. https://doi.org/10.1007/s11071-009-9500-5

Hadi, M. N. S., & Arfiadi, Y. (1998a). Optimum Design of Absorber for MDOF Structures. *Journal of Structural Engineering*, *124*(11), 1272–1280. https://doi.org/10.1061/(ASCE)0733-9445(1998)124:11(1272)

Hadi, M. N. S., & Arfiadi, Y. (1998b). Optimum Design of Absorber for MDOF Structures. *Journal of Structural Engineering*, *124*(11), 1272–1280.

https://doi.org/10.1061/(ASCE)0733-9445(1998)124:11(1272)

Haskul, M., & Kisa, M. (2021). Free vibration of the double tapered cracked beam. *Inverse Problems in Science and Engineering*, *29*(11), 1537–1564.

Kim, H.-S., & Kang, J.-W. (2012). Semi-active fuzzy control of a wind-excited tall building using multi-objective genetic algorithm. *Engineering Structures*, *41*, 242–257. https://doi.org/10.1016/j.engstruct.2012.03.038

Kim, Y., You, K., & Kim, H. (2008). Wind-induced excitation control of a tall building with tuned mass dampers. *The Structural Design of Tall and Special Buildings*, *17*(3), 669–682. https://doi.org/10.1002/tal.372

Koo, J.-H., Ahmadian, M., Setareh, M., & Murray, T. (2004). In Search of Suitable Control Methods for Semi-Active Tuned Vibration Absorbers: *Journal of Vibration and Control*. https://doi.org/10.1177/1077546304032020

Leung, A. Y. T., & Zhang, H. (2009). Particle swarm optimization of tuned mass dampers. *Engineering Structures*, *31*(3), 715–728. https://doi.org/10.1016/j.engstruct.2008.11.017

Ohtori, Y., Christenson, R. E., Spencer, B. F., & Dyke, S. J. (2004). Benchmark Control Problems for Seismically Excited Nonlinear Buildings. *Journal of Engineering Mechanics*, *130*(4), 366–385. https://doi.org/10.1061/(ASCE)0733-9399(2004)130:4(366)

Ok, S.-Y., Song, J., & Park, K.-S. (2008). Optimal performance design of bi-tuned mass damper systems using multi-objective optimization. *KSCE Journal of Civil Engineering*, *12*, 313–322.

Ok, S.-Y., Song, J., & Park, K.-S. (2009). Development of optimal design formula for bi-tuned mass dampers using multi-objective optimization. *Journal of Sound and Vibration*, *322*(1–2), 60–77.

Paksoy, M., & Aggümüş, H. (2022). MR Sönümleyicili Yarı Aktif Ayarlı Kütle Sönümleyicisinin Uyarlamalı Kontrolü. *Avrupa Bilim ve Teknoloji Dergisi*, *33*, 68–73.

Sakai, C., Ohmori, H., & Sano, A. (2003). Modeling of MR damper with hysteresis for adaptive vibration control. *42nd IEEE International Conference on Decision and Control (IEEE Cat. No.03CH37475)*, *4*, 3840–3845 vol.4. https://doi.org/10.1109/CDC.2003.1271748

Terasawa, T., Sakai, C., Ohmori, H., & Sano, A. (2004a). Adaptive identification of MR damper for vibration control. *Undefined*. https://www.semanticscholar.org/paper/Adaptive-identification-of-MR-damper-for-vibration-Terasawa-Sakai/d3c8367e399761b180eb13c9e63d2335fbc64acd

Terasawa, T., Sakai, C., Ohmori, H., & Sano, A. (2004b). Adaptive identification of MR damper for vibration control. *2004 43rd IEEE Conference on Decision and Control (CDC) (IEEE Cat. No.04CH37601)*, *3*, 2297-

2303 Vol.3. https://doi.org/10.1109/CDC.2004.1428732

Turan, A., & Aggumus, H. (2022.). *Implementation of Advanced PID Control Algorithm for SDOF System*. 10.

Wang, Y., & Dyke, S. (2013). Modal-based LQG for smart base isolation system design in seismic response control: MODAL-BASED LQG FOR SMART BASE ISOLATION SYSTEM IN SEISMIC CONTROL. *Structural Control and Health Monitoring*, *20*(5), 753–768. https://doi.org/10.1002/stc.1490

Warburton, G. B. (1982). Optimum absorber parameters for various combinations of response and excitation parameters. *Earthquake Engineering & Structural Dynamics*, *10*(3), 381–401.

DEVELOPMENTS IN THE FIELD OF ENGINEERING 2024

yaz
yayınları

YAZ Yayınları
M.İhtisas OSB Mah. 4A Cad. No:3/3
İscehisar / AFYONKARAHİSAR
Tel : (0 531) 880 92 99
yazyayinlari@gmail.com • www.yazyayinlari.com

ISBN: 978-625-6171-18-3